MOLECULAR CLONING AND FUNCTIONAL CHARACTERIZATION OF GENES INVOLVED IN THE BIOSYNTHESIS OF POLYUNSATURATED FATTY ACIDS IN OAT (*AVENA SATIVA* L.)

A Thesis Submitted to the
College of Graduate Studies and Research
In Partial Fulfillment of the Requirements
For the Degree of Master of Science
In the Department of Food and Bioproduct Sciences
College of Agriculture and Bioresources
University of Saskatchewan
Saskatoon, Saskatchewan
Canada

by

MATTHEW HUNTER BERNARD

PERMISSION TO USE

In presenting this thesis/dissertation in partial fulfillment of the requirements for a Postgraduate degree from the University of Saskatchewan, I agree that the Libraries of this University may make it freely available for inspection. I further agree that permission for copying of this thesis/dissertation in any manner, in whole or in part, for scholarly purposes may be granted by the professor or professors who supervised my thesis/dissertation work or, in their absence, by the Head of the Department or the Dean of the College in which my thesis work was done. It is understood that any copying or publication or use of this thesis/dissertation or parts thereof for financial gain shall not be allowed without my written permission. It is also understood that due recognition shall be given to me and to the University of Saskatchewan in any scholarly use which may be made of any material in my thesis/dissertation.

DISCLAIMER

Reference in this thesis/dissertation to any specific commercial products, process, or service by trade name, trademark, manufacturer, or otherwise, does not constitute or imply its endorsement, recommendation, or favoring by the University of Saskatchewan. The views and opinions of the author expressed herein do not state or reflect those of the University of Saskatchewan, and shall not be used for advertising or product endorsement purposes.

Requests for permission to copy or to make other uses of materials in this thesis/dissertation in whole or part should be addressed to:

The Head of the Department of Food and Bioproduct Sciences
51 Campus Drive, University of Saskatchewan
Saskatoon, Saskatchewan S7N 5A8
Canada

OR

Dean College of Graduate Studies and Research
University of Saskatchewan
107 Administration Place
Saskatoon, Saskatchewan S7N 5A2 Canada

ABSTRACT

This thesis research started with analysis of oat fatty acids by using three different transmethylation methods. Basic sodium methoxide was compared with traditional acidic methanol for the total fatty acid analysis, while diazomethane was used to analyze free fatty acids. Epoxy FAs were readily hydrolyzed to dihydroxy fatty acids under the acidic condition, which suggest an overestimation of hydroxyl fatty acids and underestimation of epoxy fatty acids in previous analyses. The sodium methoxide method proved more reliable to quantify the oat seed fatty acid composition. CDC Dancer oat seed analyzed here was comprised mostly of palmitic acid (PA), oleic acid (OA) and the polyunsaturated fatty acid (PUFA) linoleic acid (LA) in quantities of 23%, 32%, and 37% of total seed FA, respectively. As well, the seed contained small quantities of another PUFA, *a*-linolenic (ALA) and several unusual oxygenated fatty acids (UFAs), *Δ*15-hydroxy fatty acid (15HFA) and epoxy fatty acids in quantities of 0.85%, 0.68%, and 2.3%, respectively. This thesis further aimed to identify and assemble all *FAD2*-like genes from an oat Expressed-Sequence Tag (EST) database using FAD2 and FAD2-like proteins from other organisms as query sequences in order to clone all putative *FAD2*-like genes-of-interest (GOIs) from oat. From the contig assemblies of retrieved oat ESTs, four distinct, putative genes were identified. From the *Δ*12-desaturase (FAD2) queries, a putative *FAD2*-like (*AsFAD2*) gene was identified; the *Δ*15-desaturase (FAD3) queries revealed two putative oat *FAD3*-like (*AsFAD3-1* and *AsFAD3-2*) genes, while an *ω*-3 desaturase (FAD7) query identified a fourth putative full-length *FAD6*-like coding sequence of two possible lengths, *AsFADX* and *AsFADX+*. The GOIs were then subcloned into a yeast expression vector and functionally characterized. AsFAD2a and AsFAD2b both demonstrated *Δ*12 desaturation on 18:1-9*c* substrate. AsFAD3-1 had no activity on any substrates present, while AsFAD3-2 exhibited weak *Δ*15-desaturation activity specifically on 18:2-9*c*,12*c*. Finally, AsFADX converted 18:1-9*c* to 18:2-9*c*,12*c*, while AsFADX+ had no activity. Then, a comparative analysis of transcript levels of these GOIs via quantitative real-time PCR (qRT-PCR) was performed across oat germinating seed, root, leaf, and developing seed. *AsFAD2* transcript abundance was generally much higher than *AsFAD3-1* and *AsFAD3-2* in all tissues. *AsFAD3-1* mRNA level was highest in developing seed tissue, slightly lower in leaf tissue, and lowest in root. *AsFAD3-2* mRNA was highest in germinating seed, and lowest in leaf tissue. In summary, the data produced from this thesis could be used to enhance breeding efforts for establishing oat cultivars with healthier oil content.

ACKNOWLEDGEMENTS

I would like to take this opportunity to acknowledge everyone without whom this thesis would not have been possible.

First I would like to thank my supervisor Dr. Xiao Qiu for recognizing my potential and offering me the opportunity to enhance my education at this level, as well as for his support and guidance throughout this project. His depth of knowledge and patience as a mentor has been instrumental in preparation for my professional career. For technical assistance and additional guidance throughout this project, I would also like to thank Dr. Dauenpen Meesapyodsuk. Her extensive knowledge and experience were invaluable, and her leadership was very much appreciated.

For their diverse expertise and counsel, I would also like to thank my committee members, Dr. Aaron Beattie, Dr. Mark Smith, Dr. Robert Tyler, and Dr. Darren Korber. I am thankful to all the advice and guidance offered to ensure the success of the project.

Working with other labs within the college and sharing lab equipment made some days much more efficient; for this, I would like to thank all my colleagues in the Department of Food & Bioproduct Sciences, the Department of Plant Sciences and the Department of Soil Sciences for their willingness to work together. I would also like to thank Dallas Kessler and Agriculture and Agri-Food Canada for providing oat seed.

Much was learned in discussions with my colleagues; I wish to thank all my fellow students and professors in the College of Agriculture & Bioresources, who have since become good friends, for their insightful discussions either within the discipline of molecular biology, or in those areas less familiar to me. I would especially like to thank my labmates, without whom this project would have been incredibly challenging. Our discussions covering everything from molecular biology, agriculture, weather, travel, culture, and language added much amusement and enjoyment over the duration of this project; these things learned from one another are the unofficial results of the degree and the memories will be cherished.

Finally, I cannot continue without acknowledging the patience and understanding of my family and friends from my personal life. Their support throughout my academic journey has been vital in helping me achieve this level of success, and I cannot properly put into words how meaningful that support has been.

This convergence of agriculture and dietary nutrition is dedicated to my parents, whom have always offered their unwavering support and guidance through every trial, tribulation, and triumph that I have encountered.

"*There are more things in heaven and earth…than are dreamt of in our philosophy."*
(Shakespeare, 1.5.167-8)

TABLE OF CONTENTS

LIST OF TABLES

LIST OF FIGURES

LIST OF ABBREVIATIONS

15HFA	Avenoleic Acid; 15-OH 18:2-9*c*,12*c*
ARA	Arachidonic Acid; 20:4-5*c*,8*c*,11*c*,14*c*
aa	Amino Acid
AAFC	Agriculture & Agri-Food Canada
ALA	*α*-Linolenic Acid; 18:3-9*c*,12*c*,15*c*
AsFAD	Avena sativa Fatty Acid Desaturase
AsFAH	Avena sativa Fatty Acid Hydroxylase
AtFAD	Arabidopsis thaliana Fatty Acid Desaturase
BLAST	Basic Local Alignment Search Tool
CB	Carbenecillin, a synthetic analogue of ampicillin
cDNA	Complimentary DNA
CDS	Coding Sequence
CORE	Collaborative Oat Research Enterprise
dATP	deoxyadenosine triphosphate
DGDG	Digalactosyldiacylglycerol
DGLA	Dihomo-*γ*-Linolenic Acid; 20:3-8*c*,11*c*,14*c*
DHA	Docosahexaenoic Acid; 22:6-4*c*,7*c*,10*c*,13*c*,16*c*,19*c*
dwt	Dry weight
E. coli	*Escherichia coli*
EPA	Eicosapentaenoic Acid; 20:5-5*c*,8*c*,11*c*,14*c*,17*c*
ER	Endoplasmic Reticulum
EST	Expressed Sequence Tag
EtBr	Ethidium Bromide
FA	Fatty Acid
FAD	Fatty Acid Desaturase (protein)
FAD	Fatty Acid Desaturase (gene)
FAD2	*Δ*12 Fatty Acid Desaturase (Endoplasmic Reticulum)
FAD3	*Δ*15 Fatty Acid Desaturase (Endoplasmic Reticulum)
FAD6	*Δ*12 Fatty Acid Desaturase (Plastidial)
FAD7	*Δ*15 Fatty Acid Desaturase (Plastidial)
FAD8	*Δ*15 Fatty Acid Desaturase (low temperature-sensitive FAD7)
FADX	FAD6 or FAD7-like
FADX+	FAD6 or FAD7-like, extended
FAH	Fatty Acid Hydroxylase protein

FAH	Fatty Acid Hydroxylase gene
FAH12	*Δ*-12 Fatty Acid Hydroxylase
FAH15	*Δ*-15 Fatty Acid Hydroxylase
FAME	Fatty Acid Methyl Ester
FFA	Free Fatty Acid
GC	Gas Chromatography
GLA	*γ*-Linolenic Acid; 18:3-6c,9c,12c
GOI	Gene Of Interest
HKG	Housekeeping Gene
INVSc1	Invitrogen *Saccharomyces cerevisiae* yeast
LA	Linoleic Acid; 18:3-9c,12c
LB	E. coli growth medium ("lysogeny broth")
LCFA	Long-Chain Fatty Acid
MAS	Marker-Assisted Selection
MCS	Multi-Cloning Site
MGDG	Monogalactosyldiacylglycerol
MS	Mass Spectrometry
NCBI	National Center for Biotechnology Information
NSAID	Non-steroidal anti-inflammatory drug
OA	Oleic Acid; 18:1-9c
ORF	Open Reading Frame
PUFA	Polyunsaturated Fatty Acid
qRT-PCR	Quantitative Real-Time PCR
S. cerevisiae	*Saccharomyces cerevisiae*
SC –U	Uracil-deficient *S. cerevisiae* growth medium
tBLASTn	protein query in translated nucleotide database
TMS	trimethylsilyl
UFA	Unusual Fatty Acid
UTR	Untranslated Region
VLCPUFA	Very Long-Chain Polyunsaturated Fatty Acid
Δ(*n*)	*n*th carbon from carboxyl end
ω(*n*)	*n*th carbon from methyl end
20:3-8*c*,11*c*,14*c*	Dihomo-*γ*-Linolenic Acid, DGLA
18:1-9*c*	Oleic Acid, OA
15-OH 18:2-9*c*,12*c*	Avenoleic Acid

18:3-6*c*,9*c*,12*c*	*γ*-Linolenic Acid, GLA
18:2-9*c*,12*c*	Linoleic Acid, LA
18:3-9*c*,12*c*,15*c*	α-Linolenic Acid, ALA
20:4-5*c*,8*c*,11*c*,14*c*	Arachidonic Acid, ARA
20:5-5*c*,8*c*,11*c*,14*c*,17*c*	Eicosapentaenoic Acid, EPA
22:6-4*c*,7*c*,10*c*,13*c*,16*c*,19*c*	Docosahexaenoic Acid, DHA

1. INTRODUCTION

Oat (*Avena sativa* L.) is an annual cereal crop originating from the eastern Mediterranean area, gaining attention as a health food in recent years (Coffman, 1977). This crop has been popular as both a feed and food crop, due to its relatively unique seed composition amongst cereals: it contains cholesterol-lowering *β*-D-glucan, antioxidant & antimicrobial avenanthramides, the storage protein globulin, and an exceptionally high oil content unusually dispersed throughout the starchy endosperm (Coffman, 1977; Leonova *et al.*, 2008; Leonova *et al.*, 2010). The fatty acid (FA) composition of the seed oil is particularly interesting, not only for its quantity but also for the unique FAs present (Hamberg & Hamberg, 1996; Leonova *et al.*, 2008). In addition to the "healthy" polyunsaturated FAs (PUFAs) (Health Canada, 2012), oat seed oil contains several unusual oxygenated fatty acids (UFAs), some of which have not been observed in any other organism to date (Hamberg & Hamberg, 1996; Hamberg *et al.*, 1998; Leonova *et al.*, 2008). Despite its global yearly production of 25 million tonnes (Mt) (Agriculture Saskatchewan, 2008), the nutritional value of oat has not been optimized; thus, this thesis aimed to clone and functionally characterize genes underlying the biosynthesis of FAs in oat while establishing the most ideal method of FA analysis for such a diverse pool of FAs.

Previous analyses mostly utilize acidic methanol to transmethylate oat FAs, which may hydrolyze unusual epoxy fatty acids resulting in their inaccurate quantification (Leonova *et al.*, 2008). Therefore, this thesis research started with reanalysis of oat fatty acids by using three different transmethylation methods. Sodium methoxide is an alkaline treatment which is less conventional than the more common sulfuric methanol transmethylation procedure, due to relative cost and safety concerns (Christie, 2011). The diazomethane method can be used to specifically analyze the free fatty acid (FFA) content. After eluting the fatty acid methyl esters (FAMEs) via gas chromatography (GC), comparing results of the different methods can demonstrate whether epoxy FAs were readily hydrolyzed to dihydroxy fatty acids under the acidic condition, which could result in an overestimation of hydroxyl fatty acids and underestimation of epoxy fatty acids. Then, the most ideal transmethylation procedure can be identified for future oat seed FA analyses.

The PUFAs and UFAs are the resulting product of the activity of *Δ*12-fatty acid desaturases (FAD2s) and FAD2-like enzymes believed to have diverged from FAD2 progenitors, such as *Δ*15-fatty acid desaturases (FAD3s) or fatty acid hydroxylases (FAHs) (van de Loo *et al.*, 1995). It has been demonstrated previously that FAD2-like enzymes (both desaturases and hydroxylases) have evolved from FAD2 proteins, as those functional proteins (and thus, their underlying genes) share high homology (van de Loo *et al.*, 1995; Broun *et al*., 1998). As such, this research will attempt to search for all *FAD2*-like genes from an oat Expressed-Sequence Tag (EST) database using FAD2 and FAD2-like proteins from other organisms as query sequences, then to clone all putative *FAD2*-like genes-of-interest (GOIs) from oat. Then, the putative GOIs can be cloned into a *Saccharomyces cerevisiae* (*S. cerevisiae*) yeast expression vector, transformed into yeast cells, fed the appropriate FA substrate(s), and finally functionally characterized.

Comparative expression analyses of these GOIs via quantitative real-time PCR (qRT-PCR) is increasingly used for insight into GOI expression patterns (Rajwade *et al*., 2013); thus, it will be applied across oat germinating seed, root, leaf, and developing seed for comparative analysis of mRNA abundance patterns in oat. These data can then be used for marker-assisted breeding programs (Xu & Crouch, 2008; Kumar *et al*., 2009) to contribute to enhancing breeding efforts to continually improve oat as a health food and strengthen the Canadian agriculture industry.

2. LITERATURE SURVEY

2.1. Dietary Oil and Human Health

In a normal, healthy human diet, oil can have some of the most significant influences on an individual's overall well-being. More specifically, the types of fatty acids (subcomponents of which oils are comprised) as well as the quantities ingested on a regular basis impact the long-term health consequences of the individual (Health Canada, 2012). Fatty acids are under increasing scrutiny as they pertain to health issues especially in the North American diet, and include the omega (ω)-6 and ω-3 polyunsaturated fatty acids (PUFAs). These fatty acids have two or more double bonds, with the last double bond occurring six carbons (ω-6) and three carbons (ω-3) from the methyl end of the molecule, and may or may not include functional groups on the same molecule. These attributes all impact their function in a biological system. The physiological effects of these PUFAs in the diet can be widespread, and many reviews and studies have suggested how these dietary PUFAs may directly affect cardiovascular health, mental/neurological health, skeletal health, inflammation and immune response, and digestive tract function, amongst others (Pan *et al*., 2012; Davidson *et al*., 2011; Russo 2009; Siddiqui *et al*., 2008; Dangour *et al*., 2012; Karr *et al*., 2011; Orchard *et al*., 2012; Cleland *et al*., 2005; Simopoulos, 2002; Simopoulos, 1998).

Both ω-6 and ω-3 desaturation occur on long-chain fatty acid (LCFA) substrates, which are common in vegetable oils and, to a lesser extent, in cereal seed tissue; arguably, the most important plant PUFAs are 18:2-9*c*,12*c* (linoleic acid; LA), and 18:3-9*c*,12*c*,15*c* (α-linolenic acid; ALA) (Figure 1). Other ω-6 and ω-3 very long chain PUFAs (VLCPUFAs) crucial to human health are eicosapentaenoic acid (EPA; 20:5-5*c*,8*c*,11*c*,14*c*,17*c*), and docosahexaenoic acid (DHA; 22:6-4*c*,7*c*,10*c*,13*c*,16*c*,19*c*) (Figure 1). (For clarification, the ω-naming will be used in the context of general health discussion, while the Δ-naming will be used more specifically within biosynthesis context, as illustrated in Figure 1.)

For quantities adequate for human physiological requirements, EPA, DHA, ALA and LA must be obtained from the diet. Although small amounts of EPA and DHA can be converted

from ALA substrate in humans, they are increasingly considered "conditionally essential" due to the small amount inefficiently produced. Due to the health benefits as well as their low production endogenously, an individual's diet should provide these VLCPUFAs (Brenna, 2002; Carnielli *et al*., 1996). However, the diet must provide both essential PUFAs LA and ALA, since these two cannot be synthesized by humans (Brenna, 2002; Carnielli *et al*., 1996; Burdge *et al*., 2002). The synthesis and metabolism of these FAs are summarized in Figure 2.

Until relatively recently throughout history, the ratio of ω-6 to ω-3 fatty acids obtained through the diet was typically 1:1 or 2:1 and was ideal for human health; today in North America, this ratio has shifted to 10:1 to 25:1 (Simopoulos, 2002). Since earlier evidence was uncovered suggesting that not only the types of PUFAs but the relative ratio between ω-6 and ω-3 fatty acids is vital to whether their effect on an individual's health is beneficial or detrimental, the concept has been well reviewed and supported (Li *et al*., 1994; Simopoulos, 2002; Cleland *et al*., 2005; Schmitz & Ecker, 2008).

The effect of the recent skewed ω-6 to ω-3 ratio may be most notable as it pertains to inflammation (Simopoulos, 2002). Eicosanoids, a group of fatty acid-derived signaling molecules, have vital functions relating to the health issues mentioned; yet, in excess, certain eicosanoids are pro-inflammatory, pro-thrombotic, and/or pro-atherogenic (Box A, Figure 1) (Li *et al*., 1994; Schmitz & Ecker, 2008). As the eicosanoids with negative physiological effects are oxidized derivatives of arachidonic acid (ARA; 20:4-5*c*,8*c*,11*c*,14*c*), and ARA is synthesized from LA precursor, excessive LA is viewed as a pro-inflammatory fatty acid (Simopoulos, 2002). Furthermore, evidence suggests that ω-3 fatty acids such as ALA have antithetic effects in the presence of ω-6 fatty acids to mitigate ARA levels and thus minimize excess harmful eicosanoid levels, subsequently curtailing the dietary-induced inflammatory response and even promote biosynthesis of beneficial eicosanoids (Box B, Figure 1) such as neuroprotectants (Li *et al*., 1994; Schmitz & Ecker, 2008).The competing effects of LA and ALA in the inflammation pathway result from the Δ6 desaturase that can use both the fatty acid substrates, while concurrently, high LA can interfere with ALA desaturation and elongation (Simopoulos, 2002). Essentially, there is FA substrate competition by the enzymes (Figure 2) for ω-6 and ω-3 FAs to use in their subsequent conversion pathways (Schmitz & Ecker, 2008). Triggering the desaturase cascade from LA substrate in most mammals increases AA, which is largely the main precursor to several pro-inflammatory molecules such as prostaglandin H_2 and its eicosanoid derivatives

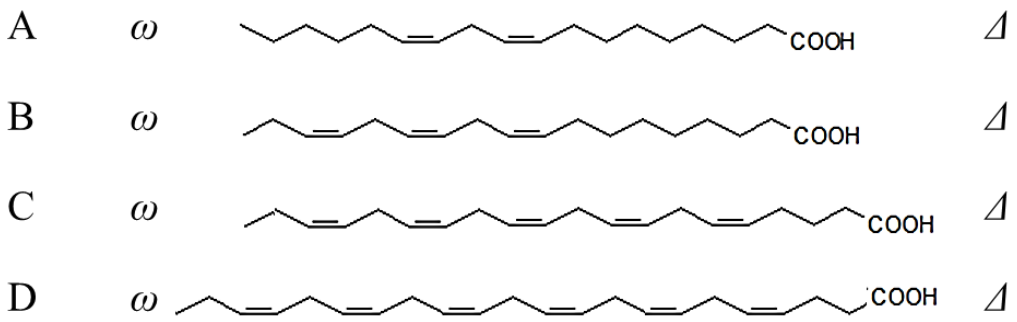

Figure 1. Linoleic Acid (A), α-Linolenic Acid (B), Eicosapentaenoic Acid (C), and Docosahexaenoic Acid (D). The relative positions of the first carbon numbered with the *ω*-nomenclature, from the methyl end, and with the *Δ*-nomenclature, from the carboxyl (polar) end (adapted from the American Oil Chemists' Society, 2012c).

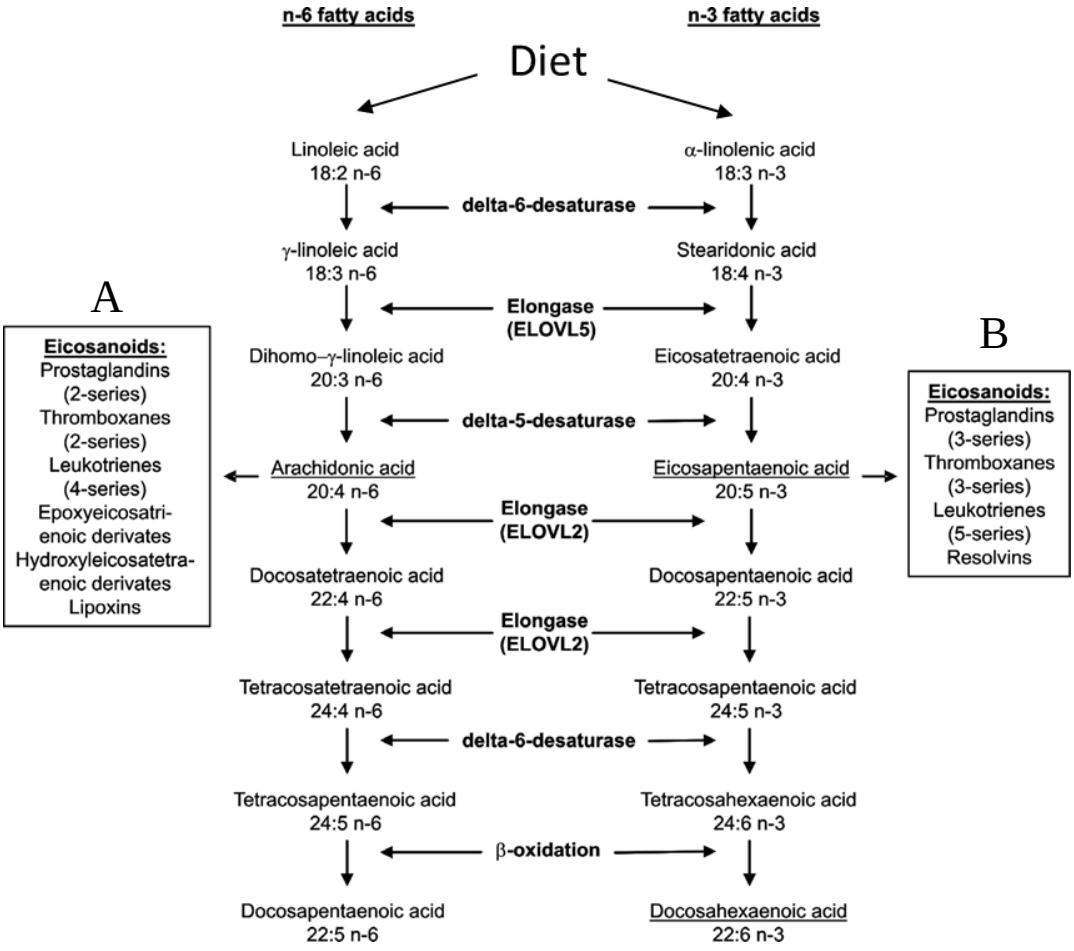

Figure 2. Overview of the *ω*-6 and *ω*-3 (or, n-6 and n-3) synthesis pathways (Adapted from Schmitz & Ecker, 2008). Boxes A and B show metabolized eicosanoids of both pathways.

(Box A, Figure 2); conversely, ALA substrate is the precursor to EPA and thus DHA biosynthesis (Salem *et al*., 1999). Hence, maximizing ALA and minimizing LA content of the same food source is conducive to human biosynthetic pathways that favour the anti-inflammatory pathway by diminishing prostaglandin H2 production – the same pharmacological goal as non-steroidal anti-inflammatory drugs (NSAIDs) (Kurumbail *et al*., 1996).

Ideally, EPA, DHA, and the two essential fatty acids LA and ALA would be obtained directly from the food sources in which they are naturally and most abundantly found, and in ideal proportions. Sufficient EPA and DHA food sources for human demands, however, are mostly limited to marine organisms (Dieticians of Canada, 2013). The accessibility and cost of including these food sources in a daily diet become increasingly challenging as proximity from the marine sources lengthens. Thus, it is important to aim for all components of a diet to have an ω-3 to ω-6 ratio as close to optimal as possible. In the prairies, a source of these FAs is oat (*Avena sativa* L.), a crop with a strong history of production, and established markets.

2.2. Oat

Oat is a tall-standing, 2-flowered dark-green cereal with 7 to 9 nodules, preferring cooler climates such as the northern plains of the United States, Great Lakes area, and southern plains of Canada. Naturally, oat is autogamic (self-pollinating) (Coffman, 1977). Oat is sought after as feed crop, although around the world it is also an important food crop as it can yield up to 100 bushels per acre (bu/acre) (Agriculture Saskatchewan, 2008). As a crop, Saskatchewan producers seed 2 million acres of oat, producing 2 million tonnes (Mt) per year, with production trending upward over 20 years (Saskatchewan Ministry of Agriculture, 2011). In Canada, 3.57Mt of oat per year is produced, accounting for 83% of total oat exports and globally; oat is a 25Mt annual commodity (Saskatchewan Ministry of Agriculture, 2011; Agriculture and Agri-Food Canada, 2010a). This annual cereal is not a new crop; it was first cultivated in the Mediterranean area more than four thousand years ago. After being brought from Europe, the first evidence of oat in North America was in 1565, and, in Canada, in 1617 (Schrickel, 1986; Coffman, 1977).

The *Avena* (*A.*) genus belongs to the Graminiae family, with a name derived from the Latin *Aveo* (“desire”), *Ava* (“nourishment”), and *Avesa* (“pasture”) (Coffman, 1977). Linnaeus (L.) first began characterizing cultivated oats in 1753 by comparing their morphologies (Coffman, 1977). Four species were initially categorized: *A. sterilis*, which dropped seeds upon maturation; *A. fatua* (“fatuous”), named to imply “without value;” *A. sativa* L. (“sativ”), meaning “sown and

cultivated;" and *A. nuda*, lacking pericarp (it has been generally accepted, however, that *A. nuda* is a sub-species of *A. sterilis*) (Coffman, 1977). *A. byzantine* has been identified as the fourth distinct group of cultivated oat. While some dispute the origins of oat, Coffman declared that all current cultivated oats evolved from *A. sterilis* (1977), while Rajhathy and Thomas conclude that *A. sativa* evolved from either *A. fatua* or *A. sterilis*.

Although these four species are distinct, they are all hexaploids and thus genetically belong to the same group. Oat exhibits polyploidy, the "heritable condition of possessing more than two complete sets of chromosomes" (Comai, 2005). The basic chromosome number (x) is 7 (Rajhathy & Thomas, 1974). Indeed, three genetic classes of oat exist: Diploid (2x=14) which includes *A. pilosa, A. ventricosa, A. prostrata, A. damascena, A. longiglumis, A. canariensis, A. wiestii, A. hirtula,* and *A. strigosa*; the tetraploids (4x=28), comprised of *A. barbata, A. vaviloviana, A. abyssinica, A. magna,* and *A. murphyi*; and hexaploids (6x=42), comprised of *A. fatua, A. sterilis, A. byzantina,* and *A. sativa*, the latter from which all cultivars today are developed (Rajhathy & Thomas, 1974).

Although the earliest forms of oat are believed to be the diploids, the tetraploids and hexaploids are generally believed to have diverged from the hybridization of various diploids to result in new combinations of two or more diploid genomes (A, B, C, and D). This resulted in more complex combinations of the A, C, or D genomes, typically to result in heterosis; speciation via polyploidy in plants is not uncommon, and it has been estimated that 15% to 35% of plants have evolved this way (Wood *et al*., 2009). Tetraploids are typically AADD or AACC (*A. magna*), but AABB also exist (*A. barbata*). These are segmental allopolyploids of hybrids of two partly homologous genomes and are bivalent in chromosome pairing. These more complex oat genomes are similar to diploids in morphology, karyotype, and biochemical properties. To date, it is unsure if the B genome is a distinct fourth genome since it is partially homologous to A and will not be discussed in this scope. While *A. magna* and *A. murphyi* are similar in morphology and hybridization of the two is possible, definite sterility exists amongst their offspring. Hybridization can occur between other tetraploid hybrids as well; when successfully hybridized, F2 generations are fertile but often regress to 2n or 4n genotype.

The hexaploids (AACCDD) are well-suited for backcrossing for desirable traits, and their interspecie fertility grants their relative ease of cultivation. The precise progenitors of this class of allopolyploids is unclear; however, with regards to karyotype, pairing, morphology, and

geographical origins, *A. canariensis* and *A. strigosa* diploids are partially homologous with their A-genome, while *A. ventricosa* shows some homology with the C-genome. Furthermore, *A. magna* x *A. murphyi* crosses result in one shared chromosome with hexaploids. Conversely, *A. damascene* (diploid) exhibits no hybridization with *A. sativa*.

The genetic duplication characteristic of hexaploids acts as a buffer for mutation. They are tolerant to chromosome loss, and some chromosomal homology exists between chromosomes in *A. sativa*; this enables compensation to occur in nullisomes, and these mutants are vigorous and fertile (Coffman, 1977). Despite this evidence of duplication, during meiosis, multivalents are uncommon and hexaploids typically form 21 bivalents. Wild hexaploid species are free-threshing (seeds separate by articulation at maturity), and have extended seed dormancy; contrary to this, the cultivars retain their seeds well and maturation is comparable to wheat. These agronomic characteristics as well as nutritional elements led to the selection of *A. sativa* for cultivar development, particularly for food use (Coffman, 1977).

2.3. Oat Oil

Oat is a somewhat unique cereal for several reasons. It is high in bran, soluble fibre (β-glucans), contains avenanthramides (antioxidants) and its storage protein is globulin (Deshpande & Damodaran, 1990). It has a relatively high sulfur requirement amongst cereals, but is quite hardy as it is tolerant to moisture levels above and temperature ranges below those ideal for many cereals (Agriculture Saskatchewan, 2012; Coffman, 1977). Furthermore, it has the highest oil content of cereals reaching 16% of the dry weight (dwt) which can be highly heritable (Holland *et al*., 2001; Schrickel, 1986).

Oat seed, as a cereal, mostly stores the carbon as starch or protein in the endosperm, whereas oil stores are largely found in the embryo (Ekman *et al*., 2008). Mature oat has the most varied neutral lipids of cereal cultivars; although lipids are primarily found in the bran and germ, the highest concentration of oil bodies (up to 8% of total oil content) are transiently deposited into the sub-aleurone cells of the endosperm (Schrickel, 1986; Banas *et al*., 2007; Heneen *et al*., 2008). This partitioning of the oil into the same kernel endosperm cells where typically only starch accumulates is rare, but has been previously observed in monocots (Alexander & Seif, 1963; Oo *et al*., 1985). Furthermore, oat is unique in that the oil is synthesized and accumulated relatively early in the development of the seed, while starch develops throughout the course of the seed development, although mechanisms are not yet fully understood (Ekman *et al*., 2008).

What is more, oat contains some minor quantities of oxygenated UFA variants mostly derived from PUFA precursors, a HFA and several epoxy FAs, in addition to the more common PUFAs previously mentioned (Leonova *et al*., 2008; Figure 3).

In this thesis, the cereal's exceptionally high total oil content and its quality are of interest. Of the total fatty acid content in oat, the pro-inflammatory LA can be as high as 43%; in contrast, the ALA (that can attenuate the potentially negative effects of LA) has only been found in amounts as high as 2% (Leonova *et al*., 2008; Table 1).

In cultivated *A. sativa*-derived cultivars, highest LA quantities were found in Allyur (43.1%), Fakir (43.1%), and Astor (41.5%). Some other notes of interest include a negative correlation comparing polar lipid (PL) to triacylglycerol (TAG) as well as to 18:1-9*c*, but PL was positively correlated with 18:2-9*c*,12*c* content in hexaploids (Leonova *et al*., 2008). Alleles for high oil content in *A. sativa* and *A. sterilis* were found to be complementary. In wild oats, LA content is higher than oleic acid (OA) only in tetraploids, although this genetic class also had lower overall oil content (Leonova *et al*., 2008).

Improving oat as a source of ω-3 and ω-6 fatty acids for human health necessitates deeper genetic insight of the cereal on which breeders and producers can capitalize. One challenge is that the oat genome has not yet been fully annotated. So to date, attention must be given to the genetic sequences underlying the ω-3 and ω-6 fatty acid biosynthesis in oat. The focus of this thesis is to elucidate all potential genes responsible for encoding enzymes similar to fatty acid desaturases (FAD-like) which most likely confer catalytic mechanisms responsible for PUFA synthesis in oat: *Avena sativa* Δ12 fatty acid desaturase (AsFAD2), and *Avena sativa* Δ15 fatty acid desaturase (AsFAD3).

2.4. Main Functions of PUFAs

As discussed, PUFAs from plants are indeed beneficial to human health. Yet, PUFAs in the plant cell membrane and the ability of plants to control and adjust their presence and composition are very pragmatic to their survival in their changing environments. The biosynthetic pathways of the vast variety of lipids or derivatives found in plants, as well as their functions, can be complex. Plant lipid fate within the organism may be essential to its survival, can be multifaceted, or may even be unknown under the context in which they have been studied to date.

Table 1. Oat Seed Fatty Acid Compositions of Various Cultivars (Percent of Total Fatty Acid) (Adapted from Leonova *et al*., 2008)

Cultivar	14:0	16:0	16:1	18:0	18:1-9	18:1-11	18:2	18:3	20:1	20:x	7-OH 18:2	15-OH 18:2	Epoxy 18:x
Astor	0.2	16.4	0.3	1.3	34.4	1.0	41.5	1.6	0.7	0.2	0.0	2.4	0.4
Lodi	0.2	16.4	0.3	1.4	34.5	1.0	40.9	1.6	0.7	0.2	0.1	2.3	0.5
Borrus	0.3	16.2	0.2	1.3	36.5	1.0	39.1	1.6	0.8	0.2	0.1	6.1	0.3
Spear	0.2	16.0	0.2	1.5	34.6	1.2	40.5	1.7	1.0	0.3	0.1	3.8	0.6
Wright	0.3	17.5	0.3	1.5	39.9	1.2	35.6	1.2	1.0	0.3	0.1	2.2	0.4
Fakir	0.2	15.1	0.1	1.3	35.1	1.1	43.1	1.5	0.5	0.1	0.1	3.0	0.4
Allyur	0.2	17.4	0.4	1.2	31.4	1.3	43.1	2.1	0.8	0.2	0.1	3.2	0.4
Argamak	0.2	16.0	0.1	1.6	36.2	1.0	40.8	1.3	0.8	0.3	0.1	3.1	0.3
Torch	0.2	16.1	0.3	1.7	36.7	0.9	39	1.3	0.7	0.3	0.1	1.9	0.3
Kynon	0.2	13.9	0.1	0.8	40.4	1.0	38.3	1.4	0.9	0.3	0.1	3.1	0.4
mean	0.2	15.9	0.2	1.4	35.8	1.1	40.4	1.5	0.8	0.2	0.1	3.1	0.4

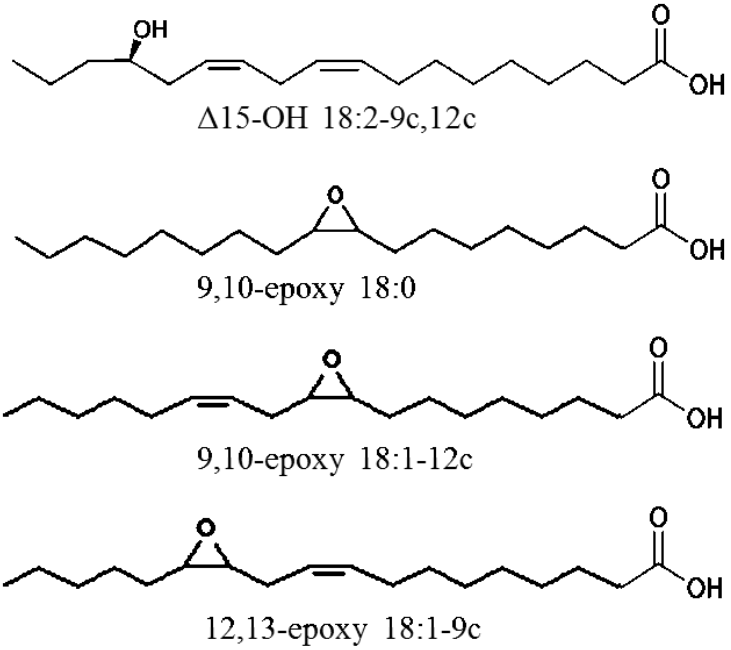

Figure 3. The minor oxygenated oat UFAs (Adapted from Christie, 2012b & Buist, 2004).

Of the diverse functions contributed to a plant by these complex molecules, there are some outstanding and generally accepted characteristics (van Meer *et al*., 2008). Generally, lipids fulfill three main roles in the organism: for energy stores or as physical material reserves for further molecular structure biogenesis, mostly as neutral TAGs or steryl esters; as signal molecules and messengers of molecular recognition/signal transduction across membranes; and as an amphiphatic lipid-derived barrier between the cell contents and the external environment, while allowing for aggregation or dispersion of specific proteins integrated in the membrane itself (van Meer *et al*., 2008). Through these three main functional contributions within the cell, lipids offer vital adaptability for the organism's survival.

The fluid characteristic of the cell membrane allows for proper aggregation or dispersion of membrane-bound proteins as mentioned, facilitating the lateral movement for the appropriate healthy-state receptor-ligand reactions to occur (Helmreich, 2003). Other activities directly impacted by the physical state of a membrane include translocation of small molecules and ion channel function (Sukharev, 1999), receptor-associated protein kinases (Wood, 1999) and sensor proteins (Tokishita & Mizuno, 1994).

The cell membrane is the primary site of environmentally-induced stress damage, since it is the separating barrier between the cell and the environment; as such, it is crucial for an organism to have the capacity to adjust membrane composition to adapt to the stress effects (Rodriguez-Vargas *et al*., 2007). More specifically, the membrane lipids create a dynamic barrier that, depending on the environmental temperature and the membrane lipid composition, can transition between solid (ordered) or fluid (disordered) phases, or dynamically exhibit two fluid phases (liquid-ordered and liquid-disordered) simultaneously (van Meer *et al*., 2008; Laroche *et al*., 2001). The membrane property changes are accomplished by adjusting the degree of movement as well as spatial positioning of each lipid comprising the membrane. The ability of lipid movement within the membrane as well as their positioning result largely from the physical structure of each fatty acid specie (and their relative abundances) from which the membrane is composed (Murata & Los, 1998), although the actual phase transition temperatures may vary depending on the ambient temperatures imposed on the cell (Laroche *et al*., 2001). There is evidence suggesting membrane lipid unsaturation directly affects membrane fluidity (Tasaka *et al*., 1996). These altered membrane lipid profiles are thus largely the aggregate sum of physically-modified end-product fatty acids that result from a lipid-modifying, membrane-bound

enzyme (or enzymes) acting upon one or several lipid substrate precursors, whose activity is induced by environmental stresses. Often, the stressors are temperatures lower than what is ideal.

This adaptation of various plant tissues to tolerate temperature extremes has been known for decades and thoroughly reviewed (Lyons & Raison, 1970; Graham & Patterson, 1982; Nishida & Murata, 1996; Murata & Los, 1998; Browse & Xin, 2001; Los & Murata, 2004). Without the ability to adapt to reduced temperatures, the cell membrane is prone to physical damage due to the ice crystals formed (Morris *et al*., 1988) or due to equilibration from exposure to the hyperosmotic condition outside the cell (Wolfe & Bryant, 1999), or biochemical damage of oxidative stress resulting from thawing (Hermes-Lima & Storey, 1993). Preventing the membrane from rupturing while maintaining its fluidity is critical for ensuring biochemical processes can ensue as normal and thereby enabling the survival of the organism as a whole.

As plants are obligated to adapt to the sometimes unpredictable temperatures inflicted by nature, mechanisms have arisen to induce a cascade of events to result in modified membrane lipid profiles (Murata & Los, 1998; Los & Murata, 2004). Particularly, the ability to increase the degree of unsaturated fatty acids of the membranes at lower temperatures has evolved in order to maintain fluidity and counter the otherwise normal tendency of the membrane to transition phases and lose fluidity (Tasaka *et al*., 1996). The mechanisms of cold-induced membrane lipid unsaturation are not thoroughly understood, but there is insight into the area. To date, it is believed that a membrane phase that increases membrane rigidification alters the physical conformation of membrane proteins, triggering transcription of one or more of three classes of cold-inducible genes (Inaba *et al*., 2003). It is believed that these triggers activate transcription of various genes involved with sulfate transport, histidine kinase (involved with cross-membrane signal transduction), RNA helicases, and RNA-binding proteins (potentially involved with transport or localization, or post-transcriptional regulation) which catalyze increased fatty acid desaturase transcription and/or activity (Inaba *et al*., 2003). Just as the diversity of the structures and functions of membrane lipids contribute to their function in the cell, so too do their abundance and proportions.

The plant seed is a self-contained package assembled to bring all its genetic material from one generation to the next, with the necessary nutrients for this to occur. Once germination begins, the nutrient stores of the seed are diminished as they are redirected to the growing cotyledons, until the plant has established the ability to photosynthesize (Ekman *et al*., 2008).

Storage forms of carbon include protein, starch and oil; TAGs, of which oil is mostly comprised, are created during seed development as sucrose is directed from the leaves (Ekman *et al*., 2008). The physiological demands specific to the plant define the lipid profile.

2.5. Biosynthesis of PUFAs: Fatty Acid Desaturation

FADs belong to a unique sub-category of oxygenases, one of two classes of enzymes that can activate atmospheric dioxygen (O_2) to catalyze one of several possible reactions (the other type, oxidase, is outside of the scope of this study) (Bugg, 2003). Typically, mono- or di-oxygenases result in the addition of one or two oxygen atoms into the catalytic product, respectively (Bugg, 2003). Similarly to oxygenases, desaturases involve the abstraction of hydrogen from a fatty acid substrate; yet, in contrast, desaturases do not incorporate oxygen into the product but rather create a double bond from the single bond precursor (Brash *et al*., 2012; Buist, 2004). Functionally, FADs introduce a double bond into an acyl chain, involving the reduction of a molecule of O_2 with products being a FA with a new double bond, and water. At each double bond created, the first hydrogen abstraction occurs at the carbon atom closer to the carboxyl end; this is also the rate-limiting step of desaturation (Brash *et al*., 2012). The resulting double bond is typically *cis* (*c*) conformation, although small amounts of *trans* (*t*) conformation can occur (Shanklin & Cahoon, 1998; Brash *et al*., 2012). The general reaction is illustrated in Figure 4A. FADs, in general, can be soluble or integral membrane enzymes; membrane-bound FADs may be localized in the endoplasmic reticulum (ER) or plastid (Shanklin & Cahoon, 1998), although the main site of lipid biosynthesis occurs by membrane-bound enzymes in the ER (Bell *et al*., 1981).

The O_2–dependent fatty acid desaturation or hydroxylation reaction is dependent upon two main factors (Buist, 2004). First, the orientation of the β carbon-hydrogen bond(s) (relative to the half-filled orbital of the carbon radical of the substrate) as indicated by white arrows in Figure 4, and secondly by the positioning of the diiron hydroxyl relative to the two carbons of the substrate on which the enzyme will act (Figure 4, A & B). Therefore, these O_2–dependant reactions are generally believed to be regio- and stereo-specific, respectively, which probably accounts for their highly-specific (and sometimes bifunctional) nature. A third factor, the ligand and thermochemical environment of the diiron complex, has also been theorized to affect the reaction completion (Buist, 2004).

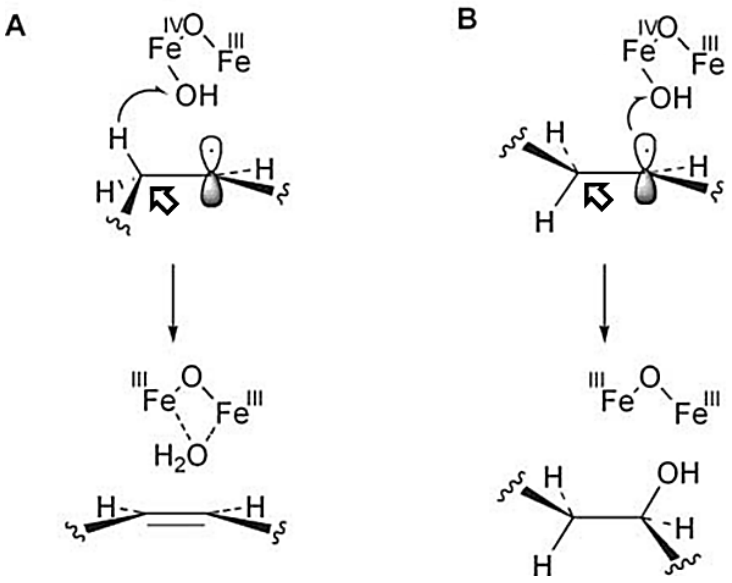

Figure 4. A general mechanism for fatty acid desaturation (A) and hydroxylation (B). These generally-accepted reaction mechanisms illustrate the slight but relatively stringent differences of the outcomes of the oxygen-bound diiron complex of the FAD or FAH enzyme relative to the specific position and orientation of the FA substrate. The interaction of the half-filled orbital of a carbon-centered radical intermediate is indicated by the half arrow. Roman numerals indicate oxidation state (Adapted from Buist, 2004).

In higher organisms such as oat, double bonds of long-chain (16C to 20C) FAs are established aerobically via the action of FADs (Shanklin & Cahoon, 1998). This method of desaturation is more energetically costly than the anaerobic method (Bloch, 1969) facilitated by some lower organisms such as *E. coli*. This evolution of desaturation is thought to have occurred after the transition from anaerobic fermentation to the more efficient aerobic respiration had already occurred which, overall, sanctioned more available energy for desaturation as well as other energetically-costly processes (Shanklin & Cahoon, 1998). Each desaturation event to produce a new double bond requires two electrons donated from a reducing source; for ER-bound FADs, this source is NADH, and for plastidial FADs, NADPH (Shanklin & Cahoon, 1998). In both cases, the electron pairs are first transferred from the donor source to a carrier protein via a flavoprotein transfer step. For the ER proteins, the flavoprotein is cytochrome b_5 reductase, while the plastid employs ferredoxin-$NADP^+$ oxidoreductase; the electron carrier proteins in the ER and plastid are cytochrome b_5 and ferredoxin, respectively (Shanklin &

Cahoon, 1998). In lower organisms, the function of FADs is likely to allow for responsiveness to environmental conditions, to allow adjustment of membrane fluidity and thus enhance their adaptability and evolutionary potential.

Several functional and genetic characteristics are conserved between FAD2s and FAD3s (Browse *et al*., 1993; van de Loo, 1995; Broun *et al.*, 1998b; Napier, 2007). Membrane-bound FADs are present not only in higher plants, but also fungi, mammals, insects, and cyanobacteria (Shanklin *et al*., 1994). The high homology between FAD2s and FAD3s has been known for quite some time. In 1990, the *Δ*12-oleate desaturase gene from the cyanobacterium *Synechocystis* PCC6803 was characterized in hopes of introducing better cold-tolerance to plants (Wada *et al.*, 1990). Not long after, Arondel *et al.* deduced the amino acid sequence of the product of a *FAD3* from *Brassica napus* using the homologous cDNA of a closely related organism, *Arabidopsis thaliana* (1992). The following year, the highly homologous relationship between the *FADs* was documented by Browse *et al*. (1993), not only uncovering homology between FAD-producing genes, but high genetic conservation across kingdoms.

In 1994, a study was conducted by Shanklin *et al*. comparing the peptide sequence similarities of several eukaryotic FADs, each demonstrating enzymatic activity at one of the *Δ*6, *Δ*9, *Δ*12 and ω-3 positions of 18-carbon fatty acids. Aside from the obvious desaturase activity of each membrane-bound FAD, the likelihood of genetic homology was further suggested by the enzymatic catalytic commonalities of each: the requirement of iron for catalytic activity, the catalytic inhibition following the addition of metal chelators, their stereospecificity, and finally the kinetic isotope effects necessary to cleave C-H bonds. Moreover, O_2 was required for all these enzymes to activate.

Iron (Fe) is an ideal catalyst with these enzymes, as it is a Group 8 transition metal: its oxidation states span -2 to +6, it is reactive with both oxygen and water and can thus give rise to cations (IUPAC, 2013). The characteristics of shared catalytic sites led to further indications of homology between FADs, particularly when compared with the Mossbauer absorption spectrum of the only purified FAD, *Δ*9-stearoyl-CoA-desaturase from rat liver (Strittmatter *et al*., 1974). The spectrum of such a FAD enzyme exhibits the pattern of that of an oxo-bridged diiron cluster, as identified in hemerythrin, ribonucleotide reductase, and other model compounds by Sanders-Loehr *et al*. (1989). Chosen for their catalytic characteristics, bacterially-produced, oxo-bridged diiron cluster-containing hydroxylases with unknown structures were compared to this: one from

an alkane hydroxylase from *Pseudomonas (P.) oleovorans*, and one from the *P. putida* methane monoxygenase with hydroxylase activity (Shanklin *et al*., 1994). A third enzyme exhibiting this catalytic centre, stearoyl-acyl carrier protein *Δ*9 desaturase originating from plants was also compared. Enzyme activity of all three enzymes was found to be O_2-activated, with these oxo-bridged diiron clusters (Figure 4) as the catalytic centre, adding evidence of divergence from one ancestral origin and further suggesting that not only FADs but FAHs are highly conserved and homologous (Shanklin *et al*., 1994). Later, Shanklin and Cahoon compared the primary structures of known diiron-binding proteins which interact with O_2, such as methemerythrin, R2, and a subunit of ribonucleotide reductase, disclosing a highly conserved motif within a four-*α*-helix bundle, $[(D/E)X_2H]_2$ (1998). After searching for homologs of this sequence in GenBank, several enzymes proved to contain this sequence, and due to the nature of the UFA-producing enzymes in which they were found, this sequence was proposed to be the consensus diiron-binding motif (Shanklin & Cahoon, 1998).

Prior to determining the amino acid sequence of these enzymes, Shanklin *et al*. identified conserved regions between all FADs and FAHs known at the time; the highest degree of similarity, 85%, was found amongst some *Δ*15FADs of plants (1994). Three specific histidine (HIS)-rich "boxes," in sum containing eight conserved HIS residues, were identified in all proteins, with the following sequences: $HX_{(3\text{ or }4)}H$, $HX_{(2\text{ or }3)}HH$, and $HX_{(2\text{ or }3)}HH$ (where numbers represent number of undefined or variable amino acids [X] between HIS residues; slight variability can occur depending on source organism). The HIS-boxes, to date, are conserved within each enzyme class as well; for example, all of the first HIS-box in FAD2s will have the pattern H(XY)HH. There was also high conservation of interval sequence length separating the three boxes. When the HIS residues were mutated in the *Δ*9-oleate desaturase, loss of enzymatic activity resulted, likely due to the inability of the HIS-lacking catalytic centre to properly bind ferric iron (Los & Murata, 2004). And, accounting for the homology between FADs and FAHs, it is reasonable to postulate that these conserved motifs are essential for desaturase as well as hydroxylase activity (Figure 4).

To investigate structural orientation of FADs within the cell, hydropathy analysis was performed on two oxo-bridged diiron membrane proteins, an alkane hydroxylase and a xylene monooxygenase (Shanklin *et al*., 1994). This identified specific hydrophilic regions (containing the HIS boxes) interrupted by two hydrophobic regions in the amino acid sequence. The

hydrophobic regions were long enough to span a membrane, strongly suggesting a membrane-bound characteristic, and the HIS boxes are believed to be on the cytosolic side of the membrane for fatty acid substrate modification. These characteristics were apparent in all FADs in the study. In 2001, Dyer and Mullen confirmed that both the C-termini and N-termini of FAD2s and FAD3s are oriented on the cytosolic side of the ER membrane. Soon after, McCartney *et al*. determined that both of these FAD types are co-translationally inserted into the ER membrane by means of a signal recognition particle (SRP)-mediated mechanism (2004). A study by McCartney *et al*. surveyed the C-termini of various membrane-bound enzymes, including FAD2s and FAD3s (2003). Both FAD2s and FAD3s contain conserved motifs, although unique depending on which position the FAD acts upon. These conserved motifs are both pentapeptide sequences of the C-termini: an aromatic amino acid-containing -YNNKL motif in FAD2, and a dilysine ER retrieval motif, -KSKIN, in FAD3. The localization of these FADs in the ER membrane is facilitated by the recognition of the retrieval motif pentapeptide sequences by post-ER compartments, enabling co-translational integration of the enzyme into the membrane. As McCartney *et al*. describe, two molecular targeting signals are required (2003). One signal sorts the molecules into the ER, while the second one retains or retrieves proteins in the ER from other pathway compartments. Mutation of these conserved pentapeptide sequences resulted in less efficient localization of the enzymes at the membranes, and thus reduced enzyme activity. Meesapyodsuk *et al.* confirmed the catalytic necessity of two conserved amino acid residues relative to the HIS boxes for different desaturation activities: two residues preceding the first HIS box, and ten residues in front of the second HIS box (2007). Meesapyodsuk *et al.* also found C-termini sequences to be significant in regioselectivity of desaturases, as ratios of Δ12 to Δ15 desaturated C18 FAs were affected after the adjustment of the C-termini (2007). The abundant evidence suggesting the high homology and close evolutionary relationship between FAD2s, FAD3s, and FAHs, may be imperative when investigating oat genes involved in PUFA biosynthesis.

2.6. Biosynthesis of Epoxy & Hydroxy Fatty Acids

The enzymes responsible for synthesizing HFAs and epoxy FAs are believed to be divergent of a FAD2 progenitor, and utilize similar FA substrates as those of FADs (van de Loo *et al*., 1995; Broun *et al*., 1998a). Both FA epoxygenases and hydroxylases are believed to be extraplastidial and localized in the ER membrane of the plant, catalyzing substrate to product

reactions on FA substrate subcomponents of phosphatidylcholine (PC), although there is variation in their catalytic mechanisms. Both types of UFAs are mostly found in the seed, in contrast to many PUFAs which can be found throughout various tissues.

To date, three distinct biosynthetic pathways have been identified for the biosynthesis of epoxy FAs, although they all replace a double bond of a FA substrate with an epoxy group. One pathway catalyzes this transformation via a FAD2-like epoxygenase (Lee *et al*., 1998), while another similar pathway achieves the same end-product but via a p450-like epoxygenase (Cahoon *et al*., 2002). A third epoxygenation pathway catalyzed by the activity of a peroxygenase was more recently confirmed (Meesapyodsuk & Qiu, 2011). As the biosynthesis of epoxy FA in oat has been elucidated, it is outside the scope of this study (Meesapyodsuk & Qiu, 2011).

In the context of cloning genes related to PUFA biosynthesis, oat offers a minor, unique opportunity to confirm a new FAH. As oat contains several oxygenated UFAs (Leonova *et al*., 2008), aside from the FADs in this study and the epoxy FA-producing peroxygenase, there remains only one unknown PUFA-related oat gene (encoding for another UFA-producing enzyme) to characterize : *Δ*15 fatty acid hydroxylase (FAH15). Moreover, it is the only known source of avenoleic acid (15-OH 18:2-9*c*,12*c*; 15HFA) (Hamberg & Hamberg, 1996). In cultivated *A. sativa*-derived cultivars, highest avenoleic acid content was uncovered in Borrus (6.1%), Spear (3.8%), and Allyur (3.2%). Furthermore, in wild and cultivated oat, locations of avenoleic acid included 12.7% and 9.8% in phospholipid, 1.2% and 1.0% in 1,3-DAG, and 0.4% and 2.4% in TAG1, respectively. Aside from these neutral lipid fractions, all other locations were comprised of less than 1.0% avenoleic acid. Although epoxy fatty acids have been UFAs of interest in the past, analyses confirmed significantly higher levels of 15-OH 18:2-9c,12c than epoxy fatty acids (Meesapyodsuk & Qiu, 2011; Hamberg & Hamberg, 1996; Ishimaru & Yamazaki, 1977; Leonova *et al*., 2008). Cultivars typically had lower OA than LA, yet had lower 15HFA content, suggesting the hydroxylase in wild oat has higher activity than in cultivars.

15HFA, although present in very small quantities in the oat seed, may impose undesirable physiological effects once ingested (Leonova *et al*., 2008). Hydroxy fatty acids are known to have laxative effects and induce uterus contraction via interaction with prostaglandin EP_3 receptors, as well as cause abnormal myoelectric patterns in mammalian small intestine resulting in altered motility (Tunaru *et al*., 2012; Mathias *et al*., 1978). Minimizing or eliminating this

UFA would enhance the healthfulness of oat even further. Because the hydroxylase responsible for producing this unusual fatty acid is hypothesized to be divergent of and highly homologous to a FAD (van de Loo *et al*., 1995; Hamberg *et al*., 1998), this study will also attempt to clone and functionally characterize the putative *Δ*15 hydroxylase, FAH15.

The precise biosynthesis behind this HFA production in plants is unknown, although plant FA hydroxylases are believed to have diverged from a FAD2 (van de Loo *et al*., 1995). In contrast to the PUFAs and epoxy FAs, though, large quantities of the HFA in oat have been found on a digalactosyldiacylglycerol (DGDG) rather than PC (Hamberg *et al*., 1998; Figure 5). This 15HFA was present in an estolide at the *sn*-2 position of the DGDG; this makes the oat HFA somewhat unique, and even more unusual is their presence as an oxygenated FA in a galactolipid. This combination is rare not only in plants but in general, and has only been observed previously in algae (Jiang & Gerwick, 1990; Jiang & Gerwick, 1991).

van de Loo *et al*. (1995) identified the first *Δ*12 fatty acid hydroxylase (FAH12) in *Ricinus communis* L. (castor bean) that has high homology to a FAD2 from *Arabidopsis*. As the lipid content of castor bean is nearly all 12-hydroxyoctadec-cis-9-enoic acid (ricinoleic acid; 12-OH 18:1-9) which is derived from oleic acid substrate, and FAD2 introduces a double bond at the *Δ*12 position of oleic acid, it was hypothesized that the FAH12 was likely derived from FAD2 (van de Loo *et al*., 1995; Figure 6). After transformation of *Nicotiana tabacum* – to which ricinoleic acid is not endogenous – with the FAH12 clone, GC-MS confirmed production and accumulation of ricinoleic acid in the *Nicotiana tabacum* seeds.

Furthermore, a FAH12 of non-plant origin was cloned and functionally characterized in *Claviceps purpurea* (Meesapysodsuk & Qiu, 2008). By isolating RNA from tissue in which the FAH was known to be present, cDNA was derived for PCR amplification using highly conserved sequences of fungal FADs for consensus sequences (both *Δ*12 and *Δ*15); likewise, primers were developed, and homology of the successful clones with other plant and fungal FADs was validated via BLASTp database searches (Meesapyodsuk & Qiu, 2008). Furthermore, they confirmed function of this previously-uncharacterized *FAH12* in yeast via the identification of its product, as the product was non-endogenous to the new host.

A study by Broun *et al*. strongly supports the homology of FADs and FAHs (1998a). Comparing the amino acid sequences of FAD2s of several species revealed seven critical conserved amino acid residues; in the FAHs of the same position, some of these residues were

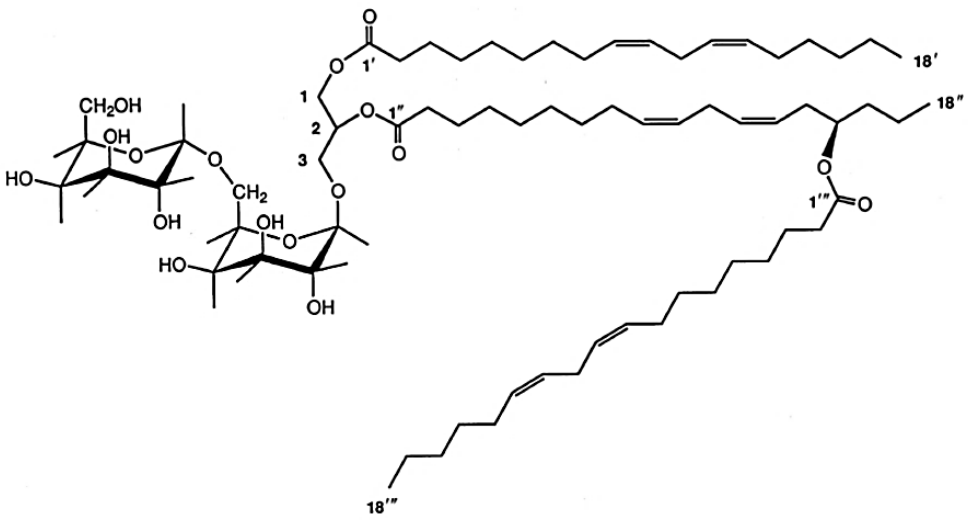

Figure 5. The sn-2, *Δ*15-OH 18:2-9*c*,12*c* estolide-containing DGDG (1-[(9′*Z*),(12′*Z*)-octadecadienoyl]-2-[(15″R)-{(9‴*Z*),(12‴*Z*)-octadecadienoyloxy}-(9″*Z*),(12″*Z*)-octadecadienoyl]-3-(*α*-D-galactopyranosyl-1-6-*β*-D-galactopyranosyl)-glycerol) (Adapted from Hamberg *et al*., 1998).

divergent. The FAH12 of *L. fendleri* showed 81% identity with the FAD2 of *A. thaliana*, and 71% identity with the FAH12 of *R. communis.* Using site-directed mutagenesis, the seven residues in the FAH12 of *L. fendleri* were replaced with the corresponding equivalent residues from FAD2 of *A. thaliana*, and vice versa. Both mutated enzymes showed dual functionality, both desaturating and hydroxylating oleic acid, and verifying the highly homologous nature of the enzymes. By focusing on those closest to the catalytic HIS sites, the conserved residues were further narrowed down to discover only six of these residues were required to convert the FAD to a FAH, and only four needed for conversion of the FAH to a FAD. The homology of these enzyme types is thought to be paralleled in FADs and FAHs with activity at other molecular positions. Although the majority of these studies focuses on enzymes having activity on the substrate *Δ*12 position, the theory will be applied to *Avena spp.* enzymes putatively thought to have activity on the *Δ*12 and *Δ*15 positions of substrates, as illustrated in Figure 7.

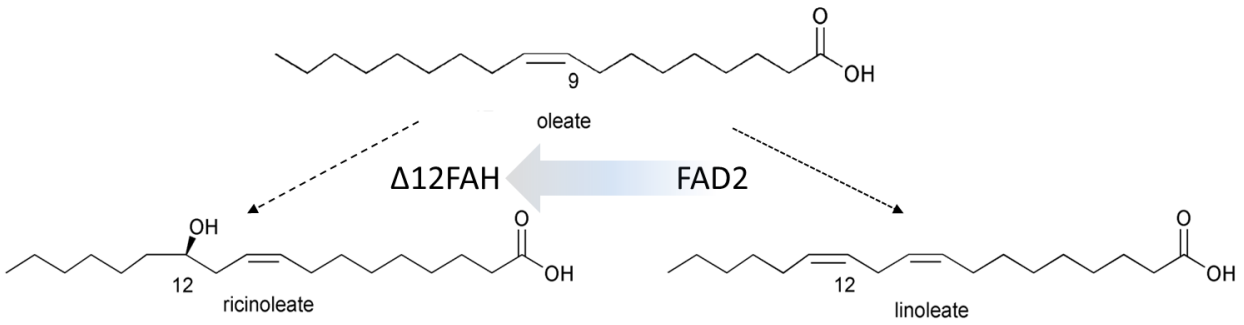

Figure 6. The conversion of oleic acid to either linoleic acid, by a FAD2, or to ricinoleic acid (in castor bean) by a FAD2-divergent hydroxylase, Δ12FAH. The dashed and dotted arrows show the known pathways through which substrate is converted to product, while the solid arrow indicates the evolutionary relationship between the two enzymes (Adapted from van de Loo *et al*., 1995; Buist, 2004).

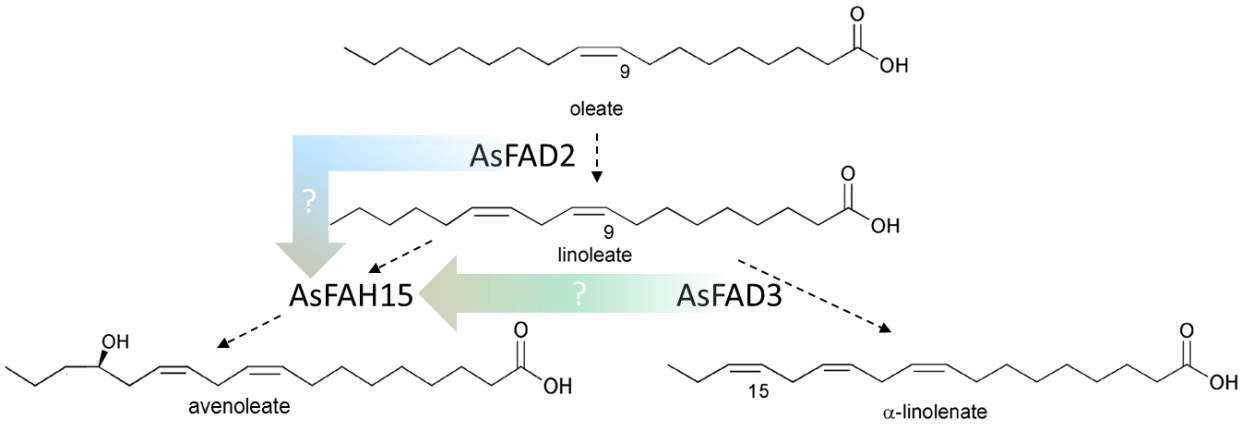

Figure 7. The putative biosynthetic pathway of avenoleate (*Δ*15-OH 18:2-9*c*,12*c*) in oat seed. The dashed arrows show the putative pathways through which oleic acid substrate is converted to either Δ15-OH 18:2-9*c*,12*c* or 18:3-9*c*,12*c*,15*c*, while the solid arrows with question marks indicate potential divergence of the oat *Δ*15FAH from either a FAD2 or FAD3 progenitor. As=*Avena sativa*

Other requirements, in addition to those suggested previously, may have effects on PUFA and UFA production and on their accumulation (Napier, 2007; Lu *et al*., 2009). Since cytochrome b_5 is the preferred electron donor for many plant FA-modifying enzymes, and thus cytochrome b_5 reductase is required, expression of this reductase in the transgenic plant is also crucial – particularly for those expressing a hydroxylase (Carlsson *et al*., 2011). The high accumulation of the HFA ricinoleic acid in castor bean, derived from oleic acid and with little to no accumulation at its site of synthesis at the membrane, further suggests that there are additional mechanisms required in addition to the modifying enzyme (Napier, 2007). In *Arabidopsis*, a study by Lu *et al*. distinguished a gene whose product is phosphatidylcholine:diacylglycerol cholinephosphotransferase (PDCT), an enzyme that regulates TAG composition via the transfer of 18:1 to PC for modification, then brings the newly desaturated FAs for TAG synthesis (2009). PDCT is needed to transfer the PC head group from PC to DAG then to TAG, and once eliminated, lack of PDCT reduced seed TAG by 40% (Lu *et al*., 2009). Thus, presence of a functional PDCT can be crucial for significant accumulation & assembly of UFAs into TAGs.

Abiotic factors may also be significant for the successful accumulation of PUFA and UFAs in seeds. A study by Los and Murata (1998) demonstrated noticeable differences in the presence and concentrations of different unsaturated FAs in *A. thaliana* with changes in temperatures; a lower temperature triggered more production of desaturated FAs and to higher degrees of desaturation. A higher level of desaturation maintains membrane fluidity at lower temperatures (Los & Murata, 1998). Although the study was focused on desaturase activity, it suggests that if the function of the hydroxylase in developing tissue is fully understood, then control over the catalyst of its production may be achieved in a manner similar to that of desaturases.

Once the genes involved in the biosynthesis of PUFAs in oat have been identified, oat breeders can exploit these as targets for marker-assisted selection (MAS) in breeding programs. Selecting for or against specific PUFA-related traits by targeting these GOIs will enhance the efficiency by which new, healthier oat cultivars can be established. The practicality of this concept has been successfully achieved and reviewed (Xu & Crouch, 2008; Kumar *et al*., 2009). This will contribute to both the accessibility of healthier food options, and to enhancing the Canadian agriculture economy.

3. RESEARCH STUDIES

3.1. Study 1: Oat Fatty Acid Survey

3.1.1. Abstract

In attempts to expand the genetic diversity available for oat breeding efforts aiming to optimize oat oil for human health, the FA composition of oat has been examined previously. However, these studies typically neglect UFAs such as HFAs and epoxy FAs; these UFAs are naturally present in very small amounts. Epoxy FAs are prone to degradation via the acidic conditions of the typical transmethylation process, employed previously. A broken epoxy group could result in two free hydroxyl groups on consecutive carbons; artifacts of the transmethylation process can overestimate total HFA and underestimate total epoxy FA content. To determine presence, identity, and relative quantity of PUFAs and UFAs as well as more common FAs for establishing the complete FA profile, oat seed FAs were extracted from CDC Dancer cultivar and transmethylated with three different methods: a typical acidic method used 1% sulfuric methanol for comparison to the second basic method which used sodium methoxide, and the third method employed diazomethane to allow identification of free fatty acids (FFAs) only. To discriminate HFAs from the pool of oat seed FAs, trimethylsilyl (TMS) derivatization was also carried out on a duplicate of each sample. TMS treatment of HFA derivatizes any free hydroxyl group present on a FA through an etherification reaction (Langer, 1958; Christie, 2011); the derivatized molecule acquires a different overall polarity relative to its non-derivatized form, discernible by a shifted peak on the chromatogram output of the TMS-derivatized sample. Chromatograms were generated for each sample via gas chromatography (GC), and mass spectrometry assisted identification of UFAs via GC-MS. Additionally, the derivatized duplicates from both alkaline and acidic treatments can be compared to distinguish whether or not poly-hydroxyl transmethylation artifacts result. The comparisons showed that the epoxy FAs were indeed degraded in the acidic method resulting in an overestimation of HFAs in previous studies and inaccurate identification of a dihydroxy FA that was actually an artifact from the acidic conditions. The reliable alkaline-treated sample was used to quantify the oat seed FAs.

The major proportions of the total FAs were comprised of 18:2-9*c*,12*c*, 18:1-9*c*, and 16:0, in quantities of 37.3%, 31.9%, and 23.1%, respectively. The UFA were 2.35% and 0.68% for total epoxy FAs and 15-OH 18:2-9*c*,12*c*, respectively. The proportion of the main PUFA of interest in this study, 18:3-9*c*,12*c*,15*c* was present as 0.85% of total FAs. Quantities of all FAs here were in agreement with previous literature, except that 15HFA quantity was approximately 4-fold lower and epoxy FA quantity was more than 4-fold higher than mean values in literature.

3.1.2. Hypothesis

Analyses of oat seed FAs to date have overestimated HFA content and underestimated epoxy FA content due to the acidic transmethylation procedure used, as epoxy FAs are sensitive to acid and yield unnatural hydroxy groups once hydrolyzed from acidic conditions. Because of this, employing a basic transmethylation procedure will preserve all UFA integrity and thus give a more reliable overall FA profile of the mature seed, allowing accurate identification of the PUFAs and UFAs of interest to this study.

3.1.3. Experimental Approach

3.1.3.1. Oat Tissue Growth and Harvest

A paper filter was placed in the bottom of 2 gallon pots, and then filled with Sunshine LG3 peat growth mix. About 20 seeds were inserted 4 cm below the surface, and pots were watered with tap water 2-3 times per week, as needed. Water-soluble fertilizer (20-20-20 N-P-K) was mixed with water starting 10 days post-emergence, and added at a rate of 0.35g/L once per week. After 2 weeks, 30g of slow-release fertilizer (14-14-14 (N-P-K)) was spread over the surface of the growth medium of each pot. Within the growth chambers, a photoperiod of 18 hours was used, with a 22°C day temperature, and 16°C night temperature at ambient relative humidity.

Once tillering began, pots were weeded back to 6 plants per pot. Those plants removed were harvested for leaf, stem, and root tissue, placed immediately in 50mL Falcon tubes in liquid nitrogen for transport, and stored at -80°C. The remaining plants were allowed to grow to milky-stage seed; at each watering, tillers were cut at the crown level to allow the main culm to grow. Once milky-stage seeds were developed, hulls were removed and seeds immediately placed in a 50mL Falcon tube in liquid nitrogen for transport to -80°C for storage. Concurrently, leaf, stem, and root tissue were harvested and stored in the same fashion.

Seeds were germinated by placing seeds in between several folds of paper towel inside a petri dish. The paper was regularly dampened at room temperature to keep moist over 7 days, and stored in aluminum foil to keep dark.

3.1.3.2. Fatty Acid Analyses

Ten seeds were placed in a dichloromethane (CH2Cl2)-washed 15mL glass screw-top tube, and soaked in 6mL chloroform/methanol (2:1 v/v). After 15 minutes, the seeds were ground as fine as possible using a glass rod. The total sample and solution was centrifuged at 2500 rpm for 5 minutes, after which the total supernatant was transferred to a new CH2Cl2-washed 15mL glass tube. 2mL of 0.9% NaCl water was added, and again centrifuged at 2500 rpm for 5 minutes. The chloroform phase was extracted, and divided into three equal portions, each aliquoted into a new CH2Cl2-washed 15mL glass tube. The three aliquots were dried under a stream of N2 gas, and the protocols Total Fatty Acid – Basic method, Total Fatty Acid – Acidic method, and Free Fatty Acid methods were performed.

3.1.3.2.1. Total Fatty Acid – Basic method

FAs were methylated using a basic treatment to preserve the acid-sensitive epoxy groups of the epoxy FAs. To one N_2-dried sample, 2mL of 0.5M sodium methoxide was added. The sample was incubated at 50°C for 30 minutes, and then cooled on ice. The sample was then acidified with 6M glacial acetic acid to pH 3-4 dropwise with a Pasteur pipette. Then, 1mL of 0.9% NaCl water and 2mL of hexane was added; the tube was centrifuged at 2500rpm for 5 minutes. The hexane phase was transferred to a clean CH_2Cl_2-washed 15mL glass tube and set aside. 2mL hexane was added to the remaining water phase for a second extraction. This solution was centrifuged at 2500 rpm for another 5 minutes, and this separated hexane phase was combined with the first hexane phase and then dried under a stream of N_2 gas. 100µL was added to resolubilize the lipid sample, and this volume was divided into two clean insert-containing GC screw-top vials. One of these was used directly for GC analysis. The other was dried under a stream of N_2 gas, followed by addition of 50µL trimethylsilylating reagent (TMS), 30 minute incubation at 80°C, and then analyzed by GC-MS.

3.1.3.2.2. Total Fatty Acid – Acidic method

To another one of the N_2-dried samples, of 2mL of 1% (v/v) sulfuric methanol was added and allowed to sit at room temperature for 5 minutes. The sample was then incubated for 60 mins

at 80°C. The samples were cooled on ice before adding 1mL of 0.9%NaCl H_2O and 2mL hexane. The tubes were then vortexed and centrifuged for 5 mins at 2500 rpm. The upper phase was extracted with at 2mL glass pipette, placed in a new CH_2Cl_2-washed 15mL glass tube, and dried under nitrogen gas. 100µL of hexane was added to the dried sample, gently vortexed, after which 50µL from each sample was aliquoted in duplicate to insert-containing screw-top GC vials. Sample in one tube was analyzed directly via GC, while 50µL of TMS was added to the other, incubated at 80°C for 30 minutes, and analyzed via GC-MS.

3.1.3.2.3. Free Fatty Acid

To the final N_2-dried aliquot, 50µL methanol and 100µL diazomethane were added. The sample was incubated at room temperature for 5 minutes, then dried again under a stream of N_2-gas. After drying, 100 µL ethyl acetate was added; after resolubilizing the lipid sample, the volume was separated into two 50 µL aliquots, each in a clean insert-containing screw-top GC vial. One was analyzed directly via GC-MS, while the other was dried under N_2-gas. 50µL TMS was added, incubated at 80°C for 30 minutes, and then analyzed via GC-MS. A FA standard sample was analyzed with all GC and MS samples. The standard contained the following FAs: 14:0, 14:1, 15:0, 16:0, 16:1-9c, 17:0, 18:0, 18:1-9*c*, 18:1-11*c*, 18:2-9*c*,12*c*, 18:3-6*c*,9*c*,12*c*, 18:3-9*c*,12*c*,15*c*, 20:0, 20:1-5*c*, 20:1-8*c*, 20:1-11*c*, 20:2-11*c*,14*c*, 22:0, 22:1-13*c*, 24:0, 24:1-15*c*, and 26:0.

3.1.4. Results

3.1.4.1. Oat Tissue Growth and Harvest

CDC Dancer was grown to 23 days post flowering to allow seed to reach the milky-stage of development. Seeds were harvested by hand and immediately placed in a 50mL plastic Falcon tube cooled by suspension in liquid nitrogen. Samples were either used directly, or stored at -80°C. Root, stem, and leaf tissue were also harvested at the same time in the same manner and stored at -80°C for RNA isolation.

3.1.4.2. Fatty Acid Analyses

The alkaline sodium methoxide fatty acid methyl esterification and the acidic sulfuric methanol fatty acid methyl esterification methods were performed on duplicates of the same oat lipid samples. Both methods are used to transmethylate all fatty acids esterified on neutral lipids

such as triacylglycerols (TAGs) and on polar lipids such as glycolipids (GLs) and phospholipids (PLs). In the acidic treatment, the fatty acid is protonated to result in an oxonium ion, which then undergoes exchange reaction with an alcohol resulting in an intermediate; finally, the intermediate becomes an ester after losing a proton. In contrast, in the basic condition, the fatty acid forms an anionic intermediate from an ester, and can then form a new ester with a methyl group.

Samples were analyzed via GC-MS, thus identity comparisons are in the form of chromatographic peaks representing relative retention time in the GC column; identities were verified by using a FA standard (not pictured) containing FAs with known identities and retention times as well as MS spectra which could be compared to an MS spectra library containing spectra of previously-identified compounds.

3.1.4.3. Total Fatty Acid – Basic method

Using the basic methyl esterification protocol, the FAs of both the FAME sample and the TMS-derivatized FAME (TMS FAME) sample were analyzed using GC-MS (Figure 8).

Common FAs were identified by comparing relative retention times with a FA standard (not pictured), as well as GC-MS. UFAs whose positions did not coincide with those of the standard were investigated with GC-MS. As it was believed the shifted peak between the chromatograms A & B of Figure 8 was 15-OH 18:2-9*c*,12*c*, MS was performed on the labelled 15HFA peak (Figure 8A) to verify; the results here agree with data from the MS library (Figure 9).

One peak shifted after TMS derivatization, as indicated by an asterisk in Figure 8 B. The mass spectrum of this peak was compared with that of a published TMS-derivatized 15HFA spectrum (Figure 10).

Figure 9 and Figure 10 confirm the only peak that had shifted (in Figure 8) represents the 15HFA, and provides evidence of the mild nature and thus appropriateness of this method for FA analysis of samples containing such UFAs as the epoxy FAs were not degraded (maintained positions) across both chromatograms of Figure 8 while the HFAs can be selectively identified.

The identities of the epoxy FA peaks (or, those unshifted peaks with elution times different from the FAs of the standard) in Figure 8A were also investigated via MS to provide evidence of the reliability of the mild nature of the alkaline method (Figure 11).

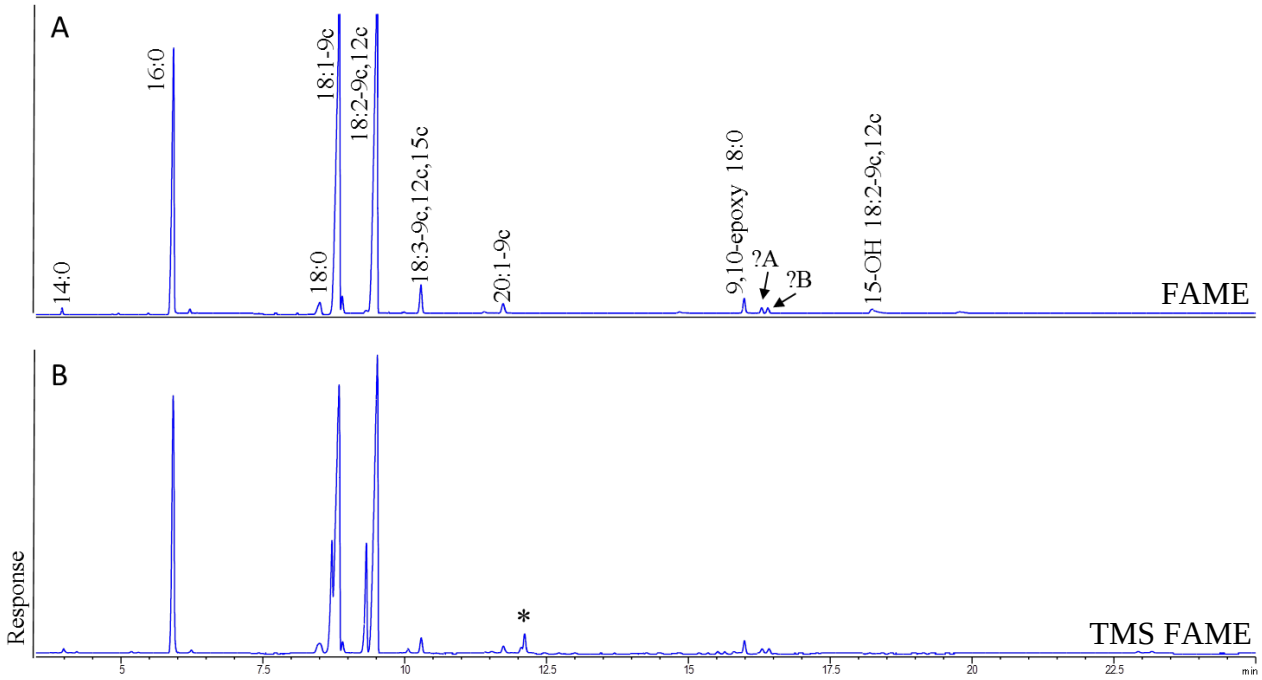

Figure 8. GC analysis of FAMEs of CDC Dancer mature seeds derived from the basic transmethylation (A) and of the duplicate TMS-derivatized FAMEs (B). One shifted peak between the two treatments is indicated by an asterisk.

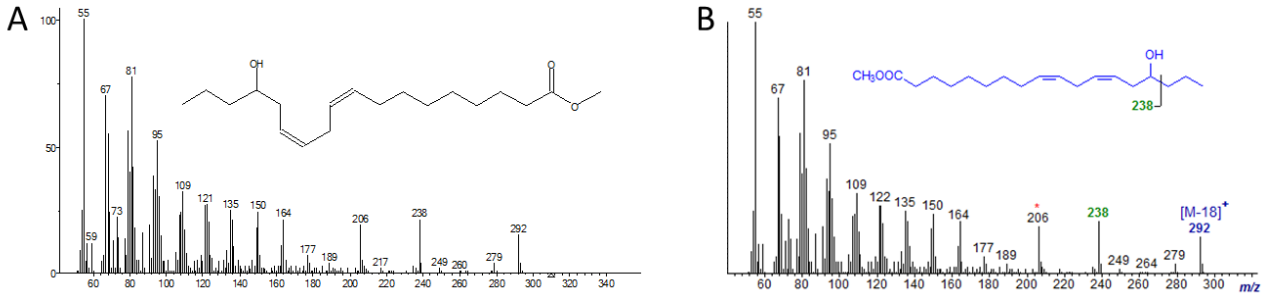

Figure 9. Mass spectrum and predicted structure of the 15HFA FAME.

The spectrum of the 15-OH 18:2-9*c*,12*c* peak in Figure 8A (A), compared to the published spectrum of the same HFA (B) (Christie, 2012)).

Figure 10. Mass spectrum and predicted structure of the TMS-derivatized putative 15HFA FAME. Spectrum of the peak marked with an asterisk in Figure 8B, compared to the published spectrum of the same derivatized HFA (American Oil Chemists' Society, 2012).

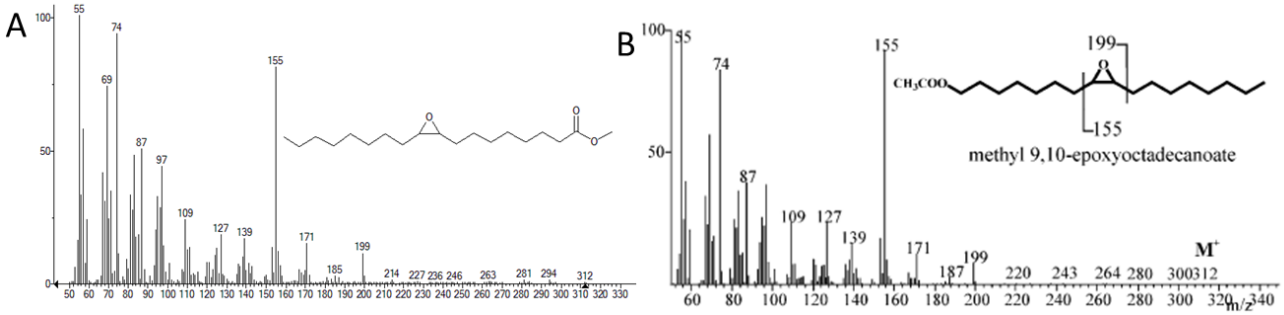

Figure 11. MS spectrum of 9,10-epoxy 18:0 peak (as labelled in Figure 1A) (A), compared to a published spectrum (B, Meesapyodsuk & Qiu, 2011).

The MS spectrum (Figure 11A) of the larger epoxy peak of 9,10-epoxy 18:0 (labelled in Figure 8A) is identical to the published spectrum (Figure 11B), confirming its presence here. The predicted identities of the two minor epoxy FAs, with peaks labelled "?A" and "?B" in Figure 8A, were less definitive.

The mass spectrum (Figure 12A) from peak "?A" is similar, but not identical to the reference spectrum of methyl 9,10-epoxy-octadec-12-enoate (9,10-epoxy 18:1-12*c*), while the spectrum from peak "?B" is less clear yet the main ionic species of which it is comprised are similar to the reference for methyl 12,13-epoxy-octadec-9-enoate (12,13-epoxy 18:1-9*c*). It is worth noting the high similarity between the spectra of both the 9,10-epoxy 18:1-12*c* and 12,13-epoxy 18:1-9*c* standards (Figure 12), which increases difficulty in distinguishing between the two FAs in a sample; this is especially true for samples with very small amounts of the two FAs, which increases the background noise of a sample and results in a more challenging comparison

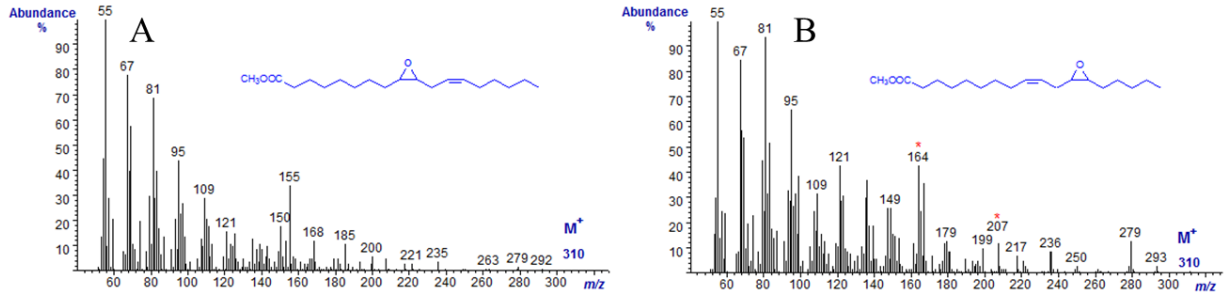

Figure 12. Literature mass spectra of 9,10-epoxy 18:1-12 and 12,13-epoxy 18:1-9 (Christie, 2012b)

of samples either lacking the entire ionic profile, or with additional ions. However, our lab group has previously identified low levels of 9,10-epoxy 18:1-12*c* and 12,13-epoxy 18:1-9*c* in oat seed, and retention times agree with peaks in Figure 8. Therefore, these two peaks might be the two epoxy fatty acids.

The relative quantities of each FA, as represented by peaks in Figure 8 A, are summarized in Table 2. Quantification proportions were determined by calculating the relative proportion of the chromatogram peak area of each individual FA to the total peak area of all FAs in the chromatogram (Table 2).

The major fatty acids in oat seeds were linoleic acid accounting for about 37%, oleic acid for more than 30% and palmitic acid for about 23%. Among UFAs, three epoxy fatty acids comprised just over 2%, four-fold higher than in literature (Table 1) with 9,10-epoxy 18:0 making up about 1.5%, and 9,10-epoxy 18:1-12*c* and 12,13-epoxy 18:1-9*c* both accounting for just below 0.5% each. 15-OH 18:2-9*c*,12*c* comprised less than 1% of total FAs, three-fold lower than levels in literature (Table 1). 7-OH 16:0 was undetected here, and aside from the minor UFAs, FA composition was in agreement with literature.

In Figure 8B, an unexpected peak appears beside each of the peaks representing 18:1-9*c* and 18:2-9*c*,12*c*. These unexpected peaks are inconsistent across samples (Figure 8A vs. Figure 8B) and are also inconsistent with literature; GC-MS was unable to confirm an identity for these peaks.

Table 2. CDC Dancer mature seed fatty acid composition (percent of the total FAs)

Fatty Acid	Replicate 1	Replicate 2	Replicate 3	Mean percent of total FA ± SD		
14:0	0.12	0.03	0.05	0.07	±	0.05
16:0	22.82	24.33	22.02	23.05	±	1.17
16:1-9*c*	0.14	0.42	0.13	0.23	±	0.16
18:0	1.01	1.51	0.98	1.17	±	0.30
18:1-9*c*	32.65	31.08	31.95	31.89	±	0.79
18:1-11*c*	2.38	0.45	2.89	1.91	±	1.29
18:2-9*c*12*c*	36.34	37.65	37.93	37.31	±	0.85
18:3-9*c*,12*c*,15*c*	0.72	1.07	0.75	0.85	±	0.19
20:0	0.14	0.03	0.05	0.08	±	0.06
20:1-9*c*	0.34	0.50	0.42	0.42	±	0.08
9,10-epoxy 18:0	1.52	1.26	1.66	1.48	±	0.21
9,10-epoxy 18:1-12*c*	0.50	0.48	0.34	0.44	±	0.09
12,13-epoxy 18:1-9*c*	0.55	0.43	0.31	0.43	±	0.12
15-OH 18:2-9*c*,12*c*	0.77	0.75	0.52	0.68	±	0.14

3.1.4.4. Total Fatty Acid – Acidic method

A sulfuric methanol protocol was employed to demonstrate the inaccurate identification of HFAs due to presence of epoxy FAs which are prone to degradation by acidic conditions. The FAMEs as well as TMS-derivatized FAMEs analyzed via GC-MS are shown in Figure 13. In contrast to the alkaline method, this protocol resulted in a shift of three distinct peaks, shown in Figure 13.

As the FA standard used in GC analysis did not include the UFAs, the identities of the UFAs (represented by peaks in the insert, Figure 13A) were investigated with GC-MS, and the spectra and their predicted FA structures were determined (Figure 14). Those identifiable were labelled as "?A," "?B," and "?C" in the chromatogram insert (Figure 13A).

Identities of some peaks in the chromatogram in Figure 13A were unclear, and labelled as "?A," and "?B," and "?C." As the epoxy FAs were undetected, peaks "?A" and "?B" are probably the minor epoxy FAs 9,10-epoxy 18:1-12 and 12,13-epoxy 18:1-9. Peak "?C" had MS

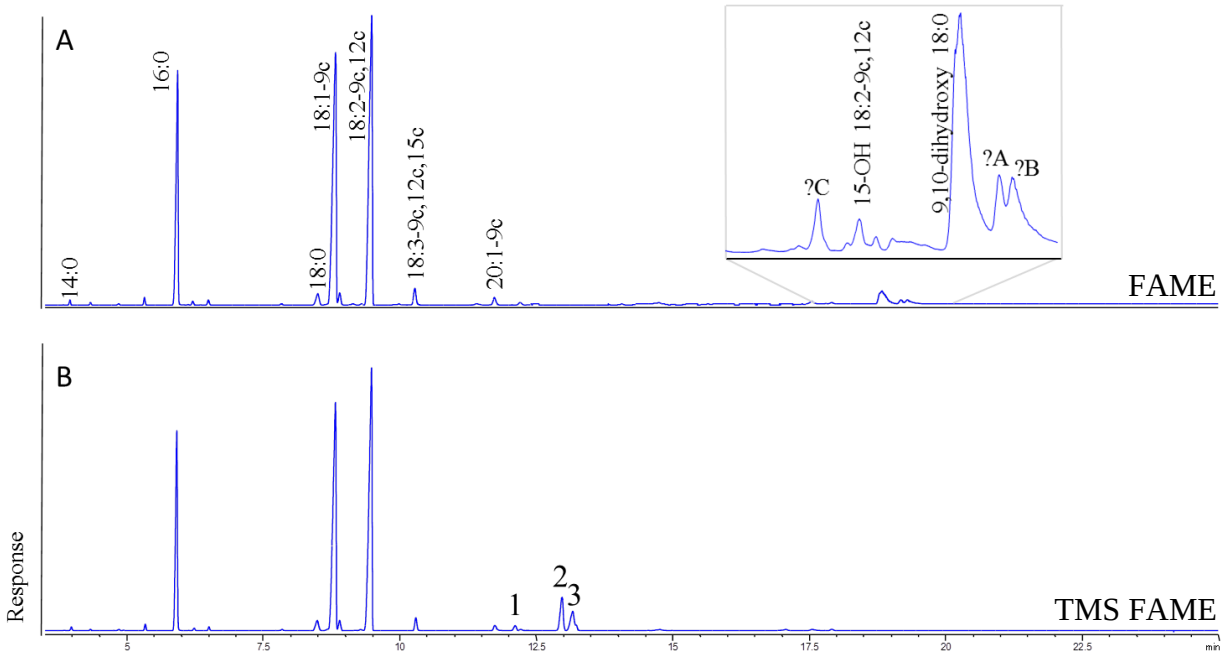

Figure 13. GC analysis of FAMEs of CDC Dancer mature seed derived from the acidic transmethylation (A) and of the duplicate TMS-derivatized FAMEs (B). Shifted peaks are indicated with numbers 1, 2 and 3. Question marks indicated peaks having no clear predicted identities based on the MS spectra library. The insert shows a magnified region of the chromatogram with UFAs.

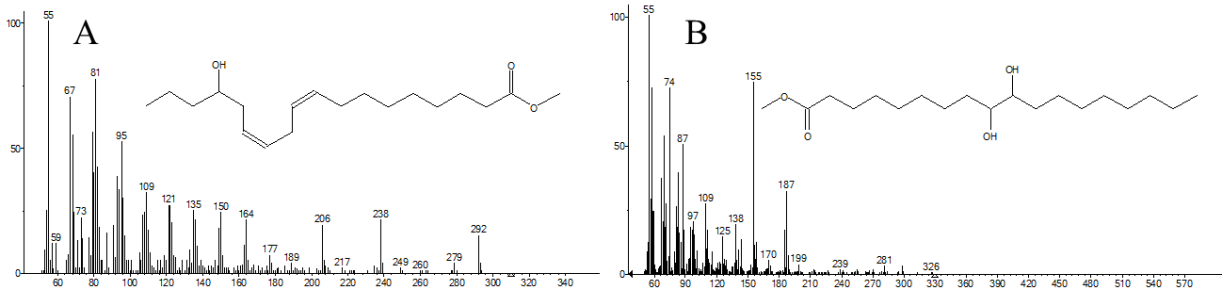

Figure 14. **The predicted identities of the UFA FAME peaks labelled in Figure 13A insert**: 15-OH 18:2-9c,12c (A), and 9,10-dihydroxy 18:0 (B) probably derived from hydration of 9,10-epoxy-18:0 (as shown in Figure 11).

library matches of very low probability, including various epoxy and hydroxy FA structures. As oat seed has been documented to contain very small quantities of 7-OH 18:2 (Table 1) yet was undetected in this study, it is likely that peak "?C" represents this hydroxy FA. Ideally, the sample could be run with a standard known to contain these epoxy FAs, however they were unavailable.

In Figure 13B, the UFAs represented by the shifted peaks 1 and 2 were identified by reference to an MS spectra library after GC-MS analysis (Figure 15) for comparison to the non-derivatized FAMEs in Figure 14.

As expected with this method, identification of the UFA peaks proved to be more challenging than in the basic treatment. Peaks 1 and 2 (from Figure 13B) were identified as the TMS-derivatizations of 15-OH 18:2-9c,12c and of 9,10-dihydroxy 18:0, which supports the initial hypothesis that the acidic method degrades the epoxy group (as the dihydroxy was not identified in the basic-treated sample). Peak 3 in Figure 13B, however, was less definitive, and several possible identity matches were retrieved from the MS library, all with low predicted probabilities.

Given the inconsistencies of MS data of this acidic treatment, the presence of a dihydroxy FA not found in the basic-treated sample, and observations previously made in our lab group, it can be extrapolated that Peak 3 is probably a dihydroxy FA artifact induced from the conditions and degraded from one or two of the monounsaturated epoxy FAs. The width of the base of Peak 3 also suggests that perhaps two molecular species are inseparable.

These results also provide evidence that acidic methods will overestimate HFA and underestimate epoxy FA content; in addition to being inaccurate with regards to epoxy FA quantity, the acidic treatment is also inconsistent with the amount of the epoxy FAs measured by the basic transmethylation method. Thus, this method is less reliable and not ideal for FA analysis of samples containing both HFAs and epoxy FAs.

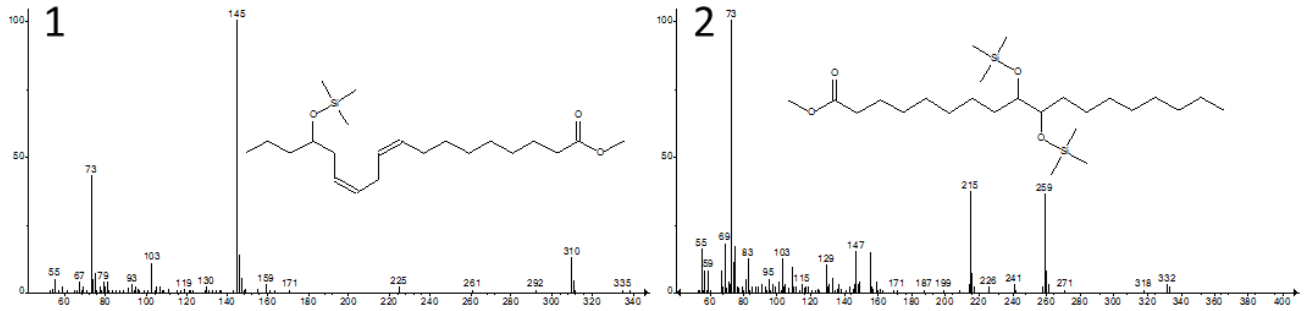

Figure 15. Mass spectra of the peaks 1 and 2 from Figure 13B. Peak 1 was identified as the TMS-derivatized FAME of 15HFA, and Peak 2 as the TMS-derivatized FAME of 9,10 dihydroxy octadecanoic acid (probably derived from hydration of 9,10-epoxy-18:0).

3.1.4.5. Free Fatty Acid

To investigate whether UFAs were present in the FFA form, a third protocol was employed. Conditions used for this diazomethane protocol allow rapid reaction of diazomethane with non-esterified FAs to result in fatty acid methyl esters, and can therefore provide methyl esters representing FFA content of oat seed. Several FAs were identified in the FFA form in mature oat seed (Figure 16 A). A duplicate of the same sample (Figure 16 B) was derivatized with TMS to identify if the presence of any FFA form of a HFA, epoxy FA or dihydroxy groups resulting from degraded epoxy FAs as described above.

Two prominent peaks appearing in both Figure 16A and B remain unidentifiable, as indicated on the chromatograms with "?". Since they maintained their retention times across both chromatograms, they must not be HFAs, nor be artifacts of hydrolyzed epoxy FAs. Neither peak aligned with the FA standard, nor was any obvious matching identity found with GC or MS. However, in Figure 16A, the bases of the two unidentified peaks are quite spread out and seem to encompass >1 molecule as if there were multiple compounds present with very similar elution times that were inseparable. In addition, there is a small peak near 18.5 mins in Figure 16A, but neither GC or MS could confirm it as anything other than background noise.

The relative proportions of the common FFAs were relatively quantified as described for the first two methods (Table 3). As this method solely analyzes FFA form, the abundance of each FA is relative within the pool of FFAs only. The composition of this pool is specifically the FFA content of the oat seed; their abundance relative to all FAs of the seed would be too small to have

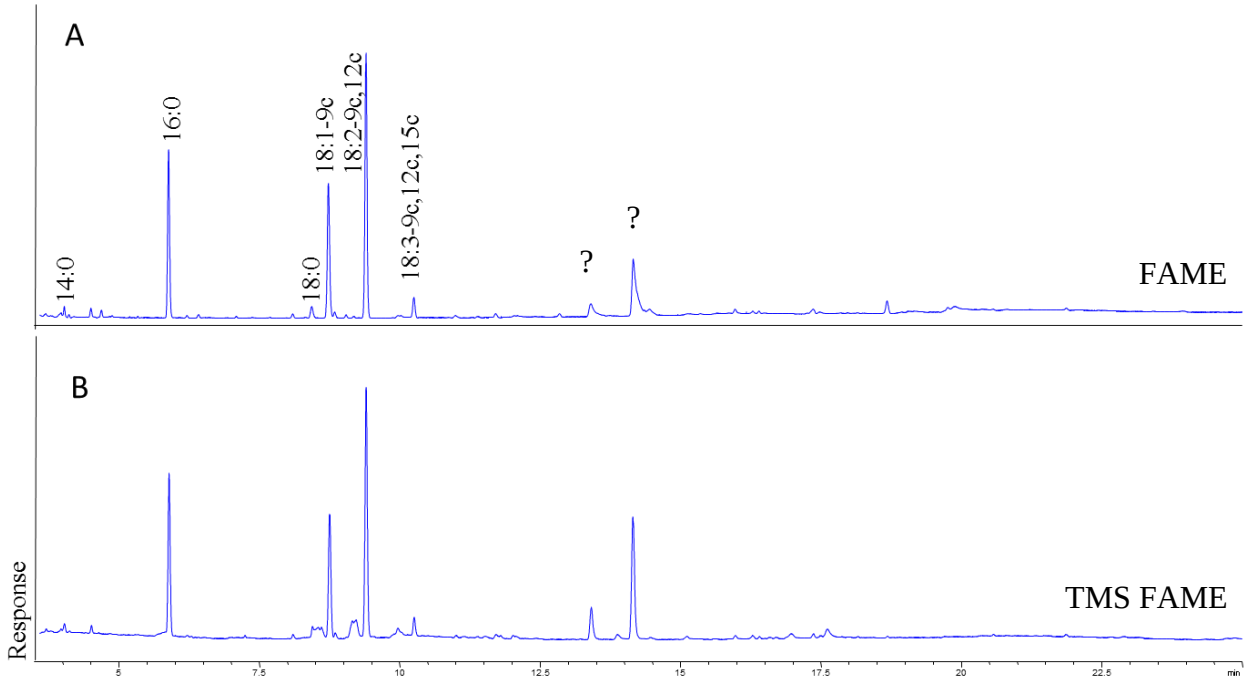

Figure 16. GC analysis of FFAs of mature CDC Dancer seed. A duplicate of the diazomethane methylated sample (A) was derivatized with TMS (B).

Table 3. Individual FFA percentages of total FFAs. The "?" denotes quantity of the identified peaks.

FFA	Relative Abundance (% of total FFA)
14:0	0.7
16:0	20.7
18:0	1.7
18:1-9c	20.0
18:2-9c,12c	40.1
18:3-9c,12c,15c	3.0
?	13.8

significance in comparing their quantities to fatty acids derived from the other forms.

3.1.5. Discussion

To determine the FA composition of CDC Dancer oat seeds, fatty acids were transmethylated from lipids that had been extracted from the seeds using three different methods. Two of the methods, an alkaline and an acidic treatment, were used to compare their effectiveness for analyzing UFA-containing lipids for the same total fatty acids from the seed lipids. The total FA composition of the mature oat seed (Table 2) was largely consistent with the other cultivars examined in the study by Leonova *et al.* (2008). Although CDC Dancer seed did not have the highest 15HFA content when compared with their study, both 18:2-9*c*,12*c* and 18:3-9*c*,12*c*,15*c* content of CDC Dancer was higher than the mean values of their study.

As the sodium methoxide was used to preserve sensitive epoxy groups, peaks representing epoxy FAs should not shift after TMS derivatization (Figure 8 B). Thus, any peaks in a new position when compared to Figure 8 A represent a HFA. Figure 8 reveals only one peak had shifted after derivatization, which was confirmed to be the 15HFA (Figure 9). However, the study by Leonova *et al*. (2008) consistently shows higher 15HFA content than results in this study. Their FA extraction methods include a sulfuric methanol step and derivatization step as well, but do not include specific information about epoxy fatty acids; this is relevant since harsh acidic conditions can cause deterioration of the cyclic epoxide structure, opening the epoxy ring to result in di-hydroxy artifacts (Greenspan & Gall, 1956). The resulting hydroxyl groups are free to bind with TMS, as would any naturally-occurring hydroxy group. The overestimation of 15HFA may be due to the influence of a hydrolyzed epoxy group in the FA.

This is further reinforced when comparing the total epoxy FA content; in this study, the epoxy FA content (Table 2) after alkaline transmethylation is approximately three-fold higher than the results by Leonova *et al*. (2008). If the epoxide ring of a FA in the sample was broken and being detected as dihydroxy FA, the total epoxy FA content would thus be expectedly lower.

Leonova *et al*. did not examine epoxy FAs in detail as all epoxy FAs are grouped together, and detailed HFA analysis discussion is limited to 7-hydroxyhexadecanoic acid (2008). Interestingly, methods used here did not detect this HFA, perhaps due to sensitivity threshold, lack of information in the MS library, or a different GC column used. By comparing chromatograms in Figure 8 and Figure 13, it can be suggested that acidic degradation of some

epoxy FAs is occurring and thus that method is less reliable in compiling an accurate FA profile for mature oat seed.

The predicted structures from MS analysis that lower confidence are two monounsaturated epoxy fatty acids which have been shown to exist in oat previously (Meesapyodsuk & Qiu, 2011). 9,10-epoxy 18:1-12*c* & 12,13-epoxy 18:1-9*c* are both produced from 18:2-9*c*,12*c* substrate; relative quantities of both substrates are abundant. However, the MS spectra predictions are somewhat limited to the information in the MS spectra library, and may not be capable of discriminating between two ionized structures with high similarity (or these two minor epoxy FAs ionize with differences below the accurate detection capabilities of the detector). Furthermore, the structures predicted via GC-MS consistently identified FAs that have never been observed in oat seed oil previously, which were always rated with very low probability and therefore increased the difficulty in identifying them. The mass spectra software likely determined the best option available when a perfect match of a structure and its ionization pattern were unavailable. Thus, for the two minor epoxy FAs (Figure 8), given the evidence here, as well as the known data regarding oat epoxy FAs, the evidence strongly supports 9,10-epoxy 18:1-12*c* & 12,13-epoxy 18:1-9*c* identities.

The MS data of the putative peak representing the 15HFA and either the closed or opened epoxy FAs were consistent with the literature (Figure 9, Figure 10, Figure 15; American Oil Chemists' Society, 2012). MS of a neighboring peak (Figure 15-2) verifies the presence of a derivative of a di-hydroxy FA which is probably the degraded product of an epoxy. Therefore, if a harsh acidic condition is used for the transmethylation process of an epoxy-containing FA pool, there is a risk of overestimating HFA content in the seed while underestimating total epoxy FA content.

The presence of small amounts of FFAs is not unusual, and they are typically present as second messengers for transferring extracellular signals, modifying metabolic processes, or altering gene expression, although the latter is typically influenced by the non-saturated LCPUFAs (American Oil Chemists' Society, 2012b). Since none of the peaks obtained in the GC analysis of FFAs shifted after TMS treatment, this indicates that there are no hydroxy (or epoxy-derived di-hydroxy artefacts) FAs in the FFA pool. This is not unexpected, since plant FFA abundance declines with increasing oil biosynthesis & seed maturity, *FAD*-like gene transcription (and the product's activity) are active during an earlier development stage, and

15HFA is esterified to form digalactosyldiacylglycerol (DGDG) (May & Hume, 1995; Hamberg & Hamberg, 1996; Napier, 2007 Hamberg *et al*., 1998). Since the plants were grown in optimal conditions in the growth chambers, the FFA content should be accurate as a result of natural biochemical processes of the plant rather than from poor environmental influence which has been shown to increase seed FFA levels (Frey & Hammond, 1975). However, oat is known to have high lipase activity, which exhibit activity even at 7.5% moisture levels (Frey & Hammond, 1975). Although extraction after grinding the sample in solution is one of the most effective methods to minimize system-induced lipase activity, acid treatment is ineffective in deactivating the enzymes completely (Frey & Hammond, 1975).

The species present and relative quantities of major FFA species in the mature seed (Table 3) largely reflect their FAME levels of the seed total FA composition (Table 2; Figure 8), although there is substantial presence of the two unknown peaks in FFA form (Figure 16). It is surprising that the clarity of the two unknown peaks in Figure 16 improves after TMS derivatization, whereas that of all others is slightly deteriorated. Neither of these peaks appears in the expected positions of the 15HFA, in the FAME or the TMS FAME chromatograms, nor do they change positions; thus, they cannot be HFAs. The small peak that appears in the FAME chromatogram at 18.5 mins is in the expected position of a HFA, and does not appear in the TMS FAME chromatogram suggesting that there was a free hydroxyl group present that was etherified by the TMS reagent; however, it was impossible to determine whether the small peaks of Figure 16B were background noise, or new peaks that shifted due to the etherified form. For all these peaks, perhaps better identification could be established by either increasing the concentration of the FA or the amount run on the GC, or by using a column with a different stationary phase or polarity.

Of particular interest to this study, in the FFA pool there are higher levels of both PUFAs relative to the monounsaturated 18:1-9*c*. Comparing FFA relative quantities of OA and LA to ALA (Table 3), ratios are 6.7:13.4:1, respectively. The ratio of total relative amounts of the same FAs in the seed (Table 2) is approximately 37:44:1. Thus, relative to ALA, OA is more than five-fold higher while LA is approximately is three-fold lower in the FFA form.

3.2. Study 2: Oat *FAD*-like gene Cloning & Sequence Analysis

3.2.1. Abstract

To identify the genes encoding enzymes involved in the biosynthesis of PUFAs and/or hydroxyl fatty acids, bioinformatics techniques were carried out. Previously-characterized FAD2, FAD3 and FAH protein sequences from NCBI databases were used as query sequences to find highly homologous EST matches from an oat-specific EST pool in CORE's sequence database using NCBI's Basic Local Alignment Search Tool (BLAST). The homologous ESTs were then assembled into contigs to establish full-length candidates for the *Avena* FAD2-like sequences. From the *Δ*12-desaturase (FAD2) queries, two isoforms of one putative *FAD2*-like ("*AsFAD2a"* and "*AsFAD2b"*) genes were found; the *Δ*15-desaturase (FAD3) queries revealed two oat *FAD3*-like ("*AsFAD3-1"* and "*AsFAD3-2"*) putative oat genes, while an *ω*-3 desaturase (FAD7) query identified a fourth putative full-length *FAD6*-like CDS, "*AsFADX"* as well as a longer variation of the same sequence, "*AsFADX+,"* which had additional 288 bp upstream of the putative translation initiation site of *AsFADX*. All were cloned from cDNAs and ligated into pGEM-T, an *E. coli* intermediate vector, for sequencing. Detailed sequence analyses were carried out with these sequences.

3.2.2. Hypothesis

FADs are well-conserved across species, and oat FAD3s and the 15FAH are believed to have diverged from a FAD2. By using previously-characterized query proteins from other organisms that have demonstrated FAD or FAH activity, putative oat *FAD*-like ORFs can be identified from an oat EST database and used as templates for designing primers. The primers can be used to clone the gene from oat seed cDNA, and then ligated into appropriate vectors for sequencing.

3.2.3. Experimental approach

3.2.3.1. Contig Construction from *Avena* ESTs

All EST sequences were obtained from either the Collaborative Oat Research Enterprise (CORE) database (United States Department of Agriculture, 2010) or from the National Center for Biotechnology Information (NCBI) database (National Center for Biotechnology Information, 2012).

Each query protein sequence was individually entered in the tBLASTn function of either the CORE database, or NCBI's public database (specific to oat ESTs as defined in the search options) using default search algorithm parameters. At least one previously-characterized protein sequence from each HIS-box-containing FAD or FAH class was used as a query sequence in the tBLASTn searches. Resulting ESTs were compiled into a single file as general oat EST-containing text files, and also divided further into cultivar-specific files. Both the general and specific sets of ESTs were used separately for constructing contigs, if adequate number of ESTs were available to cover the entire putative CDS. Putative sequences were derived from the cultivar-specific EST files, if available; otherwise, the total collection of homologous ESTs was used to construct the full-length ORF of the putative gene. ESTs were assembled using DNAstar's SeqMan offline software. Manual corrections of all outstanding nucleotide inconsistencies across assembled ESTs were performed. ORFs were determined by aligning the maximum length of the contig (putative UTRs and ORFs included) with the query sequence, and determining the translation initiation and stop codons. This was based in part on the length of the reference gene ORFs, and relative positions of the HIS-boxes as well as their initiation and stop codons; additionally, putative oat genes were determined to be distinct based on the putative UTR regions both upstream (Figure 45, 5.2) and downstream (Figure 46, 5.2) from the putative ORFs (Figure 44, 5.1). The finalized contigs were translated in DNAstar's SeqBuilder program, and aligned with the original query sequences in DNAstar's MegAlign program to verify the entire protein was translated and to verify that they contained the HIS-boxes. Primers for cloning were designed using a combination of DNAstar's PrimerSelect and the criteria described by Sambrook & Russel (2001); the putative CDS (3.2.3.1) of each GOI was used as the template. Where sequences of previously-characterized templates originating from organisms very closely related to oat were unavailable, those from well-studied model organisms *Arabidopsis thaliana* and/or characterized proteins of other plants were used (The Arabidopsis Genome Initiative, 2000).

3.2.3.1.1. *Δ*12 Desaturase/Hydroxylase query: FAD2-like

Products of previously characterized genes exhibiting activity on the *Δ*12 position of oleate substrate were used as query sequences. The *Δ*12 desaturases used as queries included those from *Arabidopsis thaliana* (AtFAD2*;* Okuley *et al*., 1994; accession number L26296.1) and the fungal *Claviceps purpurea* (CpFAD2A & B*;* Meesapyodsuk *et al*., 2007; accession

numbers EF536897 and EF536898). Other queries included enzymes with either *Δ*12 hydroxylase activity, (RcFAH12*;* van de Loo *et al*., 1995; accession number U22378), or those with dual *Δ*12 hydroxylase and desaturase activity (LfFAD2FAH12*;* Broun *et al*., 1998a; accession number AF016103; CpDesX*;* Meesapyodsuk & Qiu, 2008; NCBI accession number EU661785).

3.2.3.1.2. *Δ*15 Desaturase/Hydroxylase query: FAD3-like

Products of previously characterized genes that act upon the *Δ*15 position of α–linolenate substrate were chosen for FAD3 queries, such as that of *Arabidopsis thaliana* (AtFAD3*;* Arondel *et al*., 1992; accession number L01418) and those *of Linum usitatissimum* (LuFAD3A *&* B*;* Vrinten *et al*., 2005; accession numbers DQ116424 and DQ116425).

3.2.3.1.3. *ω*-3 Desaturase/Hydroxylase query: FAD7-like

A chloroplast membrane-bound FAD7 from *Arabidopsis thaliana* with *ω*-3 desaturase activity on 16:2 and 18:2 substrates to produce linolenic and hexadecatrienoic acids, respectively, was used as the query sequence (AtFAD7*;* Iba *et al*., 1993; accession number D014007).

The putative CDS from each contig assembly or assemblies were used as templates on which to design primers for amplification of each putative GOI target from cDNA template.

3.2.3.2. Isolation of total RNA

CDC dancer germplasm was selected for experiments. All seeds were found and obtained from Agriculture & Agri-Food Canada's Genbank (2010; 2012). The total RNA was isolated from the developing seed tissue of CDC Dancer cultivar using Invitrogen's TRIzol Reagent (Invitrogen, 2010a). The reagent is a solution of phenol, guanidine isothiocyanate as well as proprietary components designed for effective isolation of the RNA, by disrupting cells, dissolving their components, and inhibiting RNase. It is ideal since it can be performed in one hour on a large number of samples.

For each tissue type in all RNA extractions, 200 mg of oat tissue was kept frozen with liquid nitrogen and ground with a mortar and pestle. 1mL of TRIzol Reagent per 50-100mg of sample was added to prevent DNA contamination of the RNA sample. To phase separate the sample, it was incubated at 5 minutes at room temperature for total dissociation of the nucleoprotein complex. 0.2mL of chloroform per 1mL of TRIzol Reagent (from

homogenization) was added, capped, and shaken for 15 seconds by hand. The sample was then be incubated for 2-3 mins at room temperature, centrifuged for 15 mins at 4ºC at 12,000xg, then the aqueous phase (containing the RNA) was pipetted out by holding the sample tube at 45º angle. This aqueous phase was placed in a new sample tube for RNA isolation.

0.5mL of 100% isopropanol (per 1mL of TRIzol Reagent from homogenization) was added to the aqueous phase, incubated at room temperature for 10 mins, then centrifuged at 12,000xg for 10 minutes at 4ºC, after which the RNA wash was performed. This is done by taking the RNA pellet, washing with 1mL of 75% ethanol (per 1mL of TRIzol Reagent from the initial homogenization), vortexed, and centrifuged at 7500xg for 5 minutes at 4ºC. The wash was discarded, the pellet air or vacuum dried for 5-10 mins, and resuspending the pellet in RNase-free water (or 0.5% SDS solution) via passing the solution up and down several times in a pipette. Concentrations were measured with a Nanodrop spectrophotometer. Remaining samples were stored at -80°C.

3.2.3.3. First-strand cDNA Synthesis

Using Invitrogen's SuperScript III (Invitrogen, 2004) the cDNA was synthesized. This system utilizes a reverse transcriptase from Moloney Murine Leukemia Virus (M-MLV) and is purified and modified to minimize RNase H activity (to minimize RNA/DNA hybrids) and increase thermal stability for synthesizing cDNA, from 100bp to 12kbp in length, up to 55ºC.

Using 5 µg of total RNA, 1 µL of oligo(dT)20 (50 µM), 1 µL of 10mM dNTP at neutral pH, and 13 µL of water was added to a nuclease-free microcentrifuge. The mix was heated to 65 ºC for 5 mins and incubated on ice for 1 minute. The contents were briefly centrifuged, after which 4 µL 5X First-Strand Buffer, 1 µL 0.1M DTT, 1 µL RNaseOUT Recombinant RNase Inhibitor, and 1 µL of SuperScriptIII RT was added. The solution was mixed via pipetting up and down, then incubated at 55 ºC for 30-60 mins, followed by reaction inactivation by heating to 70 ºC for 15 mins. cDNA used as template in cloning was diluted 1/10, and remaining cDNA was stored at -20°C.

3.2.3.4. Primer Design, DNA polymerase selection, PCR amplification

3.2.3.4.1. Primer Design

Primers designed are listed in Table 4 to Table 7 based on the criteria described by Sambrook and Russell (2001).

Table 4. *AsFAD2* primers

Target	Sequence (5'→3')	Description
AsFAD2	[1]TTGAATTCGCC**ATG**GGTGCCGGTGGCAGGATG	*AsFAD2* sense primer
	[1]CTGAATTCAT**CTA**GAACTTGTTGCTGTAC	*AsFAD2* antisense primer
	ACGAGTGGAGCACCAGGC	*AsFAD2* nested antisense primer

Restriction sites underlined; [1]EcoRI site; translation initiation & termination sites in bold.

Table 5. *AsFAD3* primers

Target	Sequence (5'→3')	Description
AsFAD3-1	TTGAATTCAGCC**ATG**GCCGCGGAAGC	*AsFAD3-1* sense primer
	TAGAATTCTA**TCA**CTTGTGCTTGTCAGTTC	*AsFAD3-1* antisense primer
	AGGTGGCCGACGACGCTGTTGAGC	*AsFAD3-1* nested sense primer
AsFAD3-2	GCCATGGCCCCCGCA**ATG**	*AsFAD3-2* sense primer
	TCACTTTTGCTTGCCATTTTTCGTC	*AsFAD3-2* antisense primer
	GGCCAGTGCCGGTGCTCAAAC	*AsFAD3-2* nested sense primer

Restriction sites underlined; translation initiation & termination sites in bold.

Table 6. *AsFADX* & *AsFADX+* primers

Target	Sequence (5'→3')	Description
AsFADX	[1]TTAAGCTTCG**ATG**TCTGAAGATTATGGGTTCAAAC	*AsFADX* sense primer
	[2]GCTCTAGA**TCA**AGCATAATCTGGCATGAACTTC	*AsFADX* & *AsFADX+* antisense primer
	AGGCGCAATTAAATGGCACAGTTC	*AsFADX* nested primer
AsFADX+	[1]TTAAGCTTGG**ATG**CGCGCGCGCACTCC	*AsFADX+* sense primer

Restriction sites underlined; [1]HindIII site; [2]XbaI site; translation initiation & termination sites in bold.

For screening insert presence and orientation in the vectors (the intermediate pGEM-T vector, and for the expression vector pYES2.0), primers flanking the MCS of each were used (Table 7).

Table 7. Generic vector-specific primers

Target	Sequence (5'→3')	Description
pGEM-T	TAATACGACTCACTATAGGG	T7 region forward primer
pYES2.0	CCTTCCTTTTCGGTTAGAGCGG	SP6 region reverse primer

3.2.3.4.2. Polymerase & PCR

To clone each GOI from cDNA, NEB's Q5® high-fidelity polymerase was used with the supplied 5X Q5® buffer or 5X Q5® high-GC enhancer, and dNTP and primer concentrations of 200µM and 0.5µM, respectively (New England Biolabs Inc., 2013). ~200ng of template cDNA was used per reaction. PCR amplification was carried out in 35 cycles, consisting of 1 or 2 stages. The first attempt was with one stage for 35 cycles. If two stages were required due to low or no amplification from the first attempt, the first part included 10 cycles with an anneal temperature (T_m) ~5°C below the recommended T_m of the primer pair used, then the next 25 cycles had the anneal temperature increased to ideal T_m. The 2-part process helped eliminate the non-specific binding of non-target DNA. Reaction cycles were conducted in an Eppendorf Mastercycler.

For *AsFAD2*, 0.5U of Phusion® polymerase (Finnzymes, 2012) was used in a 25µL reaction containing 3% dimethylsulfoxide (DMSO). Initially the reaction was held at 98°C for 2mins, followed by the first 10 cycles of denaturation at 98°C for 15sec, annealing at 55°C for 30sec, and elongation at 72°C for 1min; the second stage had 25 cycles of 98°C for 15sec, 59.2°C for 30sec, and 72°C for 1min. The reaction was held at 72°C for 10 minutes, then run on an agarose gel. To amplify the oat *FAD3*s, 0.5U of Phusion® polymerase was used in each reaction containing 3% DMSO. Initially the reaction was held at 98°C for 2mins, followed by the first 10 cycles of 98°C for 15sec, 54°C for 30sec, and 72°C for 45sec; the second stage had 25 cycles of 98°C for 15sec, 59°C for 30sec, and 72°C for 45sec. The reaction was held at 72°C for 10 minutes, then run on an agarose gel. For amplifying both *AsFADX* and *AsFADX+*, 0.5U of Q5® was used in a 25µL reaction with 1X of the high GC enhancer buffer. The reactions were first held at 98°C for 3mins, followed by the first 10 cycles of denaturation at 98°C for 10sec, anneal at 55°C for 30sec, and elongation at 72°C for 1min; the second stage had 25 cycles of 98°C for 10sec, 68°C for 30sec, and 72°C for 1min. Each was held for an additional 2mins at 72°C.

The sample was then run on an agarose gel with wide-toothed comb wells. Where several bands appeared on the gel and/or there is no dominant band, the total DNA from this region was isolated and extracted, followed by another amplification procedure with the same primers.

Amplicons of expected size were cut from the gel and eluted/purified using BioBasic's miniprep kit (2013).

3.2.3.5. Vector Recombination, *E.coli* Transformation, & Sequencing

For cloning the GOIs into intermediate pGEM-T vectors, a single-nucleotide dATP-overhang was added to the purified inserts. 21µL of the gel-extracted amplicon was transferred to a 0.2mL tube, followed by addition of 2.5µL of Invitrogen's 10X PCR buffer (-$MgCl_2$), 0.75µL of 50mM MgCl2, 0.5µL of 10mM dNTPs, and 0.25µL of Invitrogen Taq. The reaction mixture was incubated for 20 minutes at 72°C. The GOI with dATP overhangs was cloned into pGEM-T vector using Promega's kit (2009). 5µL of 2X rapid ligation buffer, 1 µL of pGEM-T linearized vector, 3 µL of GOI with dATP-overhangs, and 1 µL of T4 DNA (Invitrogen, 2002) ligase were combined, and ligated at 4°C overnight.

Electrocompetent TOP10 *E. coli* cells were prepared, and then transformed with the GOI/pGEM-T recombinant vectors. Transformation was carried out using an electroporator, set at 1800mV, and using glass cuvettes with 1mm gap, as follows: For each transformation, 40 µL of TOP10 cells were thawed for 3 minutes on ice, and 1 µL of the overnight ligation of the GOI/pGEM-T recombinant vector was added to these cells, and gently mixed. The 41 µL volume was transferred into the cuvette, and set on ice for 5 minutes. The cuvette was transferred to the electroporator permeabilize the cells, immediately followed by addition of 1mL liquid LB medium into the cuvette. The total sample was transferred into a plastic 15mL tube, incubated at 37°C for 1 hour, and plated on LB agar containing 100µg/mL carbenecillin (CB) for selection. The plates also contained 40µL of X-gal (5-bromo-4-chloro-3-indolyl-beta-D-galacto-pyranoside) and 40µL of 0.1M of IPTG (isopropyl *β*-D-1-thiogalactopyranoside). The plates were incubated at 37°C overnight, after which several white colonies were selected, subcultured, and screened via PCR. For PCR screening to confirm GOI presence in the intermediate vector, the same gene-specific primer pair was used in a PCR reaction. A small amount of each of the three random, individual white colonies was used as template in each reaction, ensuring that the PCR parameters reached adequate temperature to disrupt the cells and release the DNA (95°C, 5 minutes). To establish the real sequence of each GOI, plasmids of 3 GOI-positive colonies were inoculated into 5mL of liquid LB growth medium + 100µg/mL (CB) and incubated in a shaker at 37°C overnight. Plasmids were extracted from each, using BioBasic's miniprep kit (2013), and isolated plasmids were stored at -20°C. For all sequencing of samples, purified recombinant

GOI/plasmid were extracted from at least three individual colonies per GOI. 10µL of 100ng/µL of GOI/plasmid were sent to the National Research Council of Canada (NRC) at 110 Gymnasium Place Saskatoon, Saskatchewan S7N 0W9 for sequencing. After sequencing results were obtained, each of the three replicates was compared with the nucleotide sequence of the putative gene. If there were discrepancies across the three sequenced samples, the one with the highest homology to the putative sequence was selected.

For preparing the GOIs for transfer into the yeast expression vector, 1µg of GOI/plasmid DNA, 2µL of 10U/µL restriction enzyme(s) and 5µL of corresponding 5X buffer were added to 15µL water and digested for 3 hours at 37°C. The GOIs were digested from the intermediate pGEM-T backbone (for transformation and selection in *E. coli*), separated via gel electrophoresis, and purified from the gel. pYES2.0, the expression vector to be used, was digested in another reaction with the restriction enzymes compatible with each GOI to which it will be ligated. After digestion, each was electrophoresed on a gel, cut, and purified using the BioBasic kit (2013). The pYES2.0 cut and purified DNA had Calf Intestinal Alkaline Phosphatase (CIAP) added to dephosphorylate the 5' terminus in order to eliminate self-ligation prior to insert/vector ligation. The GOI:pYES2.0 were combined in a 3:1 ratio. The volumes were combined with 2µL 5X buffer, 0.5µL T4 ligase, and brought to 10 µL final volume. The reactions were incubated at 16°C overnight. TOP10 cells were then transformed with these ligations, plated on CB-containing LB agar plates, extracted and sequenced as described above.

Using the DNA map of the GOI/vector, specific restriction enzymes were chosen that, once used to digest the circular GOI/vector, would yield one of two unique patterns of varying DNA fragment lengths. The patterns of both possible outcomes of the digestion were determined by the orientation of the GOI relative to the vector backbone, and thus the digestion was performed on the plasmids extracted from the sequenced sample having highest homology to the putative template. 1µg of GOI/plasmid DNA, 2µL of 0.02U/µL restriction enzyme(s) and 5µL of corresponding 5X buffer were added to 15µL water and digested for 3 hours at 37°C and run on a gel to determine fragment sizes. Once proper orientation of the GOI in pYES2.0 was confirmed, one colony from this original stock was inoculated into 5mL of liquid LB growth medium + 100µg/mL (CB) and incubated in a shaker at 37°C overnight followed by plasmid extraction. These GOI/pYES2.0 samples were stored at -20°C until the yeast transformation.

For all gel electrophoreses, 1.2% agarose gel was run at 110V for 30mins unless otherwise specified. Each well was loaded with the total reaction volume after adding 2µL of 6X DNA loading dye to the solution, and 5µL of 1kb marker was used. For RNA, 5µL of samples + 4µL of 5X RNA loading buffer + 11µL of water was incubated at 65°C for 5 mins before loading. 20% glycerol stock of each GOI/vector-containing *E. coli* strain was stored at -80°C.

3.2.3.6. Protein Sequence Analysis

Total aa length of each protein was determined by translating the nucleotide sequencing results of each gene in DNAstar's SeqBuilder; histidine boxes were found by aligning each protein sequence with the query sequence with which its comprising ESTs were found. Protein families were predicted using NCBI's conserved domain BLAST tool (2013b), conserved motifs predicted with the same conserved domain BLAST function and with ExPASy's Prosite scan tool (NCBI, 2013; Swiss Institute of Bioinformatics, 2013a) and transit peptide predictions were performed with ChloroP and TargetP online tools (Emanuelsson, 1999; Nielsen *et al*., 1997). Membrane-spanning regions and sizes were predicted using the TMPred online tool (Swiss Institute of Bioinformatics, 2013c), which could then be compared to the predictions by the Kyte-Doolittle hydropathy plots (1982).

Kyte-Doolittle hydropathy plots were generated using ExPASy's ProtScale function (Kyte & Doolittle, 1982; Swiss Institute of Bioinformatics, 2013b). Window size was set to 19, relative weight of the window edges compared to the window center was set at 100%, weight set to linear, and without normalizing the scale. Extinction coefficients were predicted with ExPASy's ProtScale and predicted values based on measurement in water at 280nm (M^{-1} cm^{-1}).

To determine if there was probability of AsFADX+ being a type I membrane-bound protein, which would also give better insight into its likely *in vivo* cellular destination, the sequence was analyzed for predicted chloroplast transit peptide sequences. This is of particular interest for AsFADX+, since it was unclear whether the 288 bp 5' segment preceding the putative translation initiation codon of AsFADX was indeed in-frame, and since the overall length of AsFADX+ was nearly 100 AA longer than all other putative oat FADs. Both ChloroP 1.1 (Emanuelsson *et al*., 1999) and TargetP 1.1 (Nielsen *et al*., 1997) Servers were used. ChloroP 1.1 is to detect presence of chloroplast transit peptides as well as their cleavage sites, using the default settings. TargetP 1.1 was used to predict presence and subcellular location of AsFADX+ as well as the 96aa N-terminus only. For TargetP 1.1, "plant" organism was selected, scope to

"Perform cleavage site predictions," and "no cutoffs; winner-takes-all (default)." The same TargetP 1.1. parameters were run again on AsFADX+ as well as the 96aa N-terminus only, but also selecting "specificity >0.95 (predefined set of cutoffs that yielded this specificity on the TargetP test sets)" were selected.

3.2.4. Results

3.2.4.1. Contig Construction from *Avena* ESTs

To identify oat genes involved in the biosynthesis of oat PUFA and HFAs, query sequences (the previously-characterized FADs and FAHs) were entered in the tBLASTn search function in both CORE and NCBI databases. Homologous ESTs identified were assembled into contigs. Putative ORFs in these contigs were determined in the oat sequences based on overall length of the gene, presence and positions of the HIS-boxes, length of intervals between HIS-boxes, presence and positions of putative transcription initiation and termination codons, and presence of termination codons upstream the putative start codon when compared to the query sequences. All queries used returned oat ESTs that, once assembled, comprised the CDS of one of four putative sequences: one *FAD2*-like, two *FAD3*-like, and one *FAD6*-like. Four distinct, putative oat genes were identified from three different FAD query sequences: the *Arabidopsis* FAD2 (AtFAD2) yielded one oat *FAD2*-like putative gene, *AsFAD2*, comprised of 54 oat ESTs. Query using a FAD3 from *Arabidopsis* (AtFAD3) found two oat *FAD3*-like putative genes, *AsFAD3-1* and *AsFAD3-2*, comprised of 94 and 101 oat ESTs, respectively. Finally, assembly of oat ESTs resulting from a query with an *Arabidopsis* FAD7 (*AsFAD7*) resulted in a fourth putative oat *FAD6*-like gene, *AsFADX* (with a longer variation, *AsFADX+*, as a fifth putative oat gene); these were comprised of 31 and 19 oat ESTs, respectively. The contigs are listed below, and putative protein products from each of these putative ORFs are aligned in Appendix 5.1 to highlight the distinctiveness of each.

3.2.4.1.1. *Δ*12 Desaturase/Hydroxylase query: FAD2-like

Using the FAD2 or FAH12s, 5 and 49 homologous oat ESTs were retrieved from NCBI and CORE databases, respectively. The entire contig length comprising these ESTs was 1736bp, presumably comprised of a 117bp 5' UTR, 1167bp ORF, and a 452bp 3' UTR.

3.2.4.1.2. *Δ*15 Desaturase/Hydroxylase query: FAD3-like

For the first oat *FAD3*-like sequence (*AsFAD3-1*), 12 and 82 homologous oat ESTs were retrieved from NCBI and CORE databases, respectively. For the second oat *FAD3*-like sequence (*AsFAD3-2*), 12 and 89 homologous oat ESTs were retrieved from NCBI and CORE databases, respectively. The entire contig lengths for *AsFAD3-1* and *AsFAD3-2* comprised of these ESTs were 1648bp and 1436bp, respectively; *AsFAD3-1* contig consists presumably of a 175bp 5' UTR, 1164bp ORF, and a 309bp 3' UTR, while *AsFAD3-2* differs slightly with a 204bp 5' UTR, 1146bp ORF, and an 86bp 3' UTR.

3.2.4.1.3. *ω*-3 Desaturase/Hydroxylase query: FAD6-like

For the shorter oat *FAD6*-like sequence (*AsFADX*), 15 and 16 homologous oat ESTs were retrieved from NCBI and CORE databases, respectively. For the longer oat *FAD6*-like sequence (*AsFADX+*), 9 and 10 homologous oat ESTs were retrieved from NCBI and CORE databases, respectively. These entire contig lengths for *AsFADX* and *AsFADX+* comprised of these ESTs were 1597bp and 1596bp, respectively. *AsFADX* contig consists presumably of a 332bp 5' UTR, 1083bp ORF, and a 182bp 3' UTR; in contrast, *AsFADX+* differs slightly with a 43bp 5' UTR, 1371bp ORF, and a 182bp 3' UTR.

These putative ORF sequences were used to design primers for amplification from cDNA template for cloning and expression studies.

3.2.4.2. Cloning of oat *FAD*-like genes

3.2.4.2.1. Primer Design

Primers listed in Table 4 to Table 7 were used amplification of each GOI. All were obtained from Sigma-Aldrich, 2149 Winston Park Dr, Oakville, ON L6H 6J8.

3.2.4.2.2. RNA Extraction & cDNA synthesis

CDC Dancer developing seed was selected as tissue sample for RNA isolation. Before any other experiment, RNA integrity must be confirmed as poor-quality (containing impurities) or degraded RNA may compromise subsequent experiments. After the TRIzol extraction of the total RNA from developing seeds, a denatured aliquot of each was run on an ethidium bromide (EtBr)-stained gel to verify presence, quality and integrity (Figure 17).

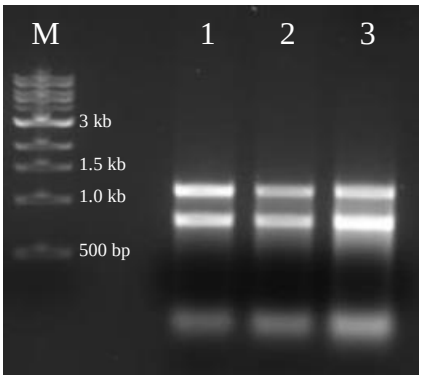

Figure 17. Biological triplicates of total RNA from milky stage CDC Dancer seed. The sample from which replicate 3 originates was used for subsequent DNAse treatment and cDNA synthesis. M=DNA marker.

As seen in Figure 17, clear bright bands representing two abundant RNA species, the 28 Svedberg units (S) and 18S ribosomal RNA (rRNA), are observed; the relative intensity ratio of the bands from these conserved molecules should be approximately 2:1. Sample 1 (Figure 17) was used as template for the reverse-transcribed first-strand cDNA. First-strand cDNA was successfully synthesized and stored at -20°C which was used for all subsequent experiments unless otherwise stated.

3.2.4.2.3. PCR amplification

The 1st strand cDNA synthesized from total RNA was used as template from which each specific gene was amplified; total PCR reactions were run on EtBr-stained agarose gels (Figure 18). Using primers targeting *AsFAD2* (Table 4), an amplicon of expected 1.2kb was amplified. For the *AsFAD3* targets, primers (Table 5) were used to amplify products of expected 1.2kb. Expected band sizes of 1.1 and 1.3kb were amplified using primers in Table 6, which targeted *AsFADX* and *AsFADX+*, respectively; amplification reactions were run on agarose gel for visualization.

Each amplicon of expected size (Figure 18) was cut from the gels, purified with the BioBasic kit, and eluted in water. To each of the purified, eluted DNA amplicons, a single deoxyadenosine triphosphate (dATP)-overhang was added to create cohesiveness with the pGEM-T vector, followed by ligation into pGEM-T vectors with T4 DNA ligase.

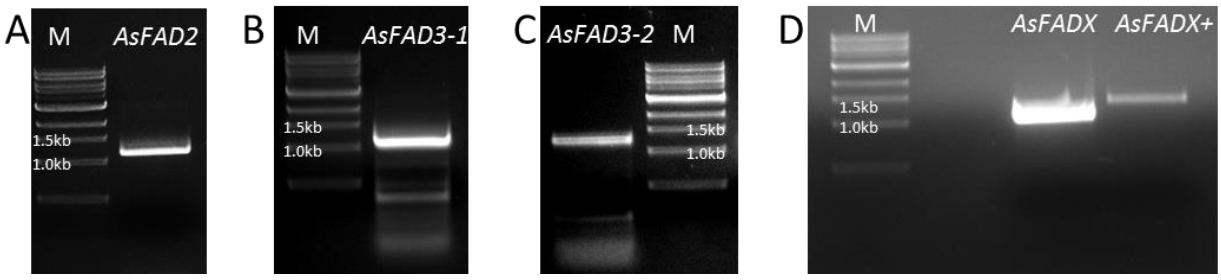

Figure 18. *FAD*-like amplicons, amplified from oat developing seed cDNA template.

AsFAD2 (A), *AsFAD3-1* (B), *AsFAD3-2* (C), *AsFADX* & *AsFADX*+ (D). M=DNA marker; kb=kilobase pair.

3.2.4.2.4. E. coli transformation

The recombinant plasmids were transformed into TOP10 *E. coli* cells via electroporation. After the electroporation was performed, selection for GOI-containing colonies was achieved by the antibiotic-containing plates, as well as the blue/white colony screening. Additionally a minimum of three white colonies from the overnight plated cultures were screened for the presence of each GOI via PCR amplification of each GOI with gene-specific primers. This was achieved by using a small amount of white colonies as template in each PCR reactions, followed by heat disruption of the cells and amplification using GOI-specific primers; PCR reaction products were run on the gel to confirm one distinct amplicon was visible in the expected position on the gel when compared to a marker.

After the colony screening, colonies positive for the GOI were inoculated into LB medium with carbenecillin overnight, followed by plasmid extraction from the cultures using the BioBasic kit. Recombinant plasmid samples from at least three different colonies were sent to Plant Biotechnology Institute (PBI) for sequencing.

3.2.4.3. Sequence Analyses

The aa sequences for each *Avena* GOI were determined after obtaining at least three nucleotide sequences of each insert inside the pGEM-T vectors extracted from *E. coli*. For each GOI, the sequence having the highest nucleotide homology to the previously-established putative CDS sequences (as described in 3.2.3.1) was determined to be the most accurate and thus the real sequence for each, and was subsequently translated to its protein product.

3.2.4.3.1. *Avena* sequence analyses: AsFAD2a

The ORF of *AsFAD2* is 1167 base pairs (bp) in length and encodes a protein 388 amino acids (aa) in length. This protein is predicted to have a molecular weight (MW) of 44,593 Daltons (Da) with an isoelectric point (pI) of 8.44. It is predicted to belong to the *Δ*12 FAD-like family (National Centre for Biotechnology Information, 2013b), and to not contain chloroplast-targeting sequences (Emanuelsson *et al*., 1999; Nielsen *et al*., 1997) (Figure 19).

```
ATGGGTGCCGGTGGCAGGATGACGGAGAAGGAGAGGGAGAAGCAGGAGCAGCTCGGCCGTGCCGACGTCG   70
 M  G  A  G  G  R  M  T  E  K  E  R  E  K  Q  E  Q  L  G  R  A  D  V

GCGCGACCCTCCAGCGCTCGCCGACGGACAAGCCGCCATTCACACTGGGGCAGATCAAGAAGGCCATCCC  140
G  A  T  L  Q  R  S  P  T  D  K  P  P  F  T  L  G  Q  I  K  K  A  I  P

ACCTCACTGCTTCCAGCGCTCGGTGATCAAGTCATTCTCCTACGTGGTCCATGACCTCGTCATCGTGGCT  210
  P  H  C  F  Q  R  S  V  I  K  S  F  S  Y  V  V  H  D  L  V  I  V  A

GCGCTCCTGTACGCCGCGCTGGTCTGGATCCCCACCCTCCCGAGCGTGCTGCAGCTGGGCGCCTGGCCGC  280
 A  L  L  Y  A  A  L  V  W  I  P  T  L  P  S  V  L  Q  L  G  A  W  P

TCTACTGGATCGTGCAGGGCTGCGTCATGACCGGCGTTTGGGTCATCGCGCACGAGTGCGGCCACCACGC  350
L  Y  W  I  V  Q  G  C  V  M  T  G  V  W  V  I  A  H  E  C  G  H  H  A

CTTCTCCGACTACTCGCTCCTCGACGACATCGTCGGCCTGGTGCTCCACTCGTGGCTGCTTGTCCCCTAC  420
  F  S  D  Y  S  L  L  D  D  I  V  G  L  V  L  H  S  W  L  L  V  P  Y

TTCTCGTGGAAGTACAGCCACCGTCGCCACCACTCCAACACCGGCTCCATGGAGCGTGACGAGGTGTTCG  490
 F  S  W  K  Y  S  H  R  R  H  H  S  N  T  G  S  M  E  R  D  E  V  F

TCCCCAAGCAGAAGGACGCGCTGGCCTGGTACACCCCATACATCTACAACAACCCCATCGGCCGGCTGGT  560
V  P  K  Q  K  D  A  L  A  W  Y  T  P  Y  I  Y  N  N  P  I  G  R  L  V

GCACATCGTGGTGCAGCTCACCCTCGGGTGGCCGCTGTACCTGTCGATGAACGCCTCGGGCCGCCCGTAC  630
  H  I  V  V  Q  L  T  L  G  W  P  L  Y  L  S  M  N  A  S  G  R  P  Y

GCGCGCTTCGCCTGCCACTTCGACCCCTACGGCCCCATCTACAACGACCGGGAGCGCATCCAGATCTTCA  700
 A  R  F  A  C  H  F  D  P  Y  G  P  I  Y  N  D  R  E  R  I  Q  I  F

TTTCGGATGTCGGTGTGGTGGCCACGGCGTTCACCCTCTTCAAGCTCGCGTCGGTGTTCGGGTTCTGGTG  770
I  S  D  V  G  V  V  A  T  A  F  T  L  F  K  L  A  S  V  F  G  F  W  W

GGTGGTGCGCATCTACGGTGTGCCGCTGCTGATCGTGAACGCTTGGCTGGTCCTCATCACCTACCTGCAG  840
  V  V  R  I  Y  G  V  P  L  L  I  V  N  A  W  L  V  L  I  T  Y  L  Q

CACACCCACCCGGCGCTGCCGCACTATGACTCCACCGAGTGGGACTGGCTGCGGGGGGGCGCTCGCCACCA  910
 H  T  H  P  A  L  P  H  Y  D  S  T  E  W  D  W  L  R  G  A  L  A  T

TGGACCGGGACTATGGCATCCTCAACCGCGTGTTCCACAACATCACGGACACGCACGTGGCGCACCACCT  980
M  D  R  D  Y  G  I  L  N  R  V  F  H  N  I  T  D  T  H  V  A  H  H  L

CTTCTCCACCATGCCGCACTACCATGCTATGGAGGCCACCAAGGCGATCAAGCCAATCCTCGGTGAGTAC 1050
  F  S  T  M  P  H  Y  H  A  M  E  A  T  K  A  I  K  P  I  L  G  E  Y

TACCAGTTCGACCCCACCCCCGTCGCCAAGGCCACATGGCGCGAGGCCAAGGAGTGCATCTACGTCGCGC 1120
 Y  Q  F  D  P  T  P  V  A  K  A  T  W  R  E  A  K  E  C  I  Y  V  A

CCACCGAGGACCGCAAGGGTGTCTTCTGGTACAGCAACAAGTTCTAG
P  T  E  D  R  K  G  V  F  W  Y  S  N  K  F  .
```

Figure 19. ***AsFAD2a*** **ORF cDNA and its translated protein sequence.** Histidine boxes are shaded.

3.2.4.3.2. *Avena* sequence analyses: AsFAD2b

A second allele of the same gene, whose products differ by 3 aa, was also confirmed; the polymorphisms occurring at base pairs 60, 688, and 756 result in amino acid variations (Figure 20). Of the five total SNPs (Figure 20), three nonsynonymous SNPs cause an amino acid substitution (Figure 21).

Both *AsFAD2a* & *AsFAD2b* are 1167 bp in length, encoding for a protein 388 aa long. The HIS-boxes are located at residues 111-115, 147-151, and 322-326, inclusively. The membrane spanning hydrophobic regions are predicted to be located at residues 63-81, 89-109, 123-143, 186-203, 258-276 (TMPred, 2013). This protein sequences are aligned in Figure 21 to illustrate the effect of the SNPs between both oat FAD2 isoforms, while comparing to the query sequence (Figure 21).

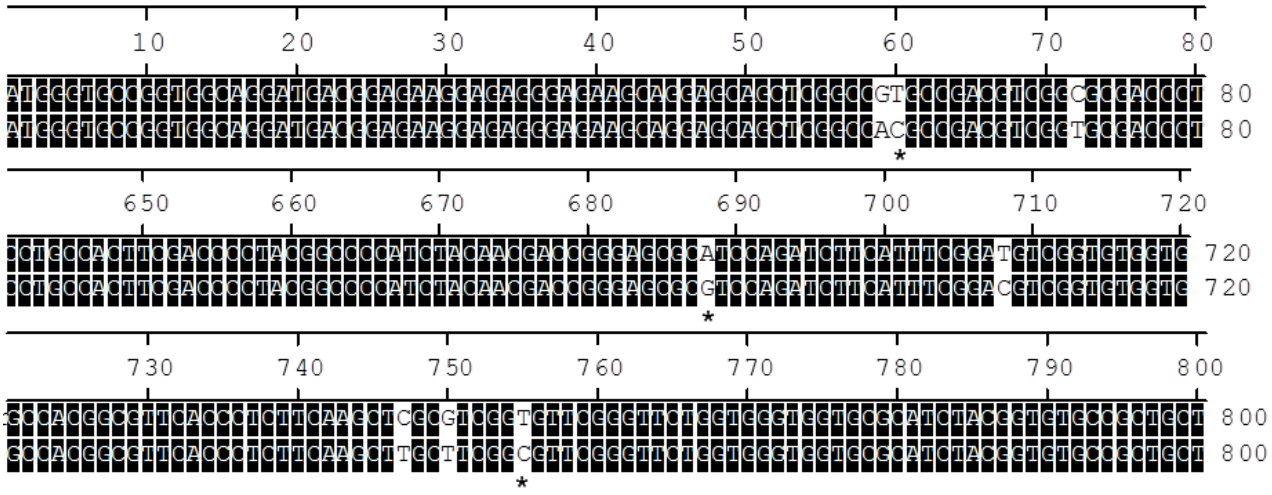

Figure 20. SNPs between *AsFAD2a* (line 1) and *AsFAD2b* (line 2). The polymorphisms occurring at base pairs 60, 688, and 756, as indicated by asterisks, result in amino acid variations.

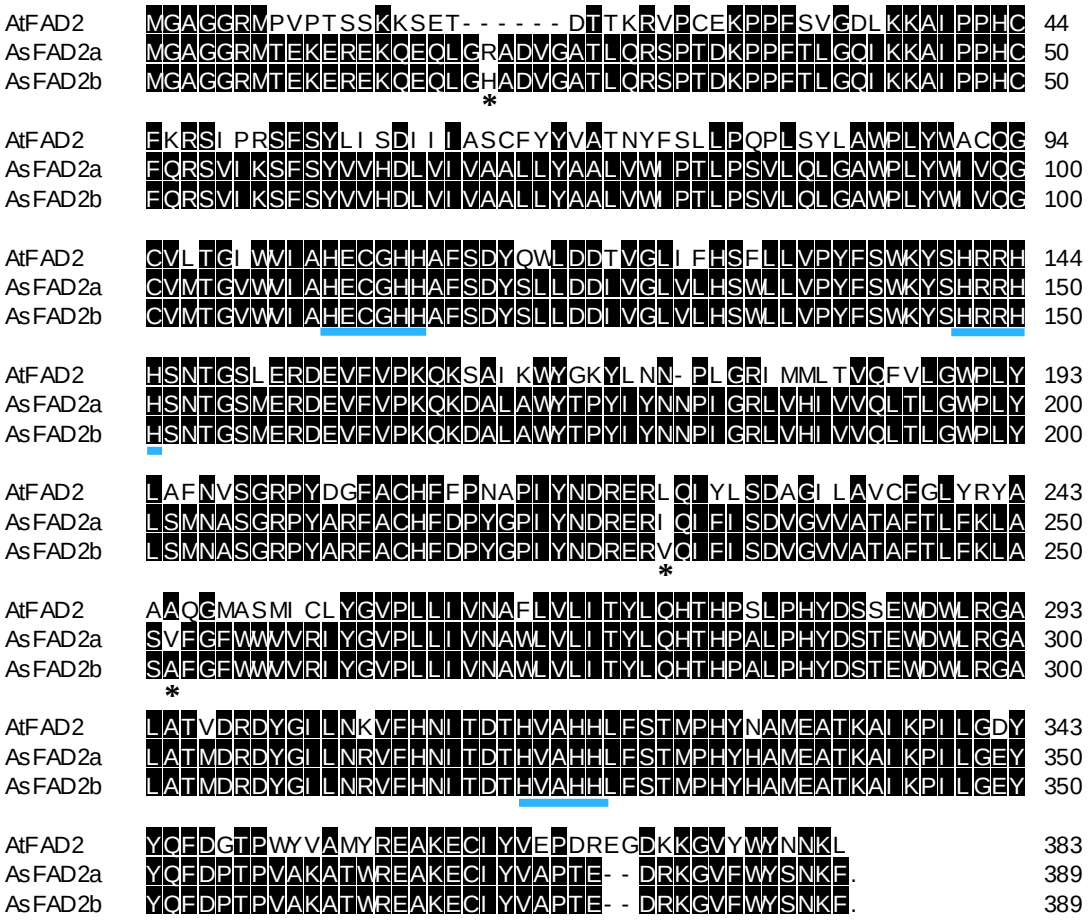

Figure 21. Query AtFAD2 aligned with both *Avena* FAD2 isoforms. Conserved residues are highlighted in black, histidine boxes are underlined, and the SNP-induced residue changes between the *Avena* FAD2s are marked with an asterisk.

Table 8. Relative percent identities of *Avena* FAD2s with their query sequences.

1	2	3	
	68.0	68.2	1
		99.2	2
			3

AtFAD2
AsFAD2a
AsFAD2b

3.2.4.3.3. *Avena* sequence analyses: AsFAD3-1

The FAD3 query retrieved ESTs of two distinct FAD3-like genes. The first, *AsFad3-1*, is 1164 bp in length and encodes for AsFAD3-1 protein of 387 aa, a predicted MW of 44,021 Da, and pI of 8.22 (Figure 22).

```
ATGGCCGCGGAAGCAATGAGGCAGCAGCGGCGGGAGCAGGAGGCCAGCTGCAAGGCCACCGAGGACCACC   70
 M  A  A  E  A  M  R  Q  Q  R  R  E  Q  E  A  S  C  K  A  T  E  D  H

GTTCCGTGTTCGACGCCGCCAAGCCGCCGCCCTTCCGCATCGGCGACGTGCGCGCCGCCGTGCCTGCCCA  140
R  S  V  F  D  A  A  K  P  P  P  F  R  I  G  D  V  R  A  A  V  P  A  H

CTGCTGGCGCAAGAGCCCCCTCCGCTCCCTCTCCTACGTCGCCCGCGACGTCGTCGTCGTGGCGGCGCTG  210
  C  W  R  K  S  P  L  R  S  L  S  Y  V  A  R  D  V  V  V  V  A  A  L

GCCGCCGCCGCCTGGGGCCTGGACAGCTGGGCCGTGTGGCCGCTCTACTGGGCGGTCCAGGGCACCATGT  280
 A  A  A  A  W  G  L  D  S  W  A  V  W  P  L  Y  W  A  V  Q  G  T  M

TCTGGGCGCTCTTCGTCCTCGGCCACGACTGTGGTCACGGGAGCTTCTCCGACAGCGGGACGCTCAACAG  350
F  W  A  L  F  V  L  G  H  D  C  G  H  G  S  F  S  D  S  G  T  L  N  S

CGTCGTCGGCCACCTGCTGCACACCTTCATCCTCGTCCCGTACAATGGCTGGAGGATCAGCCACAGGACG  420
  V  V  G  H  L  L  H  T  F  I  L  V  P  Y  N  G  W  R  I  S  H  R  T

CACCATCAGAACCATGGCCACATCGAAAAGGACGAGTCATGGCACCCGATCACCGAGGGGCTGTACCAGA  490
 H  H  Q  N  H  G  H  I  E  K  D  E  S  W  H  P  I  T  E  G  L  Y  Q

AACTGGAAGCACGGACCAAGAAACTACGCTTCTCAGTACCATTCCCGCTCCTGGCTTTCCCTGTCTACCT  560
K  L  E  A  R  T  K  K  L  R  F  S  V  P  F  P  L  L  A  F  P  V  Y  L

CTGGTACAGAAGCCCGGGCAAGACTGGCTCGCACTTCAACCCGAGCAGCGGTCTGTTTACCCCCAAGGAG  630
  W  Y  R  S  P  G  K  T  G  S  H  F  N  P  S  S  G  L  F  T  P  K  E

AGGCAAGACGTGATCATCTCCACCACCTGCTGGTTCACGATGATTGCGCTGCTCATCGGTATGGCATGCA  700
 R  Q  D  V  I  I  S  T  T  C  W  F  T  M  I  A  L  L  I  G  M  A  C

TGTTCGGCCCAGTACCGGTGCTCAAGGTCTACGGGGTTCCATATGTTGTGTTTGTGATGTGGCTTGATTT  770
M  F  G  P  V  P  V  L  K  V  Y  G  V  P  Y  V  V  F  V  M  W  L  D  L

GGTGACTTATCTTCACCACCATGGCCACCAGGATCTTCCTTGGTACCGTGGCGAGGAATGGAGCTACCTC  840
  V  T  Y  L  H  H  H  G  H  Q  D  L  P  W  Y  R  G  E  E  W  S  Y  L

CGTGGTGGCTTGACGACCGTTGACCGAGACTACGGGTGGATCAACAACATCCACCATGACATCGGCACTC  910
 R  G  G  L  T  T  V  D  R  D  Y  G  W  I  N  N  I  H  H  D  I  G  T

ATGTCATCCACCACCTCTTCCCCCAAATACCTCACTACCACCTAGTAGAAGCAACCAAGGCAGCGAGCCC  980
H  V  I  H  H  L  F  P  Q  I  P  H  Y  H  L  V  E  A  T  K  A  A  S  P

AGTATTGGGTAGATACTACCGGGAGCCGGAGAAGTCAGGCCCGCTGCCAGTTCACCTTGTCAGCGTCCTC  1050
  V  L  G  R  Y  Y  R  E  P  E  K  S  G  P  L  P  V  H  L  V  S  V  L

CTCAAGAGCTTGAGAGTTGATCACTTTGTCAGCGACGAGGGAGATGTCGTCTTCTACCAAACTGACCCCA  1120
 L  K  S  L  R  V  D  H  F  V  S  D  E  G  D  V  V  F  Y  Q  T  D  P

GCTTGAGCGGCGACAACCGGATCGGAACTGACAAGCACAAGTGA
S  L  S  G  D  N  R  I  G  T  D  K  H  K  .
```

Figure 22. *AsFAD3-1* ORF cDNA and its translated protein sequence. Histidine boxes are shaded.

The HIS-boxes occur at residues 102-106, 138-142, and 304-308 aa. This protein is also predicted to be in the ω-6 FAD families (National Center for Biotechnology Information, 2013b; UniProt, 2013). There are two N-myristoylation sites at positions 113-118 and 282-287 aa (MyHits, 2013). Although neither ChloroP nor TargetP predicted a chloroplast targeting peptide, there are five predicted transmembrane regions at positions 80-101, 114-134, 172-189, and 214-235, 240-261 aa using TMPred (Swiss Institute of Bioinformatics, 2013c).

3.2.4.3.4. *Avena* sequence analyses: AsFAD3-2

A second *FAD3*, *AsFAD3-2*, was identified using the same query sequence. The ORF of this *FAD3* gene is 1146 bp in length, and encodes for a 381 aa protein. This protein has a predicted MW of 43,415 Da, and a pI of 7.81 (Figure 23).

AsFAD3-2 has three conserved HIS-boxes at positions 96-100, 132-136, and 298-302 aa. The predicted membrane-spanning regions are at positions 63-81, 89-109, 123-143, 186-203, and 258-276 aa (Swiss Institute of Bioinformatics, 2013c). It is predicted to be part of the 'Δ12 FAD-like family' and 'FA_desaturase family' (National Centre for Biotechnology Information, 2013b). One N-myristoylation site is predicted at position 276-281 aa (SIB, 2013). No chloroplast targeting sites are predicted (Emanuelsson *et al*., 1999; Nielsen *et al*., 1997). The products of the two oat *FAD3*s are highly homologous, but can be distinguished by the N- and C-termini (Figure 24).

```
ATGGGCGCGGCGGCGAGGAGGGCGCCCGAGCAGGAGCAGAGCTGCAAGGCCACGGAGGAC   60
 M  G  A  A  A  R  R  A  P  E  Q  E  Q  S  C  K  A  T  E  D

TTCGACGCCGCCAAGCCCCCACCCTTCCGCATCGGGGACGTGCGCGCCGCCGTGCCCGCG  120
 F  D  A  A  K  P  P  P  F  R  I  G  D  V  R  A  A  V  P  A

CACTGCTGGCGCAAGAGCCCCCTCCGCTCCCTCTCCTACGTCGCCCGCGACGTCGCCGCC  180
 H  C  W  R  K  S  P  L  R  S  L  S  Y  V  A  R  D  V  A  A

GTCGCCGCGCTCGCCCTCGCAGCCTGGGGCATCGACACCTGGGCCGTCTGGCCGCTCTAC  240
 V  A  A  L  A  L  A  A  W  G  I  D  T  W  A  V  W  P  L  Y

TGGGCGGCGCAGGGCACCCTCTTCTGGGCCCTCTTCGTCCTCGGACACGACTGTGGGCAC  300
 W  A  A  Q  G  T  L  F  W  A  L  F  V  L  G  H  D  C  G  H

GGGAGCTTCTCGGACAGCGCGACGCTCAACAGCGTCGTCGGCCACCTGCTGCACACCTTC  360
 G  S  F  S  D  S  A  T  L  N  S  V  V  G  H  L  L  H  T  F

ATCCTCGTCCCATACAATGGATGGAGGATCAGCCACAGGACACACCACCAGAACCATGGC  420
 I  L  V  P  Y  N  G  W  R  I  S  H  R  T  H  H  Q  N  H  G

CACATCGACAAGGACGAGTCATGGCACCCGATTACCGAGAATGTGTACAAGGAGCTGGAG  480
 H  I  D  K  D  E  S  W  H  P  I  T  E  N  V  Y  K  E  L  E

CCAAGCACCAAGAAGCTACGCTTCTCGCTACCGTACCCGCTCCTGGCTTTTCCTGTCTAC  540
 P  S  T  K  K  L  R  F  S  L  P  Y  P  L  L  A  F  P  V  Y

CTCTGGTACAGAAGCCCTGGCAAGAACGGTTCACACTTTAACCCAAGCAGCGATCTGTTC  600
 L  W  Y  R  S  P  G  K  N  G  S  H  F  N  P  S  S  D  L  F

AGCCCCAAGGAGAGGCGTGACGTGATCATTTCAACCACTTGCTGGTTCACGATGATCGCG  660
 S  P  K  E  R  R  D  V  I  I  S  T  T  C  W  F  T  M  I  A

CTGCTCATCGCCATGGCGTGTGTGTTCGGGCCAGTGCCGGTGCTCAAACTGTACGGGGTC  720
 L  L  I  A  M  A  C  V  F  G  P  V  P  V  L  K  L  Y  G  V

CCATATGTTGTGTTTGTGATGTGGCTTGATTTGGTGACGTACCTTCACCACCATGGTCAC  780
 P  Y  V  V  F  V  M  W  L  D  L  V  T  Y  L  H  H  H  G  H

CAGGACCTCCCTTGGTATCGCGGCGAGGAATGGAGCTACCTCCGTGGTGGCCTGACGACC  840
 Q  D  L  P  W  Y  R  G  E  E  W  S  Y  L  R  G  G  L  T  T

GTGGACCGGGATTATGGGTGGATCAACAACATCCACCATGACATTGGCACTCATGTCATC  900
 V  D  R  D  Y  G  W  I  N  N  I  H  H  D  I  G  T  H  V  I

CACCACCTCTTCCCCCAAATACCTCACTACCACCTAGTGGAAGCAACTAAGGCAGCAAGG  960
 H  H  L  F  P  Q  I  P  H  Y  H  L  V  E  A  T  K  A  A  R

CCAGTACTGGGAAGATATTACCGTGAGCCGGAGAAGTCAGGTCCACTGCCAACTCACCTC 1020
 P  V  L  G  R  Y  Y  R  E  P  E  K  S  G  P  L  P  T  H  L

TTCAGCATCCTCCTCAGGAGCTTAAGAGTCGATCACTTCGTCAGTGATGTTGGAGATGTT 1080
 F  S  I  L  L  R  S  L  R  V  D  H  F  V  S  D  V  G  D  V

GTCTTCTACCAAACTGACCCAAGCTTGGACAGCGATAGCTGGACGAAAAATGGCAAGCAA 1140
 V  F  Y  Q  T  D  P  S  L  D  S  D  S  W  T  K  N  G  K  Q

AAGTGA
 K  .
```

Figure 23. *AsFAD3-2* ORF cDNA and its translated protein sequence. Histidine boxes are shaded.

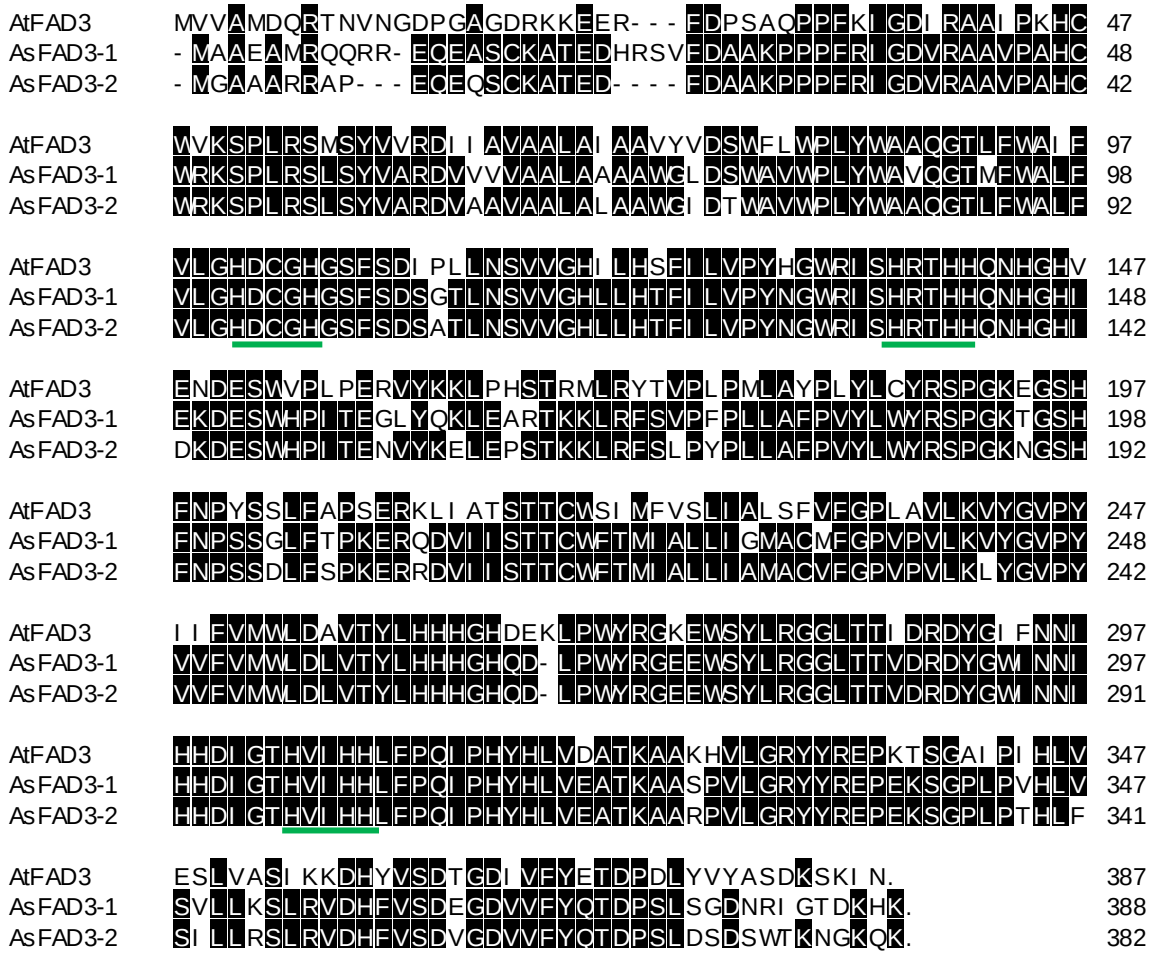

Figure 24. Both *Avena* FAD3s compared to the query *Arabidopsis* FAD3. HIS-boxes are underlined.

Table 9. Percent identity of the *Avena* FAD3s as compared to the AtFAD3.

1	2	3	
	65.9	66.9	1
		88.2	2
			3

AtFAD3
As FAD3-1
As FAD3-2

3.2.4.3.5. *Avena* sequence analyses: AsFADX & AsFADX+

The ORF of *AsFADX* is 1080 bp in length and encodes a protein 360 aa in length. This protein is predicted to have a MW of 42,309 Da with a pI of 8.17 (Figure 25).

As there was a substantial, continuous sequence upstream of *AsFADX*, with three additional putative translation initiation codons and few ESTs available in that region, it was unclear whether *AsFADX* or the longer version or both were functional genes or if one was an artifact. The longer version, *AsFADX+*, was thus also isolated after assembling the putative contig with the additional 288 bp (96 aa) region upstream from the translation initiation codon of *AsFADX*, termed '*AsFADX+*.' The region of 288 bp upstream from the putative ORF of *AsFADX*, when translated, showed a continuous segment of 96 aa, shifted out-of-frame relative to the *AsFADX* ORF by one nucleotide. In an area of seven repeated nucleotides at a position 114 bp upstream from the putative ORF of *AsFADX*, which was otherwise identical across the eight ESTs (from which that region of the contig was assembled), there was disagreement on one nucleotide across these ESTs, as well as one nucleotide gap slightly upstream of this region in two of the ESTs. Deleting the nucleotide responsible for causing the disagreement across the ESTs resulted in the entire 288 bp region at the 5' end upstream from the putative ORF of *AsFADX* to shift into frame, bringing both *AsFADX* putative ORF and the upstream region into one frame to form *AsFADX+*.). No additional putative translation initiation codons upstream of those of *AsFADX+* were identified; putative UTRs can be examined in Appendix 5.2. Once sequenced, the results showed the longer 5' region of the putative ORF of *AsFADX+* to be in-frame with the putative ORF of *AsFADX* (Figure 25) which suggests that *AsFADX* is an incomplete ORF, despite its length being more similar to the expected length of a *FAD* than that of *AsFADX+*.

AsFADX+ is 1368 bp in length and encodes for a protein 456 aa in length. This protein is predicted to have a MW of 53164Da with a pI of 9.4. Both AsFADX and AsFADX+ have three conserved HIS-boxes; these are at positions 84-88, 120-124, and 280-284 aa, and at 180-184, 216-220, and 376-380 aa, respectively. TMPred predicts four membrane spanning regions for both proteins (Swiss Institute of Bioinformatics, 2013c). These are located at residues 42-58, 62-82, 96-115, and 190-208 aa in FADX, and in FADX+ at 138-154, 158-178, 192-211, 286-304 aa.

Figure 25. *AsFADX*+ ORF cDNA and its translated protein sequence. Histidine boxes are shaded. The black arrow indicates the translation initiation codon of the shorter *AsFADX*, while the white arrow indicates the position of the nucleotide that was deleted and shifted the upstream nucleotide segment in-frame with *AsFADX* to result in three possible translation initiation codons of the putative *AsFADX*+ (indicated by the grey arrows).

Both AsFADX and AsFADX+ are predicted to each have two N-myristoylation sites at residues 73-78 and 260-265, and at 169-174, and 354-360, respectively (SIB, 2013). Both are predicted to belong to FAD-like and FA_desaturase protein families when analyzed with NCBI's conserved domain tool (2013b). Neither was predicted to have chloroplast targeting peptide sequences (Emanuelsson *et al*., 1999; Nielsen *et al*., 1997).

Additionally, the 96 aa N-terminal of *AsFADX+* was submitted separately into the ChloroP 1.1 Server and predicted to not be a chloroplast-targeting peptide sequence.

The AsFADX (and AsFADX+) product sequences yield relatively low (<30%) protein homology to the AtFAD7 with which its comprising ESTs were found (Figure 26; Table 10). (An additional alignment of AsFADX+ with all *Arabidopsis* FADs can be found in Appendix 5.3).

To investigate if the unique sequence inside the third HIS-box was consistent with another class of desturase or hydroxylase, it was aligned with other HIS-box-containing FADs and FAHs to specifically examine the HIS-box regions (Figure 27). The AsFADX sequences yield a unique aa pattern inside the third HIS-box as emphasized in Figure 27C. The third conserved HIS-box of the AsFADX sequences, although ESTs were retrieved from a FAD7 query, showed aa identity unique from all other HIS-box-containing proteins. Although the sequence is not identical within th HIS boxes, valine (V) and isoleucine (I) are extremely similar in size, structure and properties as they differ by only one carbon atom, so the catalyitic function is likely retained, and AsFADX is likely a FAD6.

Although based on the HIS-boxes, the sequences suggest that the AsFADXs are FAD6s, but this comparison shows the unique aa residue pattern inside the third histidine box of FADX & FADX+, indicated by the bracket and black arrows. Despite the aa difference, the biochemical similarity between the third HIS-box of AsFADX and that of AtFAD6 suggest AsFADXs fall under the FAD6 classification.

AsFADX+ was searched back into NCBI as the query sequence, using the tBLASTn function and general parameters not specific to any organism. Several matches were found sharing various levels of protein homology within a wide range of sequence query coverges, however each was either a mRNA/cDNA or predicted protein sequence. Of particular interest to this study, and included in the tBLASTn results was two mRNA sequences originating from the leaf (GenBank Accession # DV482249.1) and flower (GenBank Accession # GT830484.1) of

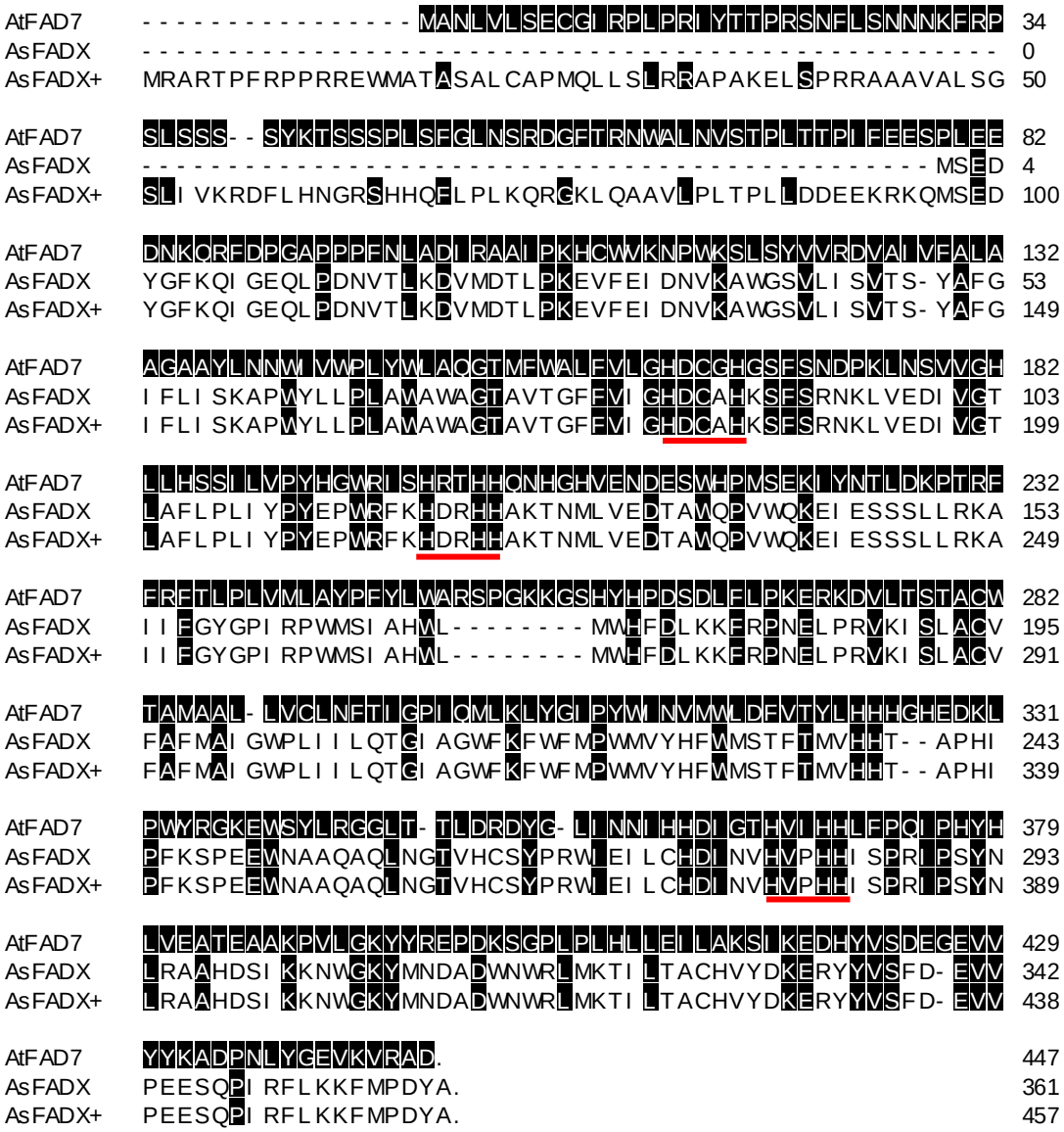

Figure 26. **The *Arabidopsis* FAD7 query aligned with both lengths of the *Avena* FAD-like sequence.** The third histidine box is unique from other FAD classes. Homologous regions are highlighted in black. Conserved histidine boxes are underlined.

Table 10. Relative percent identities of the query FAD7 and the resulting *Avena* FAD6-like protein sequences.

1	2	3		
	27.0	24.7	1	As FAD7
		100.0	2	As FADX
			3	As FADX+

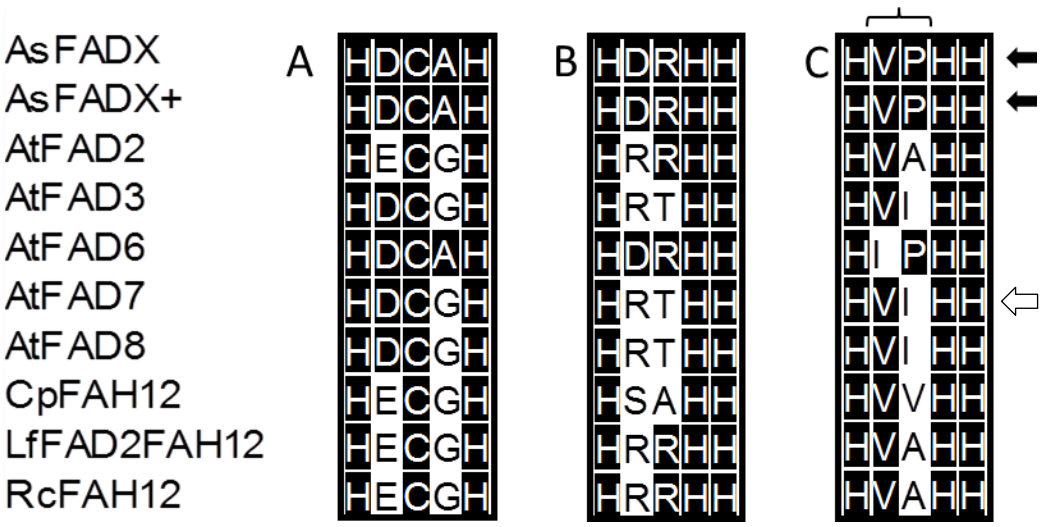

Figure 27. HIS-box protein alignment. AsFADX & AsFADX+ are shown in lines 1 and 2, with previously characterized FADs (lines 3-7), *Δ*12 hydroxylases (lines 8 & 10), and a bifunctional *Δ*12 hydroxylase/desaturase (line 11). At=Arabidopsis thaliana; As=*Avena sativa*; Rc=*Ricinus communis*; Cp=Claviceps purpurea; Lf=*Lesquerella fendleri.* Black arrows indicate the 3rd HIS-box of the AsFADX proteins, and the white arrow indicates the 3rd HIS-box of the query AtFAD7 with which they were found.

Brachypodium distachyon (*Bd*) sharing 96% and 95% protein identity (within 61% and 57% query coverage) to the AsFADX+ query sequence, respectively.

Although both of the *Brachypodium* sequences were cDNA clones, the second sequence had the same "HVPHH" sequences in the third putative HIS-box (Figure 28) with high similarity to a FAD6. This prompted a more specific search within the *Brachypodium distachyon* genome.

Brachypodium distachyon is a member of the Pooideae family of annual grasses and is a model organism of growing interest and applicability for such studies (The International Brachypodium Initiative, 2010). This grass has a relatively short flowering period and small genome, making it an ideal model; although to date it has not been explored as deeply as *Arabidopsis*, as a monocot *Brachypodium* may be more ideal as a reference to oat, although queries using FADs from either organism should be effective as dicots were not distinct from monocots until approximately 150 million years ago (Chaw *et al*., 2004).

The predicted *Brachypodium distachyon* FAD2 (Accession # XP_003574539.1, termed "BdFAD2" for these purposes and encoded by the predicted gene termed "*BdFAD2*," accession

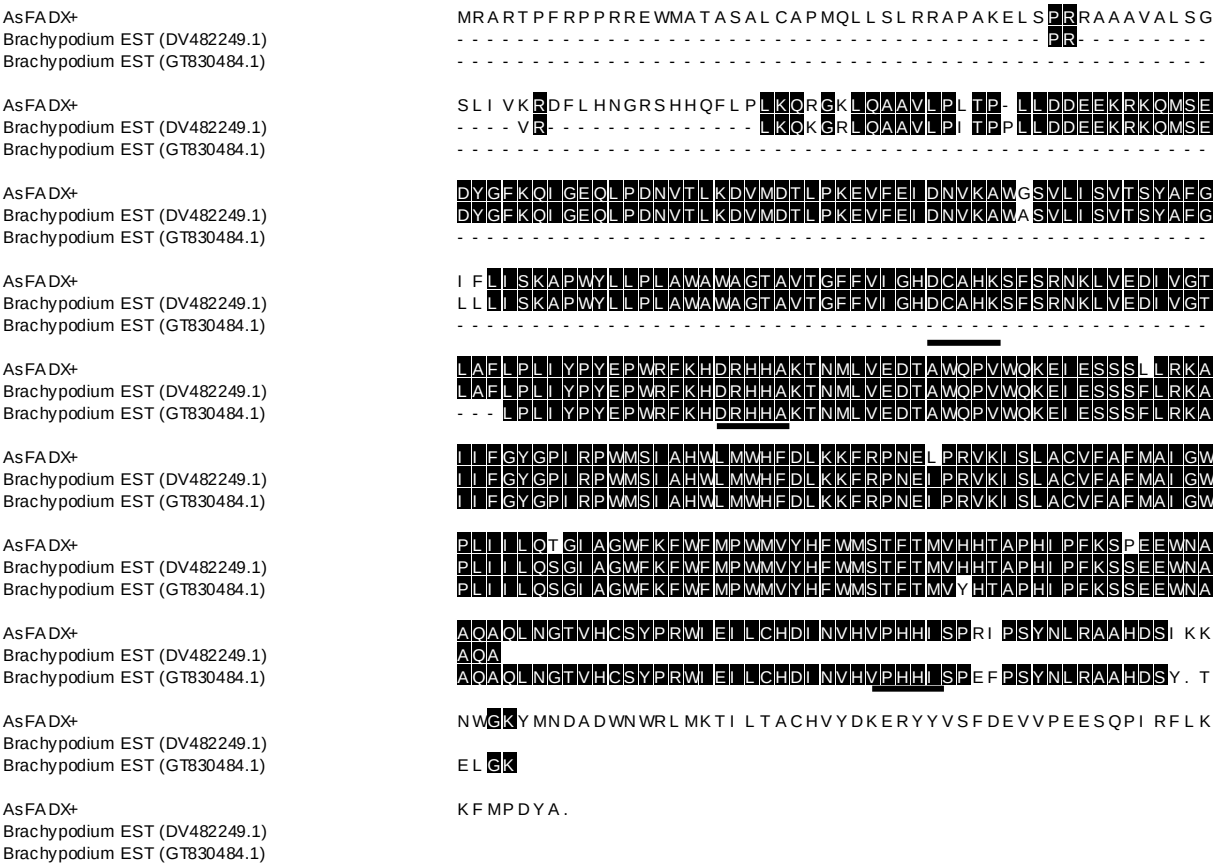

Figure 28. Protein alignment of AsFADX+ with the homologous *Brachypodium* ESTs, DV482249.1 and GT830484.1. Histidine boxes are underlined.

Table 11. Protein percent identities of both *Brachypodium* ESTs with AsFADX+.

1	2	3	
	96.2	94.0	1
		99.3	2
			3

1 AsFADX+
2 Brachypodium EST (DV482249.1)
3 Brachypodium EST (GT830484.1)

number XM_003574491) and a predicted FAD3/ω-3 desaturase (Accession # XP_003558157.1, termed here "BdFAD3" encoded by the predicted gene termed "*BdFAD3*," accession number XM_003558109.1) sequences were retrieved from NCBI to align with the AsFADX+ query sequence, as shown in Figure 29.

Figure 29. A ClustalW protein alignment of the AsFADX+ with the *Brachypodium distachyon* (Bd) FAD2 (BdFAD2) and FAD3 (BdFAD3). Histidine boxes are underlined. The arrow indicates the location of the beginning of the shorter AsFADX.

Table 12. Relative percent protein identities of the sequences aligned in Figure 29.

1	2	3		
	92.8	26.4	1	AsFADX+
		26.5	2	BdFADX
			3	BdFAD3

It is generally believed that FAD3s diverged from FAD2s, and FAHs diverged from either FAD2s or FAD3s throughout evolution. To compare these oat FAD2-like sequences of this study with the *Arabidopsis* FAD2 query as well as with the *Brachypodium* BdFAD2, all FAD-like protein sequences from this thesis were aligned with these two putative progenitors (Figure 30).

Figure 30. Protein alignment of all *Avena* FAD-like sequences in this study (sequences 2-7), compared with the AtFAD2 (sequence 1) and BdFAD2 (sequence 8). HIS-boxes are underlined.

Table 13. Relative percent identities of all *Avena* FAD-like protein sequences identified in this study, compared with the FADs of both model organisms. At=*Arabidopsis thaliana;* As=*Avena sativa*; Bd= *Brachypodium distachyon.*

1	2	3	4	5	6	7	8		
	68.0	68.2	34.2	34.9	20.1	19.6	19.9	1	AtFAD2
		99.2	36.5	37.4	20.6	19.8	20.4	2	AsFAD2a
			36.5	37.1	20.6	19.8	20.4	3	AsFAD2b
				88.2	24.9	24.4	24.7	4	AsFAD3-1
					25.1	25.1	25.7	5	AsFAD3-2
						100.0	96.4	6	AsFADX
							92.8	7	AsFADX+
								8	BdFAD2

The comparison indicated four distinct enzymes: a FAD2 (in two isoforms), two FAD3s, and a FAD6-like (with potentially a transit peptide sequence at the N-terminus, despite software prediction tools refuting this conjecture). The FADXs are slightly anomalous relative to the other oat proteins in this study based on their HIS-box sequence, and in length; AsFADX+ is nearly ~100 aa longer than the others, while AsFADX is ~20 aa shorter, and both have gaps of ~10 aa preceding the first HIS-box and ~20 aa between the first and second HIS-boxes. Generally, there is high conservation in regions surrounding the HIS-boxes, particularly ~10-20 aa preceding the first HIS-box. There are other seemingly HIS-rich regions, although outside of the conserved "HIS-box" sequences; one precedes the 3rd HIS-box by 5 aa, a second by ~50 aa, and another follows the 3rd HIS-box by ~7 aa. Amongst the oat proteins of this study, AsFAD3-2 is most similar to AsFAD2 sharing 37.6% identity, while AsFAD3-1 is slightly less homologous sharing 36.8% identity. AsFADX shares only 22.7% identity with AsFAD2, while AsFADX+ is least similar to AsFAD2 sharing 22.0% identity.

A graphical representation of the relative lengths of each oat FAD-like sequence and relative positions of each conserved region encoding for the HIS-boxes is better understood when aligned at the C-terminal ends (Figure 31).

The phylogenetic relationship between the evolutionary divergences of the oat FAD-like proteins (aligned in Figure 30) from a FAD2 progenitor can be better visualized with a phylogenetic tree (Figure 32), as well as their evolutionary relationships to other FAD and FAH classes of proteins (Figure 33).

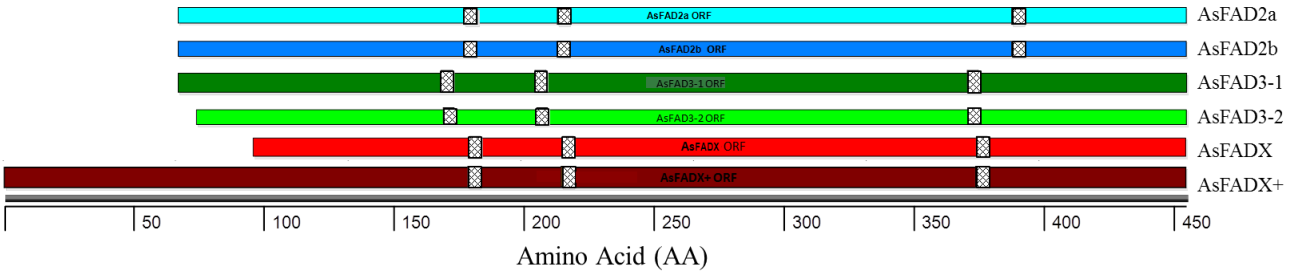

Figure 31. A graphical representation of each oat FAD-like sequence aligned from the C-terminal end. Hatched regions indicate relative positions HIS-boxes. ORF=open reading frame. As=*Avena sativa.*

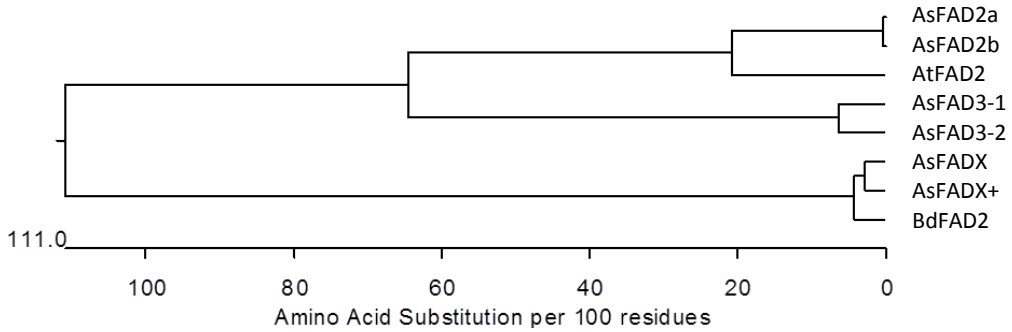

Figure 32. A phylogenetic tree comparing all *Avena* FAD-like sequences with AtFAD2 and BdFAD2. At=*Arabidopsis thaliana*; As=*Avena sativa*; Bd= *Brachypodium distachyon.*

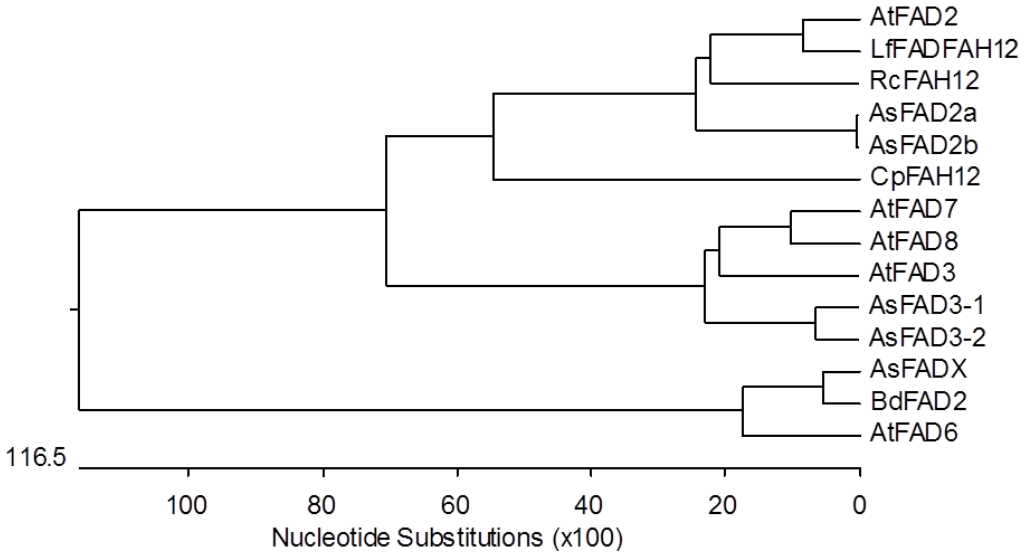

Figure 33. A phylogenetic tree comparing all *Avena* FAD-like sequences with the different *Arabidopsis* FAD queries, FAH queries, and the hypothetical *Brachypodium* FAD. As=*Avena sativa*, Bd=*Brachypodium*, At=*Arabidopsis thaliana*, Lf=*Lesquerella fendleri*, Cp=*Claviceps purpurea*, Rc=*Ricinus communis*.

As expected, the AsFAD2s are highly homologous and most closely related to the previously-characterized FAD2. The AsFAD3s are less homologous to the AtFAD2 than the AsFAD2s. Interestingly, the BdFAD2 is most closely related to the AsFADXs, although the BdFAD2 is merely a predicted protein.

In Figure 33, there are three distinct clusters of related proteins. In the first cluster, the oat FAD2s are most closely related to the castor bean hydroxylase, but are homologous with the FAHs and FAD2s, overall. The oat FAD3s are share highest homology with the AtFAD3, but are also highly homologous with the characterized FAD7 and FAD8, as observed in the second cluster. The third cluster shows the homology of the oat FADX with the characterized AtFAD6 as well as with the predicted BdFAD2

3.2.5. Discussion

As multiple codons may encode for one amino acid, the preliminary BLAST searches were based on more highly-specific amino acid sequence of the established FAD2 and FAD-like FAH enzyme sequences. The BLAST search that was employed (tBLASTn) compared the query protein sequence to any resulting matches across all six possible translated frames of the overlapping ESTs from the EST databases, which would later become the putative oat contig. Ideally, the source of query sequences would originate from plant species more closely related to oat, such as *Hordeum vulgare* or *Triticum aestivum*, rather than an oilseed such as *Brassica napus*, although the lesser-related sequences were used when information was unavailable from the more closely related organisms. As there has not been a FAH15 previously identified and characterized, and therefore no direct reference, their characterizations must begin by the extrapolation of information from indirect but evolutionarily-related sequences, a FAD2, FAD3, and FAHs.

Once new putative oat sequences were identified, their nucleotide sequences were used as the query sequence to BLASTn (nucleotide) search within the oat-specific EST database. Contigs were constructed from various oat ESTs available from the unpublished CORE database that had high protein (>67% identity) homology to the previously-established FAD or FAH query sequences. Any oat contig matches to the NCBI *FAD* or *FAH* query sequences, assumed to partially contain nucleotide sequences of the desired *FAH15*, were downloaded for assembling new oat contigs using DNAstar's SeqMan program. The new contigs were then edited for any sequencing errors or gaps in the contig consensus sequences (when compared to the queries or

amongst the total set of overlapping ESTs), translated to the putative protein sequence in DNAstar's EditSeq, and finally compared with one another as well as with their query sequences in DNAstar's MegAlign to (1) determine the full length ORFs and conserved HIS boxes are present, homologous to other FAD or FAHs; and (2) identify enough homology to confirm identity as a probable candidate as a FAH, while having adequate divergence to reasonably hypothesize to be a putative oat FAD or FAH and thus justify pursuing cloning of its gene. The putative GOIs were cloned by PCR using two specific primers at both ends of the ORF and encompassing the putative start and stop codon, and designed with specific restriction sites protruding beyond the ends of the ORF.

Given the polyploidy nature of the *Avena sativa* genome, and the common belief that hexaploids have evolved from the hybridization of either diploids with diploids, or diploids with tetraploids, thus two distinct isoforms of each *FAD*-like oat gene are expected to have originated from a tetraploid progenitor or, three paralogs of each *FAD*-like gene in hexaploids. Both FAD2 and FAD3 queries each identified two isoforms of oat *FAD2*s and *FAD3*s, respectively. Although the two AsFAD2s differed by only three amino acid residues, it was worthwhile to pursue their functional characterizations, particularly in the context of searching for a putative FAH; it has been demonstrated previously that as few as 3 amino acid changes can convert a FAD to a FAH (Broun *et al.*, 1998). Although both FAD2-like oat genes were desaturases, the substrate-product conversion efficiency difference is not unexpected.

Since 15-OH 18:2-9*c*,12*c* is known to be present in all diploid, tetraploid, and hexaploid oat classes, the evolution of the number of paralogs of the *AsFAH15* is expected to be the same as with *AsFAD3*; unexpectedly, no additional *FAD3*-like genes were identified from the ESTs available. However, it is possible that one of the putative *AsFAD3*s is actually the *AsFAH15*, in which case the two enzymes share very high homology, but the presence of only one gene coding for an AsFAD3 and one for an AsFAH15 would also be unexpected. Moreover, it is possible (to a lesser extent) that the putative AsFAD3s have dual function primarily as a *Δ*15 desaturase and secondarily as a *Δ*15 hydroxylase, considering such enzymes have been confirmed and considering the relative 18:3-9*c*,12*c*,15*c* to 15-OH 18:2-9*c*,12*c* levels accumulated in the seed. All classes of HIS-box-containing FAD-like sequences were used as query sequences to maximize the identification of homologous *FAD*-like ESTs from the oat EST database. Although query sequences from all available classes of the HIS-box-containing

proteins were queried, only four distinct *Avena* genes were defined - a *FAD2*-like, *AsFAD2*; two *FAD3*-like, *AsFAD3-1* and *AsFAD3-2*; and a *FAD6*-like, *AsFADX* (as well as an extended variation, *AsFADX+*, with additional 288bp upstream of the translation initiation codon of *AsFADX*).

As a reference to all of the oat genes and proteins here, a previously-characterized plant FAD2 from *Arabidopsis* (AtFAD2) was used in the same online tools and analyses for comparison (Okuley *et al*., 1994), as well as a predicted FAD2 from *Brachypodium* (BdFADX). Except for AsFADX+, the all *Avena* genes in this study are analogous with AtFAD2: AtFAD2 is 383 aa with the three conserved HIS-boxes occurring at positions 105-109, 141-145, and 315-319 aa. There are five predicted membrane spanning regions at positions 55-71, 83-103, 117-137, 179-196, 225-245 and 251-272 aa. There are no transit peptide sequences predicted, and unexpectedly there are no ER-targeting C-terminus sequences predicted. Table 14 summarizes sequence information of all oat genes and proteins, in comparison to the two model organism FAD2s.

Various software tools were employed to predict the number of transmembrane domains of these oat desaturases. However, the number varies with the software used. The discrepancy between the predicted number of transmembrane regions from the different tools employed suggests the unreliability of these types of tools, and therefore the hesitation with which the predicted topology structures must be taken into consideration. As well, the topology predictions require some manipulation of membrane-spanning versus integral membrane regions in order to achieve the proper putative orientation of the catalytic sites, for example the HIS-boxes, relative to one another.

With the exception of the AsFADX-type proteins, all the encoded proteins are within 10 aa of one another in length. The shorter length of AsFADX suggests that some part of the sequence is lacking and thus some length beyond that sequence should be taken into consideration. Additionally, the relative positions of the HIS-boxes aligned with the C-termini ending in nearly the same position, thus examination of the sequence upstream from the putative start codon of the ORF coding for AsFADX was logical. However, the nearest upstream start codons were substantially further than expected, based on the other *FAD*-like gene lengths, so it was unclear whether AsFADX or the longer AsFADX+ was the ORF sequence, if one was an artifact, or if it was erroneously induced by cloning procedure or as a result of an evolutionary

Table 14. Sequence detail comparisons of all oat sequences with the AtFAD2 and BdFADX.

gene	*AsFAD2a*	*AsFAD2b*	*AsFAD3-1*	*AsFAD3-2*	*AsFADX*	*AsFADX+*	*AtFAD2*	*BdFADX*
length (nt)	1167	1167	1164	1146	1083	1371	1152	1332
GC proportion (%)	64.1	64.3	60.8	59.9	41.7	44.8	49.7	43.8
protein	**AsFAD2a**	**AsFAD2b**	**AsFAD3-1**	**AsFAD3-2**	**AsFADX**	**AsFADX+**	**AtFAD2**	**BdFADX**
length (AA)	388	388	387	381	360	456	383	443
# of predicted transmembrane regions (TMPred)	5	5	5	5	4	4	6	5
# of predicted transmembrane regions (Kyte-Doolittle)	3	3	3	3	3	3	1	3

event in the plant itself. It may be possible to determine this by cloning each length for expression in yeast individually, with a different sense primer amplifying from each of the putative initiation codons. However, based on both the amino acid similarity at the histidine boxes and entire sequences, AsFADX might be a FAD6-like, chloroplast-localized desaturase.

3.3. Study 3: Functional Characterization of Putative Oat FADs in *S. cerevisiae*

3.3.1. Abstract

In order to functionally characterize these putative *Avena* genes from Study 2, each gene was cloned into a yeast expression vector, after which the recombinant vectors were used to transform *S. cerevisiae.* Fatty acid analysis of transformants indicated that both AsFAD2 isoforms as well as AsFADX demonstrated *Δ*12 desaturase activity on 18:1-9 substrate; AsFAD3-1 had no function on substrates provided, while AsFAD3-2 resulted in *Δ*15 desaturation of strictly 18:2-9,12. AsFADX+ had no function on substrates provided

3.3.2. Hypothesis

The yeast *S. cerevisiae* has been widely employed to functionally characterize eukaryotic genes involved in the lipid/fatty acid biosynthesis. In the presence of appropriate FA substrate, expression of the oat genes in yeast will elucidate the function of these putative genes.

3.3.3. Experimental Approach

3.3.3.1. Yeast Transformation

For all GOI/pYES2.0 recombinant vectors, *S. cerevisiae* INVSc1 cells (genotype: Genotype: MATa *his3Δ1 leu2 trp1-289 ura3-52/*MATα *his3Δ1 leu2 trp1-289 ura3-52*; phenotype: His-, Leu-, Trp-, Ura-) were first plated on SC medium lacking uracil (-U). Transformations were performed similar to the protocol by Gietz and Schiestl (2007). A single colony was grown in 5mL YPD overnight in a 50mL flask at 30°C on a shaker till OD_{600}=0.4/mL. This volume was then added to 50mL of pre-warmed (to 30°C) 2XYPAD medium in a 250mL flask. It was incubated on a shaker at 30°C until the OD_{600} reached 2.0/mL. The yeast was then transferred to a 50mL Falcon tube, centrifuged at 3000xg at 4°C for 5 minutes, and supernatant was discarded. The cells were washed twice with 25mL water volumes (centrifuge each time 3000xg at 4°C for 5 minutes), and then resuspended in 1mL water. This was then transferred to a 1mL microcentrifuge tube, centrifuged at top speed for 30 seconds, and supernatant was discarded. Then, the cells were resuspended in 1mL water. 100µL of the suspended cells were used for each GOI/pYES2.0 transformations to be performed. One volume was prepared for the positive control, *CpDesX* /pYES2.0 construct; this gene has confirmed *ω*-3, *Δ*15 and *Δ*12 desaturase activity (Meesapyodsuk *et al*., 2007). The cyclic, non-recombinant

pYES2.0 vector was also used to transform another volume of these competent cells as the negative control. To each of the 100µL volume, the following transformation mix was added: 240µL PEG 3550 (50% w/v), 36µL 1.0M lithium acetate (LiAc), 50µL 2.0mg/mL single-stranded carrier DNA (previously boiled for 5 minutes and set aside on ice), and 34 µL of water containing 1µg of GOI/pYES2.0 plasmid DNA (or empty vector, for the negative control). The total mixture was vortexed to resuspend the pellet, incubated at 42°C for 12 minutes, centrifuged at top speed for 30 seconds followed by discard of the supernatant, and 1mL water was added. The sample was vortexed/resuspended, and then 2µL, 20 µL, and 200µL volumes from each transformation were plated on SC –U agar plates. These were incubated for 3 days at 30°C.

3.3.3.2. Selection and Screening for Transformants

The yeast was plated on SC -U plates, deficient in uracil. Three colonies for each transformation were selected for screening. A small amount of each yeast colony was transferred to 20µL of 0.02M NaOH and incubated for 30 minutes at 95°C to disrupt the cells. 1µL of each of these solutions was used as templates for colony PCR screening. Presence and orientation were screened for each GOI via PCR using one GOI-specific primer and one pYES2.0-specific primer, as described above, for a minimum of 3 colonies per GOI.

3.3.3.3. Functional Analysis: Expression Induction and Fatty Acid Analysis

From a GOI-positive yeast colony, a toothpick was used to transfer it into 15mL of liquid SC –U medium, incubated for 2 days on a shaker at 30°C. From this sample, a required volume to achieve OD_{600}=4 in a subsequent 5mL volume was calculated. The supernatant was removed after centrifuging at 1500xg for 5 minutes, then washed twice with 1mL of water (centrifuging for 1500xg for 5 minutes after each). The pellet was then resuspended in galactose-containing SC –U induction medium, with 0.1% Tergitol, and 250µM of an appropriate FA substrate (if required) to reach a final volume of 5mL for the expression assay. The samples were incubated on a shaker for 2 days at 30°C. For those with weaker activity, slight adjustments were made for AsFAD3s and AsFADX/AsFADX+, incubating for 1 day at 30°C, 1 day at 20°C, and 1 day at 15°C, as stronger activity with FAD3s is often observed at lower temperatures.

After incubation, the entire culture was transferred to a 15mL Falcon tube and centrifuged at 1500xg for 5 minutes. The pellet was washed in a 1% Tergitol solution, then washed twice with 5mL water (centrifuged 1500xg for 5 minutes after each; final centrifuge is

after transferring to a 15mL glass screw-top tube). The pellet was dried with N_2 gas, after which 2mL of 1% sulfuric acid methanol was added. The samples were incubated for 1 hour at 80°C then cooled on ice. 2mL hexane and 1mL 0.9%NaCl water was added, then the tubes were vortexed and centrifuged for 5 minutes at 2000xg. The upper hexane phase was transferred to a new glass tube and dried with N_2 gas. 100µL of hexane was added to resolubilize the lipid, and divided equally into two insert-containing GC vials. One was analyzed directly via GC. To account for possible bifunctional (both FAD and/or FAH) activity of each putative enzyme, the other duplicate was dried under N_2 gas followed by addition of 50µL TMS and incubated for 30 minutes at 80°C, then analyzed by GC.

3.3.3.4. Substrate Specificity

Expression assays were carried out with the yeast transformants containing the functional FAD3-2/pYES2.0 plasmid. The same protocol as in 3.3.3.3 was performed, but replacing the 250µM FA substrate with the same concentration of other *ω*-6 FAs including 18:3-6c,9c,12c *γ*-Linolenic Acid (GLA), 20:3-8*c*,11*c*,14*c* Dihomo-*γ*-Linolenic Acid (DGLA), or 20:4-5*c*,8*c*,11*c*,14*c* Arachidonic Acid (AA).

3.3.4. Results

3.3.4.1. Expression of the oat *FAD*-like Genes in Yeast

After confirming the sequence, the oat GOI inserts were cut from the pGEM-T vector with appropriate restriction enzymes and inserted into yeast expression vector pYES2.0. The recombinant vectors were used to transform *E. coli* competent cells, and plated on selection medium. The transformed cells were screened via colony PCR to verify correct orientation of the insert inside the vector relative to the GAL10 promoter in pYES2.0. In addition, restriction enzyme digestion was also performed to verify proper orientation of the inserts in the vector. A restriction site (different from that of the flanking primer site) with cutting sites both inside the GOI insert as well as in the vector was selected. The plasmids that yielded the expected fragment sizes of properly-orientated inserts were used for yeast transformation. Yeast colonies were screened via PCR using gene-specific and vector-specific primers to confirm the presence and correct orientation of each GOI in pYES2.0. Yeast colonies from the selection plates that were screened positive for the properly-orientated GOI/pYES2.0 were grown in induction medium in the presence of appropriate FA substrates.

3.3.4.2. Fatty acid analysis of Products from Yeast Transformants

From GOI/pYES2.0-transformed yeast culture, FAs were extracted and analyzed with GC or GC-MS. Peaks from each sample chromatogram below were compared to a FA standard containing FAs of known identity and retention times (not pictured), or analyzed with GC-MS to compare mass spectra to a library database of known spectra.

3.3.4.2.1. Functional Characterization: AsFAD2a

From the *AsFAD2a*-transformed culture, 18:2-9*c*,12*c* was identified confirming FAD2 activity of AsFAD2a from 18:1-9*c* substrate. A TMS-derivatization was also performed on the same sample, but as this resulted in no peaks shifting, it was concluded that there is no HFA produced from substrates present (Figure 34).

Figure 34A shows the empty vector. Figure 34B shows the FAs produced by the yeast which has been transformed with the *AsFAD2a*/pYES2.0 construct; as yeast produces 18:1-9*c*, and that is the putative substrate for AsFAD2a, no FA substrates were added. Peak 1 in Figure 34B represents the 18:2-9*c*,12*c* produced by the transformant. To verify whether or not any HFA was produced, in addition to the GC-MS results, a TMS-derivatization was performed on the FAMEs; Figure 34C demonstrates that no HFA is present, as all peaks are in the same position as the non-derivatized sample.

3.3.4.2.2. Functional Characterization: AsFAD2b

An isoform of the oat FAD2 containing three SNP-induced residue changes (relative to AsFAD2a) was also characterized, and thus *S. cerevisiae* was transformed with this *AsFAD2b*/pYES2.0 vector and subjected to the same conditions as the *AsFAD2a*/INVSc1 transformants. The *AsFAD2b*/INVSc1 showed FAD2 activity as well (Figure 35), although lower quantities of its FA product resulted when compared to FAs of the *AsFAD2a* transformant.

Figure 35A shows the empty vector. Figure 35B shows the FAs produced by the yeast which has been transformed with the *AsFAD2b*/pYES2.0 construct without substrate added. Peak 1 in Figure 35B represents the 18:2-9*c*,12*c* produced by the transformant. To verify whether any HFA was produced, a TMS-derivatization was also performed on the FAMEs; Figure 35 demonstrates that no HFA is present, as all peaks are in the same position as this non-derivatized sample.

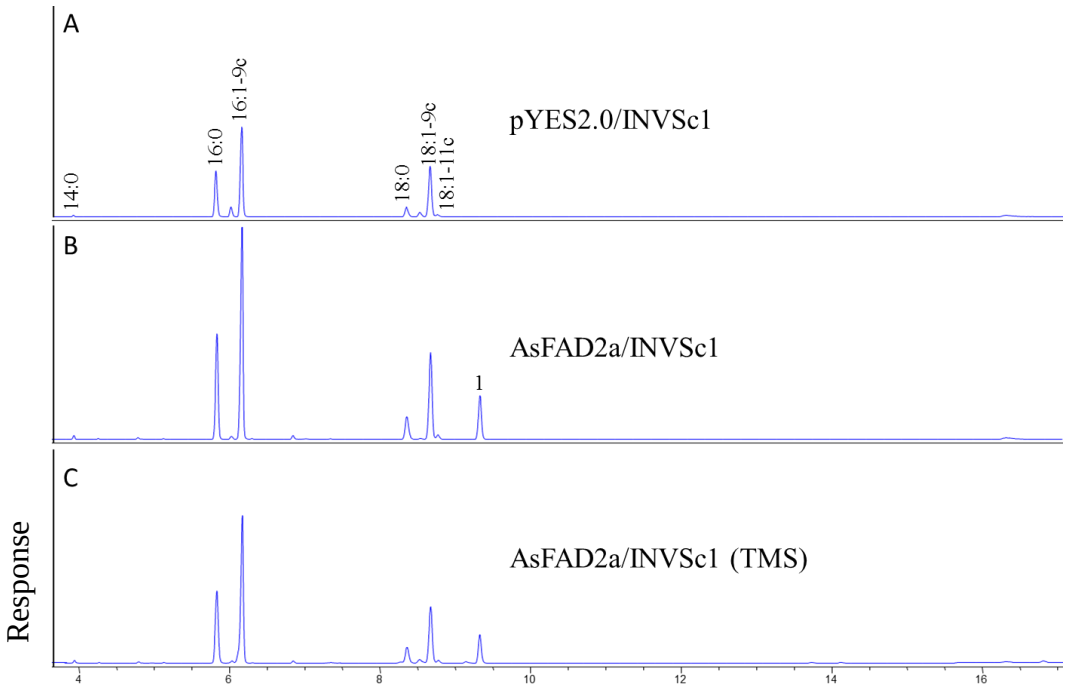

Figure 34. A GC chromatogram of the FAMEs of the empty vector control (A), *S. cerevisiae AsFAD2a* transformant (B), and the TMS-derivatized duplicate (C). Peak 1 shows the 18:2-9*c*,12*c* product produced by the transformant.

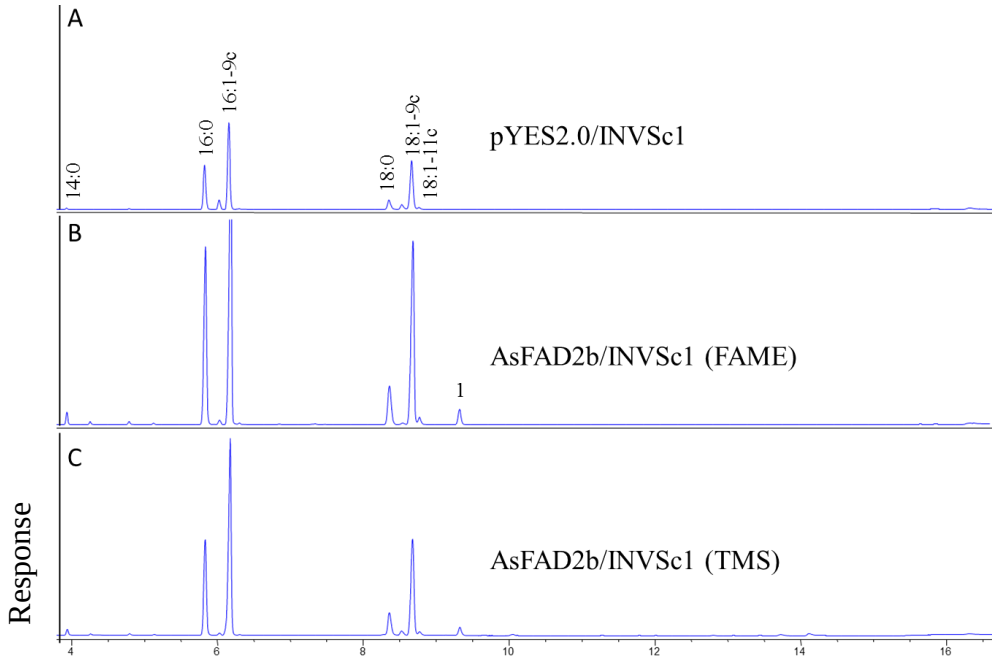

Figure 35. A GC chromatogram of the FAMEs of the empty vector control (A), *S. cerevisiae* AsFAD2b transformant (B), and the TMS-derivatized duplicate (C). Peak 1 shows the 18:2-9*c*,12*c* product produced by the transformant.

3.3.4.2.3. Functional Characterization: AsFAD3-1

Since AsFAD3-1 putatively desaturates 18:2-9*c*,12*c* to produce 18:3-9*c*,12*c*,15*c*, the LA substrate was provided to the AsFAD3-1/INVSc1 cells and FAs were extracted for GC analysis (Figure 36).

Figure 36A shows the empty vector. Figure 36B shows the FAs produced by the yeast which has been transformed with the AsFAD3-1/pYES2.0 construct without substrate added. No new peaks are observed, thus it has no FAD2 function on this substrate. Peak 1 in Figure 36C represents the 18:2-9*c*,12*c* fed to the transformant. No new peaks are observed after feeding substrate, so thus it has neither Δ12 nor Δ15 desaturase function on the substrates present.

3.3.4.2.4. Functional Characterization: AsFAD3-2

The other putative FAD3, AsFAD3-2, was also fed 18:2-9*c*,12*c* substrate with the expected outcome of 18:3-9*c*,12*c*,15*c* production. A new peak, representing 18:3-9*c*,12*c*,15*c*, was observed as is shown in Figure 37.

Figure 37A shows the GC results of the FAMEs extracted from the yeast transformed with the empty vector and analyzed via GC-MS. Figure 37B shows the AsFAD3-2 transformant without putative substrate fed. The result of feeding the same transformant with 18:2-9*c*,12*c* substrate (peak 1) can be seen in Figure 37C (and insert), and a small new peak (peak 2) identified as 18:3-9*c*,12*c*,15*c* is produced. To verify if a hydroxyl group was present on FAs produced, the FAMEs of the same sample were derivatized with TMS to observe if the peak shifted. No shift was observed, which supports the GC-MS data for the production of only 18:3-9*c*,12*c*,15*c*, suggesting that AsFAD3-2 has weak FAD3 activity. The insert shows a closer view of the region in which the new peak was observed.

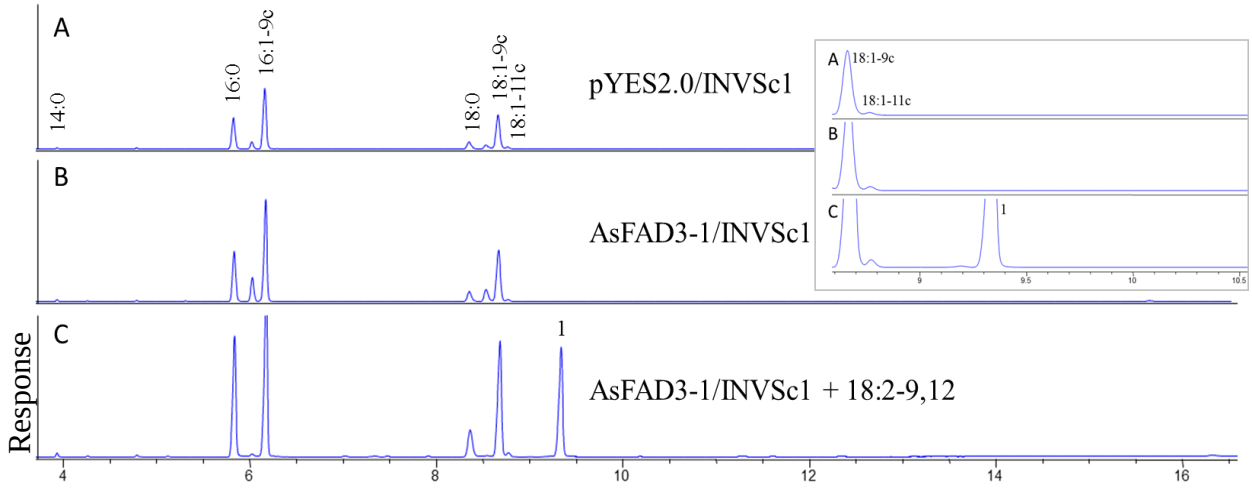

Figure 36. A GC chromatogram of the FAMEs of the empty vector control (A), *S. cerevisiae* AsFAD3-1 transformant (B), and the same transformant fed with 18:2-9*c*,12*c* substrate (C). Peak 1 shows the exogenous 18:2-9*c*,12*c*. The insert shows a closer view of the same chromatograms.

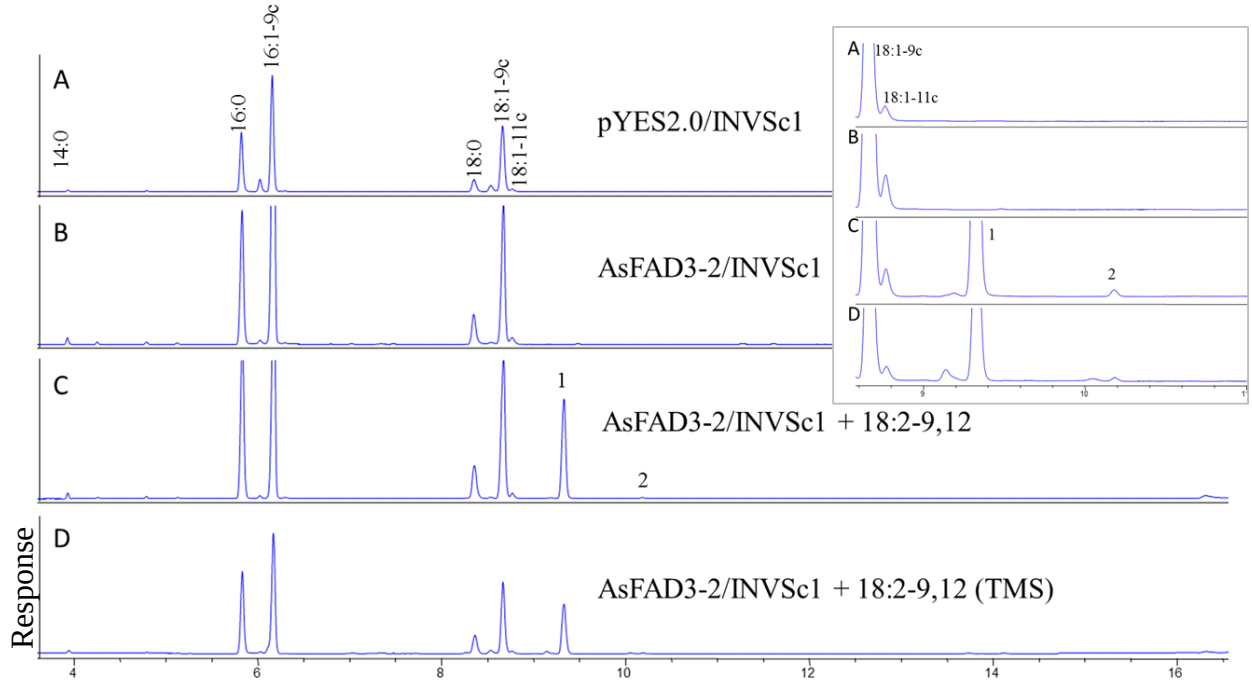

Figure 37. A GC chromatogram of the FAMEs of the empty vector control (A), *S. cerevisiae* AsFAD3-2 transformant (B), and the same transformant fed with 18:2-9*c*,12*c* substrate (C), and the TMS-derivatized FAMEs of the FA-fed transformant (D). Peak 1 shows the exogenous 18:2-9*c*,12*c*; peak 2 shows the 18:3-9*c*,12*c*,15*c* product. The insert shows a closer view of the same chromatograms.

3.3.4.2.5. Functional Characterization: AsFADX

Figure 38A shows the empty vector control. Figure 38B shows the new peak (peak 1) representing 18:2-9*c*,12*c*, produced from AsFADX activity; the insert shows a closer view of the region in which the new peak was observed. To investigate potential FAH activity of FADX, the same FAMEs in Figure 38B were derivatized with TMS, however no peaks were observed to shift, as demonstrated in Figure 38C. The Figure 38 chromatogram demonstrates that AsFADX has *Δ*12 desaturase activity on 18:1-9*c* and it is not of dual FAD2/FAD3 function, and FADX is also not a FAH (Figure 38).

3.3.4.2.6. Functional Characterization: AsFADX+

The longer form of AsFADX, AsFADX+, was also expressed in *S. cerevisiae* followed by GC-MS analysis. No activity was observed (Figure 39).

Figure 39A shows the FAME profile of the FAs extracted from the empty vector-transformed yeast cells; Figure 39B shows the FAs produced by the AsFADX+ transformed yeast cells, no new peak was observed suggesting that no endogenous substrates present are appropriate for this FAD-like enzyme, or that the longer version of AsFADX does not produce a functional protein in this yeast system used. To examine if AsFADX+ had FAD3 activity, the same construct was provided with 18:2-9*c*,12*c* substrate, as shown in Figure 39C, indicated by peak 1. However, no new peaks were observed, and it is concluded that AsFADX+ has no function on any substrates present.

3.3.4.3. Substrate Specificity

Since the yeast transformant with the AsFAD3-2 was the only sample showing activity upon the *ω*-3 position of a substrate, which is the same position on which the putative substrate is hydroxylated by the uncharacterized *Avena* FAH15, several other *ω*-3 FAs were provided to this transformant. This would determine if the oat AsFAD3-2 had strictly *Δ*15 desaturase activity on LA substrate, or if it had a general *ω*-3 desaturase activity from the methyl end of the substrate. Two more *ω*-6 FAs in addition to LA were fed as substrates to FAD3-2: Gamma-Linolenic Acid (GLA): 18:3-6*c*,9*c*,12*c* and Dihomo-gamma-linolenic acid (DGLA) 20:3-8*c*,11*c*,14*c*. Of the substrates tested, FAD3-2 only had a desaturase activity on LA. AsFAD3-2 showed no activity upon the three *ω*-6 FAs, suggesting that it is not an *ω-3* FA desaturase but rather it has activity specific to the *Δ*15 carbon of LA substrate (Table 15).

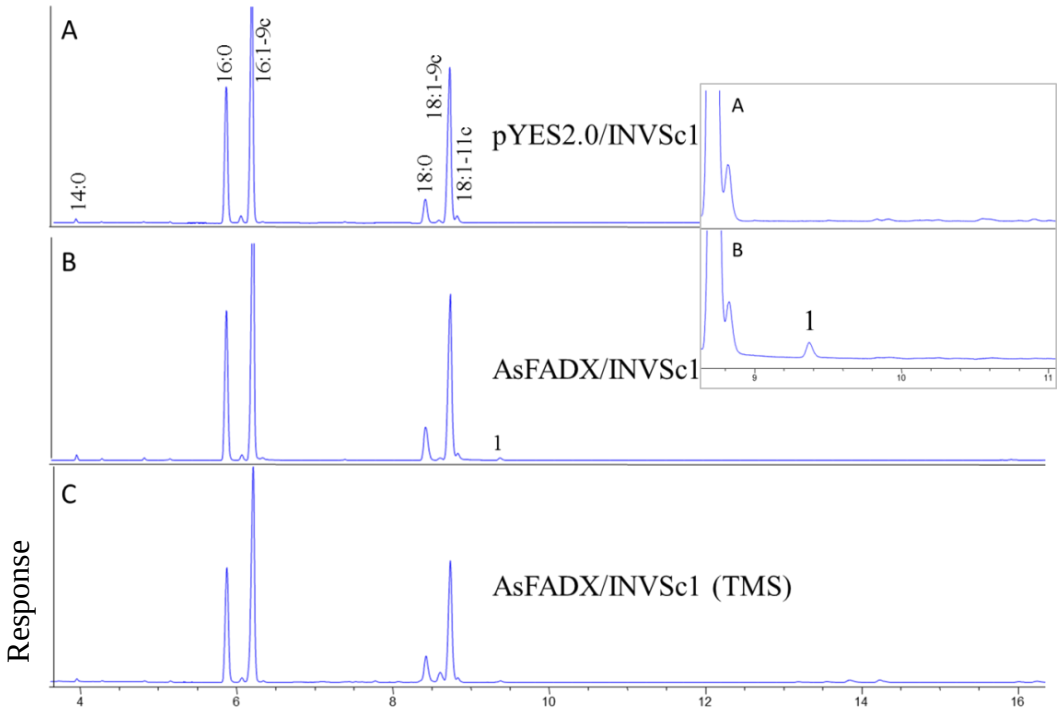

Figure 38. A GC chromatogram of the FAMEs of the empty vector control (A), *S. cerevisiae* AsFADX transformant (B), and the TMS-derivatized duplicate (C). Peak 1 shows the 18:2-9*c*,12*c* product produced by the transformant. The insert shows a closer view of the same chromatograms.

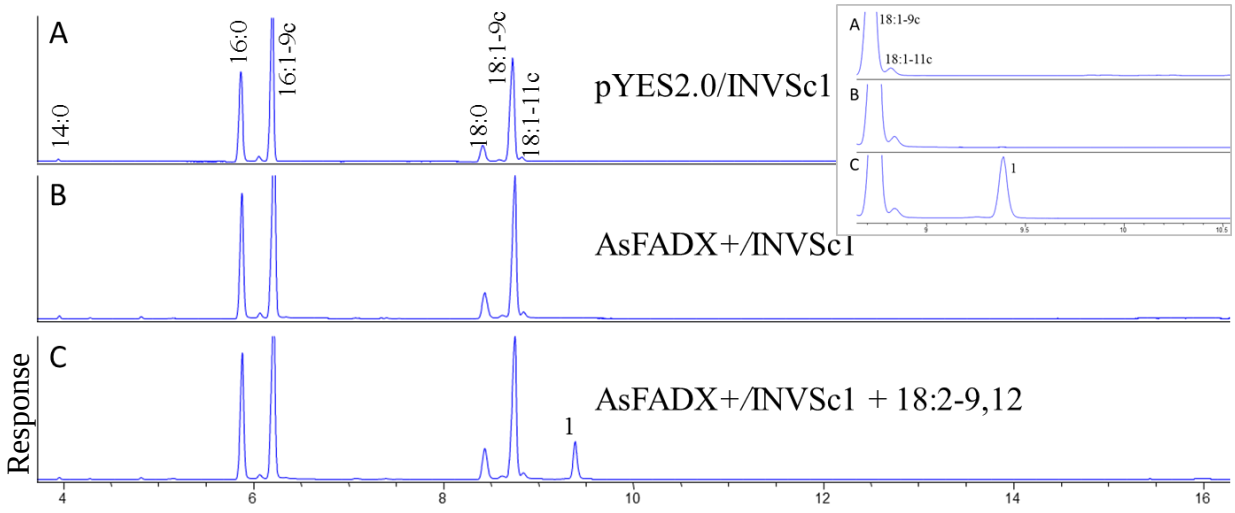

Figure 39. A GC chromatogram of the FAMEs of the empty vector control (A), S. cerevisiae AsFADX+ transformant (B), and the TMS-derivatized duplicate (C). Peak 1 shows the exogenous 18:2-9*c*,12*c* FA substrate. The insert shows a closer view of the same chromatograms.

Table 15. Substrate-to-product conversion efficiencies of oat FAD-like products in yeast.

pYES2.0 insert	Substrate	Product	Mean % ± SD	
AsFAD2a	18:1-9*c*	18:2-9*c*,12*c*	20.4	± 11.4
AsFAD2b	18:1-9*c*	18:2-9*c*,12*c*	3.92	± 3.21
AsFAD3-1	18:1-9*c*	18:2-9*c*,12*c*	0.00	
	18:2-9*c*,12*c**	18:3-9*c*,12*c*,15*c*	0.00	
AsFAD3-2	18:1-9*c*	18:2-9*c*,12*c*	0.00	
	18:2-9*c*,12*c**	18:3-9*c*,12*c*,15*c*	0.60	± 0.48
	18:3-6*c*,9*c*,12*c**	18:4-6*c*,9*c*,12*c*,15*c*	0.00	
	20:3-8*c*,11*c*,14*c**	20:4-8*c*,11*c*,14*c*,17*c*	0.00	
	20:4-5*c*,8*c*,11*c*,14*c**	20:5-5*c*,8*c*,11*c*,14*c*,17*c*	0.00	
AsFADX	18:1-9*c*	18:2-9*c*,12*c*	0.91	± 0.23
	18:2-9*c*,12*c**	18:3-6*c*,9*c*,12*c*	0.00	
AsFADX+	18:1-9*c*	18:2-9*c*,12*c*	0.00	
	18:2-9*c*,12*c**	18:3-9*c*,12*c*,15*c*	0.00	

*provided to the samples, 250μM final concentration

3.3.5. Discussion

pYES2.0 is a common vector for gene cloning and inducible expression of eukaryotic genes in yeast. pYES2.0 is a 5.9kb vector containing a *GAL1* promoter, allowing high expression in yeast induced by galactose, while being repressed by glucose, as well as *URA3*, enabling selection of uracil prototrophic genotype transformants in yeast (Invitrogen, 2008). It also contains the *CYC1* transcription terminator, and ampicillin resistance gene (for selection in *E. coli*). This vector, when used to transform yeast, is compatible with the INVSc1 strain yeast host. Other features of the vector are the *T7* promoter/priming site, which allows in vitro transcription in the sense strand, and sequencing through the insert. The multi cloning site contains the insertion site for EcoRI and XbaI, among others. The 2μ origin maintains high copy number in yeast, and the f1 origin allows rescue of a single strand DNA. Yeast hosts were successfully transformed with all GOI/pYES2.0 constructs.

3.3.5.1. AsFAD2

Efficiency of AsFAD2 activity on 18:1-9*c* substrate to produce LA in this study is consistent with other *in vivo* yeast expression studies of other FAD2s. An *Arabidopsis* FAD2 under control of the *GAL1* promoter, once transformed into *S. cerevisiae*, resulted in accumulation of 9.2, 6.4, and 0.6% LA of total FAs at incubation temperatures of 15°C, 22°C, and 28°C, respectively (Covello & Reed, 1996). Another study examining the function of FAD2s from *Exocarpos cupressiformis* and *Santalum acuminatum* also used pYES2 expression vectors for *in vivo* expression (Okada *et al*., 2013). Efficiencies of conversion of 18:1-9*c* to 18:2-9*c*,12*c* ranged from 23% to 63%, although incubation temperatures are not specified (Okada *et al*., 2013).

3.3.5.2. AsFAD3

It was necessary to feed the appropriate LA substrate to the transformants with the constructs expressing AsFAD3s, although only one of the two putative AsFAD3s had activity on substrates present. Comparing the new peak from the AsFAD3-2 sample with the empty vector control, the FA standard and the mass spectra confirm FAD3 activity of this gene. The AsFAD3 conversion of LA into ALA is relatively low when compared with efficiency of the FAD2 substrate to product conversions; however, it is not unexpected. Low conversion rates of LA to ALA in transformed yeast have been observed previously with other FAD3s (Dyer *et al*., 2004; Reed *et al*., 2000). A FAD3 (GenBank accession number L01418) from *Brassica napus* introduced into *S. cerevisiae* using the pYES2.1 vector and the same *GAL1* promoter as this study resulted in only 1.5% ALA accumulation of total FA in the yeast (Dyer *et al*., 2004). A similar study observed 1.3% conversion of LA to ALA (Reed *et al*., 2000). Accumulated ALA levels of total FA in transformant yeast have been observed at levels <1% (Dyer *et al*., 2001). The FAD3 activity may be influenced by temperature; increased ω-3 desaturation of LA substrate with lower growth temperatures was observed in both plants and transformed yeast (Gibson *et al*., 1994; Dyer *et al*., 2001). Data from Dyer *et al*. (2001) suggest that the change is a cold-induced post-transcriptional adaptation, as FAD3 transcript levels remain constant. Highest levels of accumulated ALA in *FAD3*-transformed yeast have been found to be at 20°C (Dyer *et al*., 2001) and 15°C (Dyer *et al*., 2004), although the total accumulated ALA between these

parameters differs by ~3% of total FA. 20°C is often effectively employed for *FAD3*-transformed *S. cerevisiae* for ALA accumulation (Vrinten *et al*., 2005; Dyer *et al*., 2001).

The initial putative contigs were constructed from the best-available material, and 15HFA is present in the germplasm, yet none of these genes have the hydroxylase activity. This suggests that 15HFA may be derived from a different pathway, or that it is modified in a form other than a fatty acid linked to phosphatidylcholine (PC). There is also a possibility that the original EST database either contains sequence errors, or that it is lacking necessary sequence information from the specific development stage in which the *FAH15* is actively transcribed. In that case, it would be impossible to identify an authentic *FAH15* gene.

The lack of AsFAD3-1 function on substrates provided may be due to some other possibilities. Sometimes, ORFs having high homology to cloned genes (either from the same genome, or from other organisms) known to encode functional products may arise, although produce no evident functional product as a result of some small nucleotide-induced mutation; in this event, *AsFAD3-1* would be a pseudogene (Jacq *et al*., 1977; Vanin, 1985). However, it is possible some small amount of ALA is produced but undetectable by methods used, as very little ALA is typically produced in these yeast *in vivo* assays. Moreover, conversion efficiency between two FAD3s sharing 94.5% identity (Vrinten *et al*., 2005) differed by >2%, and at such low ALA production levels as in this study may be enough to keep ALA produced below the detection threshold.

The majority of 15-OH 18:2-9*c*,12*c*, which is putatively the product of a FAD-derived enzyme, was found in digalactosyldiacylglycerol (DGDG), as an estolide thus without a free hydroxy group (Hamberg *et al*., 1998). Although ricinoleic acid, derived from OA in castor oil is thought to be structurally (and therefore, the preceding relevant biochemical processes) closely related to 15HFA production in oats, the glycolipid location of oat hydroxyl fatty acid suggests the fundamental biosynthetic mechanism(s) for this fatty acid might be different from that of castor ricinoleic acid. *S. cerevisiae* does not encode a DGDG synthase, so the galactolipid precursor to which linoleate is bound which in turn is putatively and subsequently hydroxylated would be absent, thus resulting in the complete absence of the appropriate substrate for AsFAH15.

3.3.5.3. AsFADX & AsFADX+

Initially, it was hypothesized that the longer N-terminus portion of AsFADX+ must be a transit peptide sequence to direct it into the chloroplast; this would be logical since its query sequence was the plastidial FAD7, and the region is long enough to comprise such a sequence (Bhushan *et al*., 2006). However, none of the prediction programs indicated the presence of a targeting sequence, nor do the hydropathy plots show exceptionally hydrophobic residues, a feature characteristic of transit peptides (Zhang & Glaser, 2002). Nevertheless, both CDS lengths were cloned for expression studies, as these indications may be the best tools available but are merely predictions.

AsFADX is highly homologous to a FAD6, has conserved similarities in the HIS boxes to FAD6s, has an N-terminus peptide region of similar length to that of an expected transit peptide, and exhibits *Δ*12 desaturation function. Because of the similarity to these query sequences, once AsFADX is expressed *in vivo*, the FAME GC profile should yield either 18:2-9*c*,12*c* from the yeast's endogenous 18:1-9*c* substrate, or yield 18:3-9*c*,12*c*,15*c* from 18:2-9*c*,12*c* provided to the assay. Indeed, the Figure 38 chromatogram demonstrates that AsFADX has weak *Δ*12 desaturase activity on 18:1-9*c*. This evidence suggests that AsFADX is a FAD6 with a hypothetical transit peptide sequence on the N-terminus to target it for chloroplast localization.

These results suggest that this upstream region of AsFADX+ may be a transit peptide portion of the *AsFADX* ORF. Another possibility, albeit unlikely, is that the upstream initiation codons are out of frame and the region creates an apparent artifact that is in-frame with *AsFADX*, so the start codon of the shorter *AsFADX* must be the proper start codon as this ORF did code for a functional enzyme. Another explanation is that the prediction software tools used algorithms incompatible with this AsFADX+ sequence used, and thus the prediction results were unreliable and this upstream region of AsFADX+ is indeed a transit peptide; in such a case, AsFADX+ would be destined for a chloroplast membrane and, in yeast, this uncleaved additional length of the N-terminus may cause steric hindrance to render the protein functionless, accounting for the lack of function of the longer version of the functional AsFADX. Yet, even if this N-terminus sequence is a cellular targeting sequence, the similar lengths with known targeting sequences, as well as the FAD2 activity of the shorter AsFADX, suggest that the extended portion of AsFADX+ would be cleaved and the final functional form would actually be the AsFADX. Finally, it is unclear which of the three translation initiation codons in the AsFADX+ portion is

correct. It may be possible to clone each length of the ORF for expression analysis in yeast, or knock down the unique 5' regions of the genes *in vivo*, using RNAi, for example; then, phenotypic changes could be observed.

3.3.5.4. Substrate Specificity (AsFAD3-2)

Some desaturases and hydroxylases have multiple functions. Therefore, different substrates were thus fed to the FAD3-2/pYES2.0/INVSc1 to investigate substrate specificity of the enzyme. A FAD3 from *Brassica napus* was found to have regiospecificity for ω-3 desaturation rather than a Δ15 desaturation (Reed *et al*., 2000). No activity was observed on any substrate other than the LA fed. This is consistent with results of a similar study by Vrinten *et al*. (2005) in which FAD3s were specific to only one substrate. This suggests that the activity of FAD3-2 is dependent on the Δ9 and Δ12 double bonds in the FA structure, rather than being a generic ω-3 desaturase of ω-6 FAs.

Of all the substrates present with each gene, the TMS derivatives show no peak shifts or new peaks. This suggests that either none of these *Avena* genes are hydroxylases, or that none are capable of hydroxylating any of the substrates tested in their current forms.

One major challenge of yeast *in vivo* expression studies of enzymes related to PUFA biosynthesis is the optimal temperature. In plants, PUFA biosynthesis increases with decreasing temperature, particularly below 20°C (Graham & Patterson, 1982). The ideal growth temperature for *S. cerevisiae* is 28°C, however yeast increases its 18:1-9 membrane proportion to maintain membrane fluidity when grown at lower temperatures (Rodriguez-Vargas *et al*., 2007). However, some nutrient uptake by the yeast is limited with these lower temperatures, and thus may influence the deficiency of certain amino acids as well as inhibit yeast growth (Torija *et al*., 2003; Rodriguez-Vargas *et al*., 2007; Tai *et al*., 2007).

3.4. Study 4: qRT-PCR Analysis of Oat *FAD*-like Transcripts

3.4.1. Abstract

mRNA levels of the oat GOIs were quantitatively analyzed using the real-time PCR (qRT-PCR) as an indication of their relative levels gene of expression. After normalizing expression levels relative to two internal housekeeping genes (HKGs), a comparative C_t method was used to determine relative expression levels. In general, *AsFAD2* mRNA levels were more abundant than *AsFAD3-1* and *AsFAD3-2* in all tissues, while *AsFAD3-1* mRNA levels exhibited lowest abundance. *AsFAD2* transcript level in root was lowest, abundant in relative levels 1.5 fold, 3.3 fold, and 3.8 fold higher in germinating seed, leaf, and developing seed tissues, respectively. *AsFAD3-1* transcript was least abundant, with relative transcript levels 10.2 fold, 11.6 fold, and 18.3 fold higher in root, germinating seed, and developing seed tissues, respectively. *AsFAD3-2* relative transcript abundance was 3.6 fold, 6.4 fold, and 8.0 fold higher than that of leaf tissue in root, developing seed, and germinating seed tissues, respectively. When examining different GOI transcript levels within a particular tissue, fold differences were more extreme when compared to *AsFAD3-1* levels (which were least abundant in all tissue types). In germinating seed, *AsFAD2* and *AsFAD3-2* abundance was 12.8 and 3.5 fold higher, respectively. In root, these levels were 7.3 and 2.0 fold higher than *AsFAD3-1*, respectively. In leaf tissue, *AsFAD2* and *AsFAD3-2* transcript relative abundance were 916.1 and 9.2 fold higher than *AsFAD3-1*, respectively, while in developing seed, the relative fold differences were 18.6 and 3.0 above *AsFAD3-1* transcript abundance.

3.4.2. Hypothesis

Quantitative real-time PCR (qRT-PCR) is widely used for mRNA quantification, due to its sensitivity and reliability. Conducting a qRT-PCR analysis of oat GOIs here relative to internal controls, the relative expression of each GOI across different oat tissues can be determined. Results can then be compared to the FA profile of mature seed, enhance insight into whether correlation exists between expression and activity of genes and proteins involved in PUFA biosynthesis.

3.4.3. Experimental approach

3.4.3.1. RNA Extraction and 1st strand cDNA synthesis

cDNA synthesis with a Quanta qScript cDNA synthesis kit was carried out on total RNA from biological triplicates from each germinating seed, root, leaf and milky-stage seed from tissues harvested in Study 1. Extractions were performed with a TRIzol method as described in 2.3.1 followed by Qiagen's RNeasy cleanup (Qiagen, 2013). Total RNA from each sample was thawed on ice when used. In each cDNA synthesis reaction, 1µg of RNA was added, with 1µL of qScript reverse transcriptase, 4µL of 5X qScript reaction mix, and brought to 20µL total volume with nuclease-free water. The mixtures were vortexed gently, centrifuged briefly, and reactions were carried out in a Biorad cfx connect™ real-time system thermocycler for 5 minutes at 22°C, 30 minutes at 42°C, and 5 minutes at 85°C. cDNA originating from each was diluted 1/10 and either used for quantification or stored at 4°C.

3.4.3.2. Oat Internal Control Sequences for qRT-PCR

For comparative C_t qRT-PCR studies, it has been recommended to use more than one stably-expressed constitutive gene, since they have constant expression across tissue types and development stages due to their function in basic homeostasis (Huis *et al*., 2010). The relative expression of the oat GOIs in this study were calculated using the comparative C_t method after normalizing their expression levels to two internal reference genes, similar to the method used by Pan *et al*., 2013. Two commonly used HKGs for these types of studies are glyceraldehyde-3-phosphate dehydrogenase (*GAPDH*) and *Actin* (Jian *et al*., 2008; Huis *et al*., 2010). Since the oat genome has not been sequenced, and housekeeping genes remain uncharacterized, two putative oat housekeeping genes, *GAPDH* (*AsGAPDH*) and *Actin1* (*AsActin1*), were established using the bioinformatics techniques previously described in this study. A previously characterized, 1014bp from *Triticum aestivum* (Sander *et al*., 2001; accession number FN429985) and a 1618bp *Actin1* from *Arabidopsis thaliana* (An *et al*., 1996; accession number U39449) genes were used as queries to search in the CORE and NCBI oat-specific sequence databases for selecting oat ESTs with highest homology to these two targets, as the putative oat *AsActin1* and *AsGAPDH*. Gene-specific primers for the three putative GOIs as well as for two internal controls (*Actin1* and *GAPDH*) were designed using Primer3Plus software.

3.4.3.3. qRT-PCR Primer Design

Primer sequences are listed in Table 16 and designed using the sequences in Figure 40 and Figure 41; qRT-PCR primers targeting the housekeeping genes were designed with the online Primer3Plus software (Whitehead Institute for Biomedical Research, 2006). Sequences in 3.2.4.3 were used to design the primers targeting the GOIs.

3.4.3.4. qRT-PCR Relative Quantification

From each biological triplicate, technical triplicates of each target were analyzed using a Sybr Green fluorescence SsoFast™ EvaGreen® supermix kit from BioRad (2013). From each replicate of a tissue type, 1µg of cDNA (from the Quanta syntheses) was combined with 10µL of SsoFast EvaGreen supermix, both forward and reverse primers (each at 500nM final concentration), and brought to 20µL total reaction volume with nuclease-free water; each technical triplicate reaction was prepared in 96-well white plates. Also, template-free negative controls were run in the same reaction plates. Additional negative controls with RNA added were included for each plate to verify RNA template initially extracted for cDNA synthesis was free of DNA contamination. The reactions were carried out for 30 seconds at 95°C for an initial denaturation step, then 95°C for 5 seconds/60°C for 15 seconds for 45 cycles, and then a final cycle starting at 65°C and increasing to 95°C (increasing 5°C increments each 5 seconds). qRT-PCR reactions were carried out in a Bio-Rad CFX96 detection system and corresponding CFX Manager software.

For comparing relative quantification of each GOI to multiple internal references, a normalization factor was generated from two stably-expressed housekeeping genes (HKGs). Multiple internal controls for relative Ct comparative studies have been effectively used (Pan *et al*., 2013). First, cycle threshold (C_t) values were obtained at the point that each amplification curves crossed; thresholds were set at the lowest point within the exponential phase of the curve. Mean C_t values were calculated from the technical triplicates of each HKG. The normalization factor was generated from both HKG expression levels using the geometric mean of the transcript quantity values from both HKGs. To depict expression levels graphically, expression of GOI with the lowest relative level was adjusted to equal 1, and all expression levels and SDs were adjusted to this value. Formulas 6.4.1 to 6.4.13 were used for the calculations.

Table 16. Primers used for qRT-PCR analysis.

Target	Sequence (5'→3')	Description	Target locations in Sequence (amplicon length)
AsFAD2	TTCCACAACATCACGGACAC	*AsFAD2* qPCR sense primer	943-962
	TCACCGAGGATTGGCTTGATC	*AsFAD2* qPCR antisense primer	1026-1046
			(104)
AsFAD3-1	ACCATGGCCACATCGAAAAG	*AsFAD3-1* qPCR sense primer	431-450
	AGTTTCTTGGTCCGTGCTTC	*AsFAD3-1* qPCR antisense primer	496-515
			(85)
AsFAD3-2	TGTGGCTTGATTTGGTGACG	*AsFAD3-2* qPCR sense primer	740-759
	TGCCAATGTCATGGTGGATG	*AsFAD3-2* qPCR antisense primer	870-889
			(150)
AsGAPDH	TGCACCACAAACTGTCTTGC	*AsGAPDH* qPCR sense primer	422-441
	TGCTGCTGGGAATGATGTTG	*AsGAPDH* qPCR antisense primer	491-510
			(178)
AsACTIN1	TGTGTTGCTCACTGAAGCTC	*AsACTIN1* qPCR sense primer	107-126
	TGGCAGGCACATTGAAAGTC	*AsACTIN1* qPCR antisense primer	265-284
			(89)

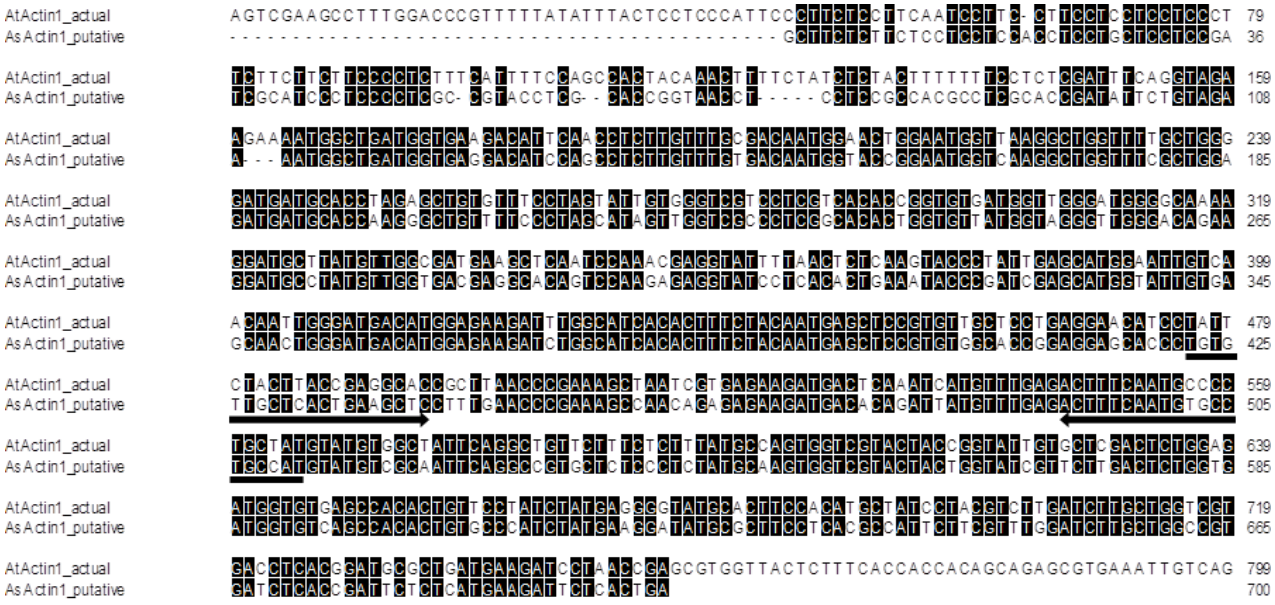

Figure 40. The *Actin1* from *Arabidopsis* (*AtActin1*) nucleotide query sequence aligned with the oat putative EST. The oat EST retrieved and used as the putative oat *Actin1* (*AsActin1*) was (ASAEN3NG-UP-091_D05). Identical nucleotides are highlighted in black. qRT-PCR primers are underlined.

Figure 41. The *GAPDH* from *Triticum aestivum* (*TaGAPDH*) nucleotide query sequence aligned with the putative oat *GAPDH*. The oat EST (ASAEN3NG-UP-105_C05) sequence was retrieved and used as the putative oat *GAPDH* (*AsGAPDH*). Identical nucleotides are highlighted in black. Primers are underlined.

$$\text{Mean Ct } (\bar{x}\text{Ct}) = (Ct_1+Ct_2+Ct_3)/3 \quad \textbf{(6.4.1)}$$

$$SD_{(\bar{x}Ct)} = \sigma_{(\bar{x}Ct)} = \sqrt{[((Ct_1 - \bar{x}Ct)+(Ct_2 - \bar{x}Ct)+(Ct_3 - \bar{x}Ct))/3]} \quad \textbf{(6.4.2)}$$

$$\text{Quantity} = (Q) = 2^{(\bar{x}Ct)} \quad \textbf{(6.4.3)}$$

$$SD_Q = (\bar{x}Ct)(SD_{(\bar{x}Ct)})(\ln(3)) \quad \textbf{(6.4.4)}$$

Normalization Factor (NF) = *n*th root of the product of the numbers, where *n* = number of HKGs used

$$NF = \sqrt{(Q_{(GAPDH)})(Q_{(Actin1)})} \quad \textbf{(6.4.5)}$$

$$SD_{NF} = (NF)[(SD_{Q(Actin1)}/(Q_{(Actin1)}x3))^2 + (SD_{Q(GAPDH)}/(Q_{(GAPDH)}x3))^2]^{0.5} \quad \textbf{(6.4.6)}$$

$$\text{Normalized Expression Level (EL)} = NF/Q \quad \textbf{(6.4.7)}$$

$$SD_{EL} = (EL)[(SD_{NF}/NF)^2+(SD_Q/Q_{GOI})^2]^{0.5} \quad \textbf{(6.4.8)}$$

$$\text{Mean EL} = (EL_{GOIa,rep1}+EL_{GOIa,rep2}+EL_{GOIa,rep3})/3 \quad \textbf{(6.4.9)}$$

$$SD_{\text{Mean EL}} = \sigma_{(\text{Mean EL})} = \sqrt{[(EL_{GOIa,rep1}+EL_{GOIa,rep2}+EL_{GOIa,rep3})/3]} \quad \textbf{(6.4.10)}$$

$$\text{Multiplication factor (MF)} = 1/EL_{(\text{of GOI with lowest expression})} \quad \textbf{(6.4.11)}$$

$$\text{Mean } EL_{(\text{Adjusted})} = (\text{Mean EL})(MF) \quad \textbf{(6.4.12)}$$

$$SD_{\text{Mean EL(Adjusted)}} = (SD_{\text{Mean EL}})(MF) \quad \textbf{(6.4.13)}$$

An X-axis arbitrary baseline for graphing was set relative to that GOI with the lowest relative transcript abundance in this study (*AsFAD3-1* in root), which was assumed to be equal to 1. Fold values were based on the normalization factor (NF) value generated from the expression levels of the two HKGs from the calculations above.

3.4.4. Results

3.4.4.1. Oat Internal Control Sequences for qRT-PCR

The putative oat *AsActin1* and *AsGAPDH* were selected as internal references for the qRT-PCR on which primers were designed. Both originated from CDC Dancer ESTs; for the oat *Actin1*, an EST (ASAEN3NG-UP-091_D05) of 700bp and 82% nucleotide homology to the

Arabidopsis query was selected as the template, and for the *AsGAPDH,* an EST (ASAEN3NG-UP-105_C05) of 689bp and 91% nucleotide homology to the *Triticum aestivum* query was selected as the template (Figure 40 & Figure 41). These oat sequences retrieved were used to design oat HKG primers for the qRT-PCR comparative expression analysis.

3.4.4.2. Primer Design for qRT-PCR

The qRT-PCR primers targeted locations in *AsFAD2, AsFAD3-2,* and *AsFAD3-2* to amplify regions of 104bp, 85bp, and 150bp, respectively. To target the *AsActin1* (Figure 40), the two primers were at nucleotide positions 422-441 and 491-510, to amplify a target size of 89 bp. To target the *AsGAPDH* (Figure 41), the two primers were at nucleotide positions 107-126 and 265-284, to amplify a target size of 178bp. These 10 primers were utilized in the following qRT-PCR steps after 1st strand cDNA was synthesized from total RNA samples of each tissue.

3.4.4.3. RNA Extraction, 1st strand cDNA synthesis

Total RNA was extracted from biological triplicates from each of germinating (7 days) seed, root, leaf, and milky-stage developing seed; after clean-up treatment, integrity and quality was screened by running an aliquot on agarose gels (Figure 42).

1st strand cDNA was synthesized from each of the biological triplicate RNA; for each of the nine cDNA samples, primers (Table 16) were employed in technical triplicate reactions for qRT-PCR and mean values of the technical triplicate reactions from each of the biological triplicates were used to relatively quantify expression levels of the GOIs (Figure 43).

3.4.4.4. qRT-PCR Data Analysis

As an equal quantity of RNA and thus cDNA was used in each reaction replicate, amplification levels of each target GOI relative to the two internal controls directly represent GOI transcript abundance in the tissue at the time of harvest. Raw data are shown in Table 22-Table 25, Appendix 5.4. The fold-differences of their expression patterns are shown in Figure 43. The baseline in this figure is set as 1 at the lowest relative expression level after the normalization (in this case, *AsFAD3-1* in leaf). The adjusted relative expression levels of all other genes across different tissues are graphed in Figure 43.

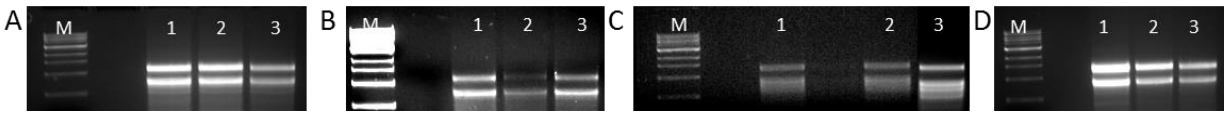

Figure 42. Total RNA extractions from biological triplicates from CDC Dancer tissues.

Germinating seed (A), root (B), leaf (C), and milky-stage seed (D). M=DNA Marker.

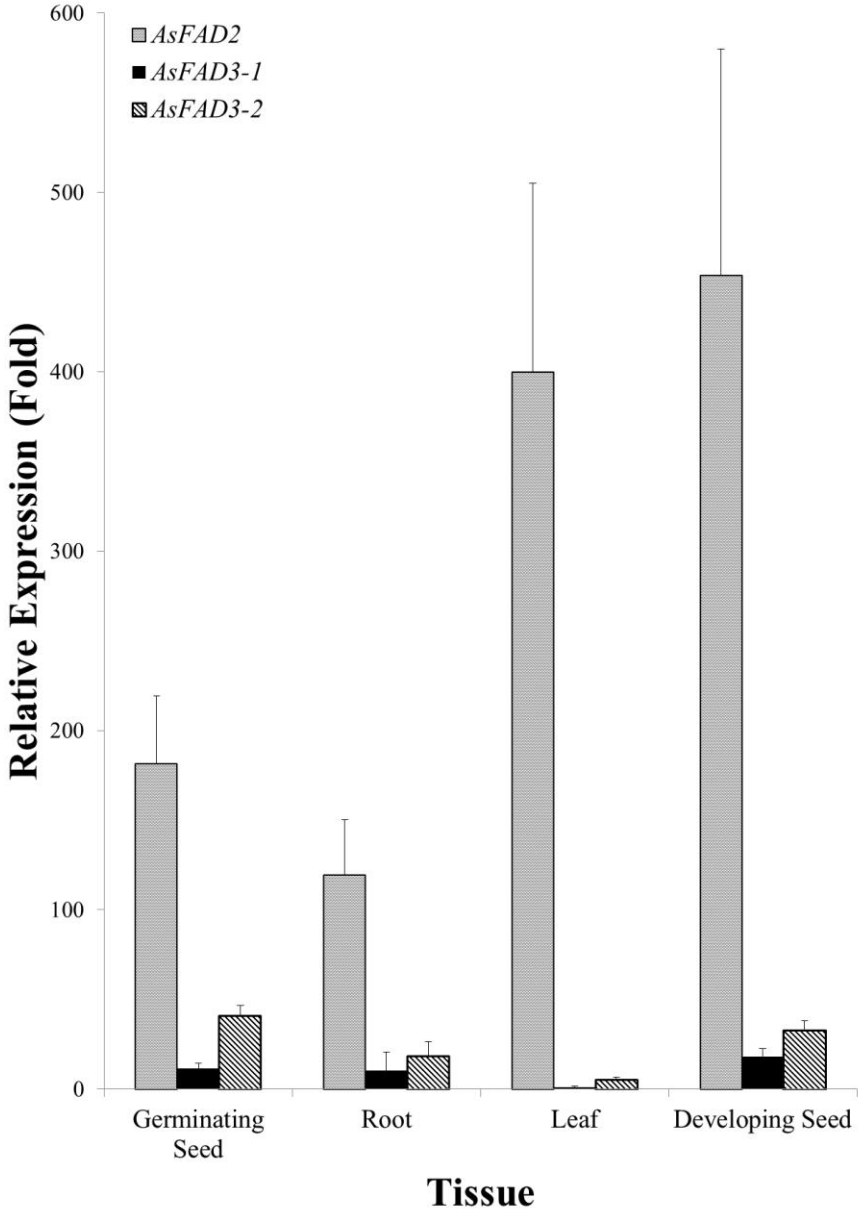

Figure 43. Relative fold-levels of *AsFAD2*, *AsFAD3-1*, and *AsFAD3-2* in various oat tissues.

Expression levels are normalized to the two HKGs, and fold-differences are relative to Leaf *AsFAD3-1* level, assigned the value of "1."

The results indicate that *AsFAD2* showed highest expression levels across all tissue types, and *AsFAD3-1* had the lowest expression in all tissues. In developing seeds, *AsFAD2* had the highest expression, followed by *AsFAD3-2* and *AsFAD3-1*, while in germinating seeds and roots the trend is the same. In leaves, the expression level of *AsFAD2* is high, but almost no expression was observed for *AsFAD3-1* and *AsFAD3-2*. The relative expression levels of these GOIs are represented numerically in Table 17 and Table 18.

Table 17. Transcript levels of each oat GOI. Abundances are shown in fold differences relative to its lowest abundance across the four tissues.

	AsFAD2	***AsFAD3-1***	***AsFAD3-2***
Germinating Seed	1.5	11.6	8.0
Root	1.0	10.2	3.6
Leaf	3.3	1.0	1.0
Developing Seed	3.8	18.3	6.4

Table 18. Relative transcript abundance of different oat GOIs within each tissue type. Abundances are shown in fold differences relative to the GOI exhibiting lowest abundance within the tissue type.

	Germinating Seed	**Root**	**Leaf**	**Developing Seed**
AsFAD2	12.8	7.3	916.1	18.6
AsFAD3-1	1.0	1.0	1.0	1.0
AsFAD3-2	3.5	2.0	9.2	3.0

3.4.5. Discussion

Relative *AsFAD2* mRNA levels were observed highest to lowest was in developing seed, leaf, germinating seed, then root tissue. For *AsFAD3-1*, highest to lowest levels were in developing seed, germinating seed, root, and leaf, while for *AsFAD3-2*, it was in germinating seed, developing seed, root, and leaf tissue.

Within each tissue type, *AsFAD2* was generally expressed much higher than the other two genes; *AsFAD3-1* was expressed at lowest levels in all tissues, with *AsFAD3-2* being expressed slightly higher than *AsFAD3-1* in all tissues.

The comparative expression data here demonstrates that there are dramatic differences between transcript levels of *FAD2s* and *FAD3s*. The ratio of accumulated LA:ALA (Table 2) in oat seeds is 44:1; this disproportionate balance is observed in relative mRNA levels of *AsFAD2:AsFAD3-1*, which is 25:1, and also reflected in *AsFAD2:AsFAD3-2*, which is 14:1 (Table 18). But since the ratio of LA:ALA accumulation compared to the ratio of expression of *AsFAD2:AsFAD3* differ by 2 fold and 3 fold, respectively, some evidence is ascertained of transcriptional regulation of PUFA biosynthesis in oat developing seed.

FAD transcript profiling studies in cereals to date are sparse. In a comparative expression study of *FAD2s* and *FAD3s* in flax, however, Rajwade *et al*. (2013) showed that relative expression of a *FAD3* was approximately three-fold higher than that of *FAD2*, and in most cultivars the ALA:LA accumulation in the seed was >3-fold, although they did not perform in-depth analyses of this apparent correlation. A study of *FAD3* transcription correlation to ALA accumulation in flax has been performed, and found high correlation between transcript levels of *FAD3* and ALA accumulation (Banik *et al*., 2011).

Interestingly, a previous study has noted low hydroxylase protein accumulation despite high levels of its transcript (Broun *et al*., 1998a). The authors suggest hydroxylase protein accumulation and thus hydroxylase activity must be controlled by a mechanism, different from the transcriptional regulation of the desaturases (Broun *et al*., 1998a). This evidence could also suggest that the rate of translation is slower, or that the hydroxylase protein itself is less stable than the desaturases, once translated, perhaps due to altered post-translational modifications in the yeast expression system. One plausible explanation could be specificity of an E3-ubiquitin enzyme for a FAH substrate over a FAD. In *S. cerevisiae*, this would increase its proteasome-mediated degradation, as E3 is known to induce ubiquination of a substrate by ligating ubiquitin

and its activating enzyme to the target substrate (Leach & Brown, 2012). From another perspective, the varying stability of the two types of proteins may be the result of the degree of sumoylation on the ubiquinated protein which, when elevated, may enhance the stability of a protein such as a FAD by antagonizing conjugation of ubiquitin to thus circumvent the ubiquination labelling of the substrate for degradation (Leach & Brown, 2012). This added complexity of the hydroxylase, considered with the lack of function of AsFAD3-1 (and assuming it is not a pseudogene or artifact) as well as definite expression of its gene, suggests there may be an additional factor required for achieving Δ15 hydroxylase activity or perhaps a more ideal *in vivo* system may be more appropriate.

4. GENERAL DISCUSSION AND CONCLUSIONS

This thesis research started with oat seed fatty acid analysis. The lipids from CDC Dancer mature seed were extracted and fatty acids were transmethylated and qualitatively analyzed via GC to determine the total FA profile; TMS derivatization was performed in duplicate to identify presence of hydroxyl groups of any UFAs. Three different transmethylation procedures were employed to contrast effectiveness of basic and acid conditions in the context of presence of epoxy and hydroxy FAs. The common FA profile of CDC Dancer was consistent with previous studies (Leonova *et al*., 2008; Dhanda, 2011), however, the basic transmethylation procedure gave better results in terms of accurate quantitation of epoxy and hydroxy FAs. Thus, this method was more reliable in examining oat samples with these UFAs.

The study was then focused on cloning and characterization of genes involved in the biosynthesis of PUFAs in oat. The oat EST databases were search for cDNA fragments exhibiting high homology to non-oat FAD2-like genes with the intention of identifying full-length oat ORFs encoding enzymes involved in PUFA and UFA biosynthesis. Using various previously-characterized FADs and FAHs as query sequences in several tBLASTn searches, one oat FAD2-like, two FAD3-like, and one FAD6-like sequence were identified. Using cDNA synthesized from CDC Dancer total RNA of the developing seed, these four distinct ORFs were cloned: *AsFAD2* (of which two isoforms, *AsFAD2a* and *AsFAD2b* were confirmed), *AsFAD3-1*, *AsFAD3-2,* and *AsFADX* (of which a second version with an extended N-terminal, *AsFADX+*, was observed and investigated). The AsFADX proteins showed an aa pattern inside the 3rd HIS-box unique from any other FAD or FAH class.

To functionally characterize the genes, all six sequences were cloned into an expression vector, the recombinant plasmids were introduced into a *S. cerevisiae* strain fed with appropriate FA substrates, if required. After inducing the expression, lipid fractions were extracted from the yeast transformants; FAs were transmethylated (with TMS derivatized duplicates) and analyzed via GC and GC-MS. Both *AsFAD2*s demonstrated *Δ*12 desaturation on OA substrate, with *AsFAD2a* having notably higher activity; *AsFAD3-1* had no function on any FA substrates

present; *AsFAD3-2* showed specific Δ15/*ω*-3 desaturation on LA substrate; and, the shorter *AsFADX* resulted in *Δ*12 desaturation while the longer *AsFADX+* had no function. Although all oat protein sequences in this study retained the conserved HIS-boxes, the third HIS-box of *AsFADX* validated a novel amino acid sequence within the HIS residues which differs from that of all other FAD and FAH enzyme classes.

Finally, a comparative expression analysis using qRT-PCR revealed relative mRNA levels of *AsFAD2, AsFAD3-1* and, *AsFAD3-2* across germinating seed, root, leaf, and developing seed tissue of CDC Dancer. Across the plant, highest relative expression of *AsFAD2* was found in the developing seed, and lowest in the root. Highest relative *AsFAD3-1* expression was in the developing seed, while *AsFAD3-2* was expressed at highest relative amounts in the germinating seed; the leaf showed lowest expression of both *AsFAD3*s.

Developments of the past decade have led to the complete genome sequencing of more than 1000 organisms (National Centre for Biotechnology Information, 2014a), of which more than 50 are plants of varying significance, genome size, and from all parts of the world (National Centre for Biotechnology Information, 2014b). These include many of the crops from which human obtain nearly half of their calories (Muthamilarasan, 2013), such as sugar beet (Dohm *et al.*, 2014), tomato (Tomato Genome Consortium, 2012), potato (Potato Genome Sequencing Consortium, 2011), cassava (Prochnik *et al.*, 2012), cannabis (van Bakel *et al.*, 2011), soybean (Schmutz *et al.*, 2010), rice (Goff *et al.*, 2002), and corn (Schnable *et al.*, 2009); others, with more immediacy to agriculture in Saskatchewan, include flax (Wang *et al.*, 2012), wheat (A-genome; Ling *et al.*, 2013), and barley (International Barley Genome Sequencing Consortium, 2012).

Barley and wheat, specifically, have many molecular markers available, centralized in online databases (Wanamaker & Close, 2014; Wheat CAP, 2007), whereas the entire genome of *Avena sativa* has yet to be sequenced and thus markers are scarce. Therefore, new oat genetic provisions can enhance insight into this unique and complex crop. This thesis has identified new pertinent information concerning PUFA biosynthesis in *Avena sativa* and can now be targeted in MAS breeding. Such insights of genetic resources are crucial in closing the information gap between oat to those of other main Canadian and Saskatchewan crops; the application of such resources in oat will increase its attractiveness as a viable option for producers in today's economy, while fostering the general availability of resources for comparative plant genomics.

Overall, data from this thesis will assist in positioning oat to be competitive with the tools of modern genomics through development of tools for molecular breeding.

5. APPENDICES

5.1. Appendix 1: Putative full-length *Avena* FAD-like sequence alignments

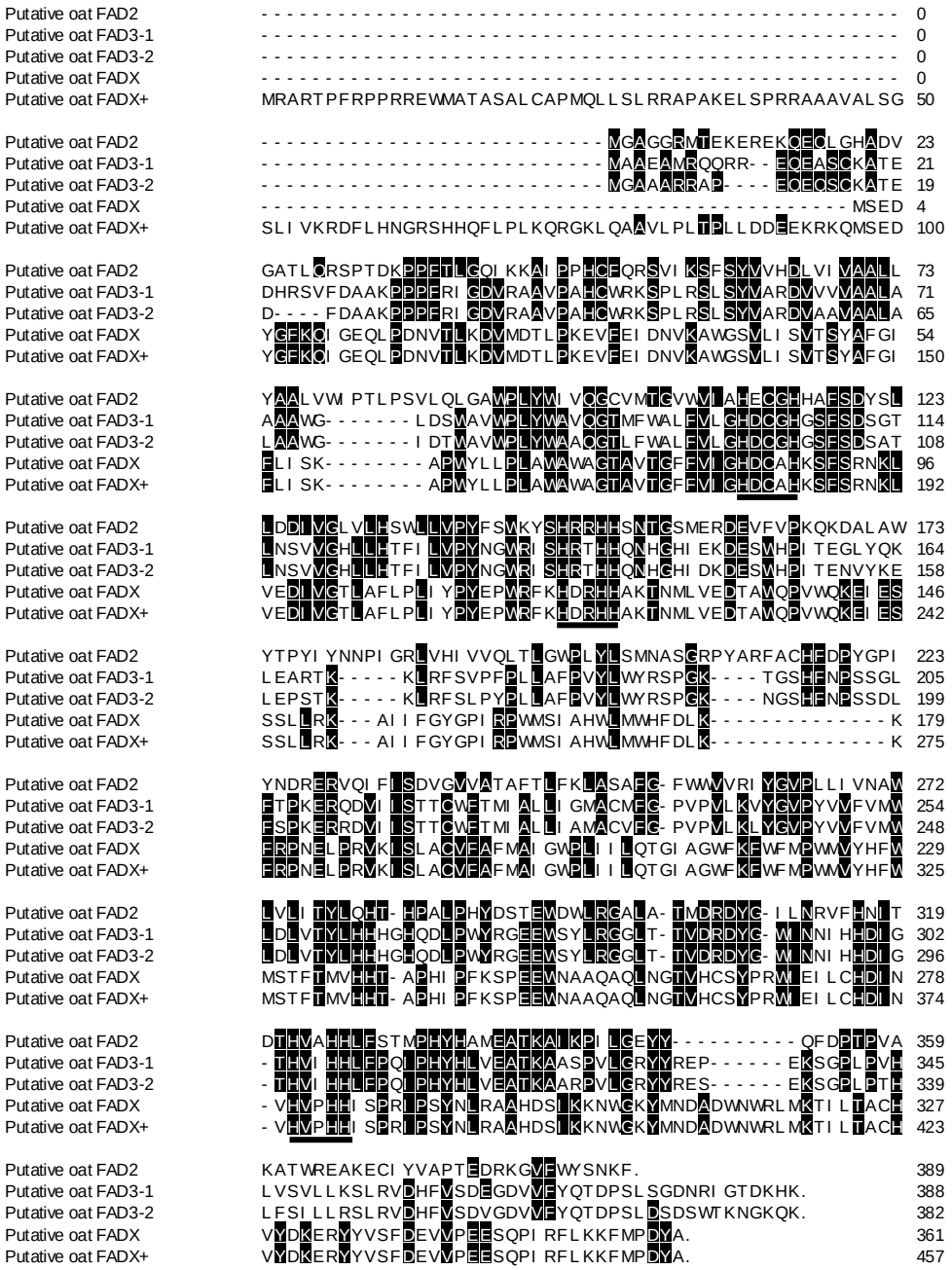

Figure 44. Putative *Avena* FAD2, FAD3-1, FAD3-2, FADX, FADX+ protein sequence alignment. HIS-boxes are underlined.

5.2. Appendix 2: Untranslated (UTR) Regions of Putative oat *FAD*-like genes

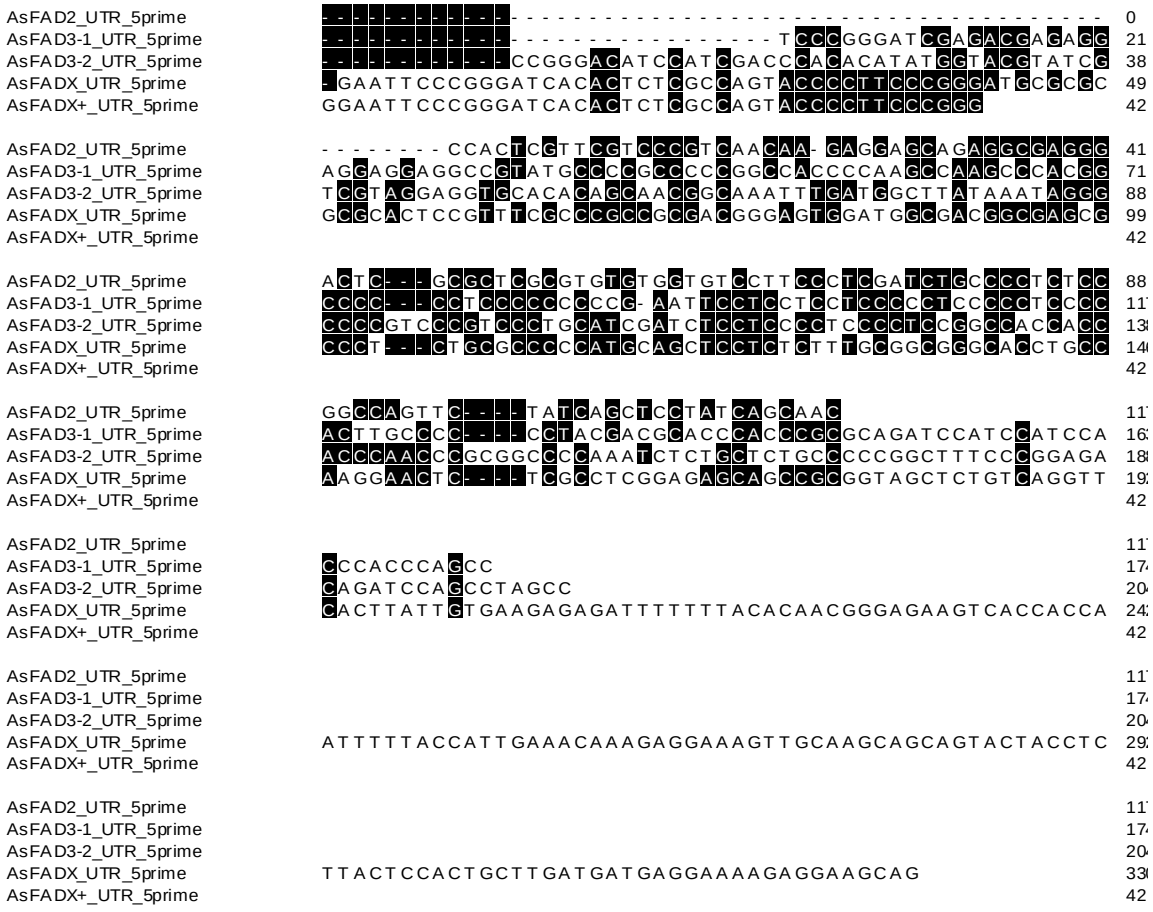

Figure 45. A ClustalW nucleotide alignment of 5' untranslated regions (UTRs) identified upstream from the putative translation initiation codon of each putative oat *FAD*-like gene CDS.

Table 19. Relative percent nucleotide identities of the 5' UTRs of each putative oat *FAD*-like gene CDS.

1	2	3	4	5		
	41.4	35.9	43.6	0.0	1	AsFAD2_UTR_5prime
		40.8	39.7	46.2	2	AsFAD3-1_UTR_5prime
			39.1	26.7	3	AsFAD3-2_UTR_5prime
				100.0	4	AsFADX_UTR_5prime
					5	AsFADX+_UTR_5prime

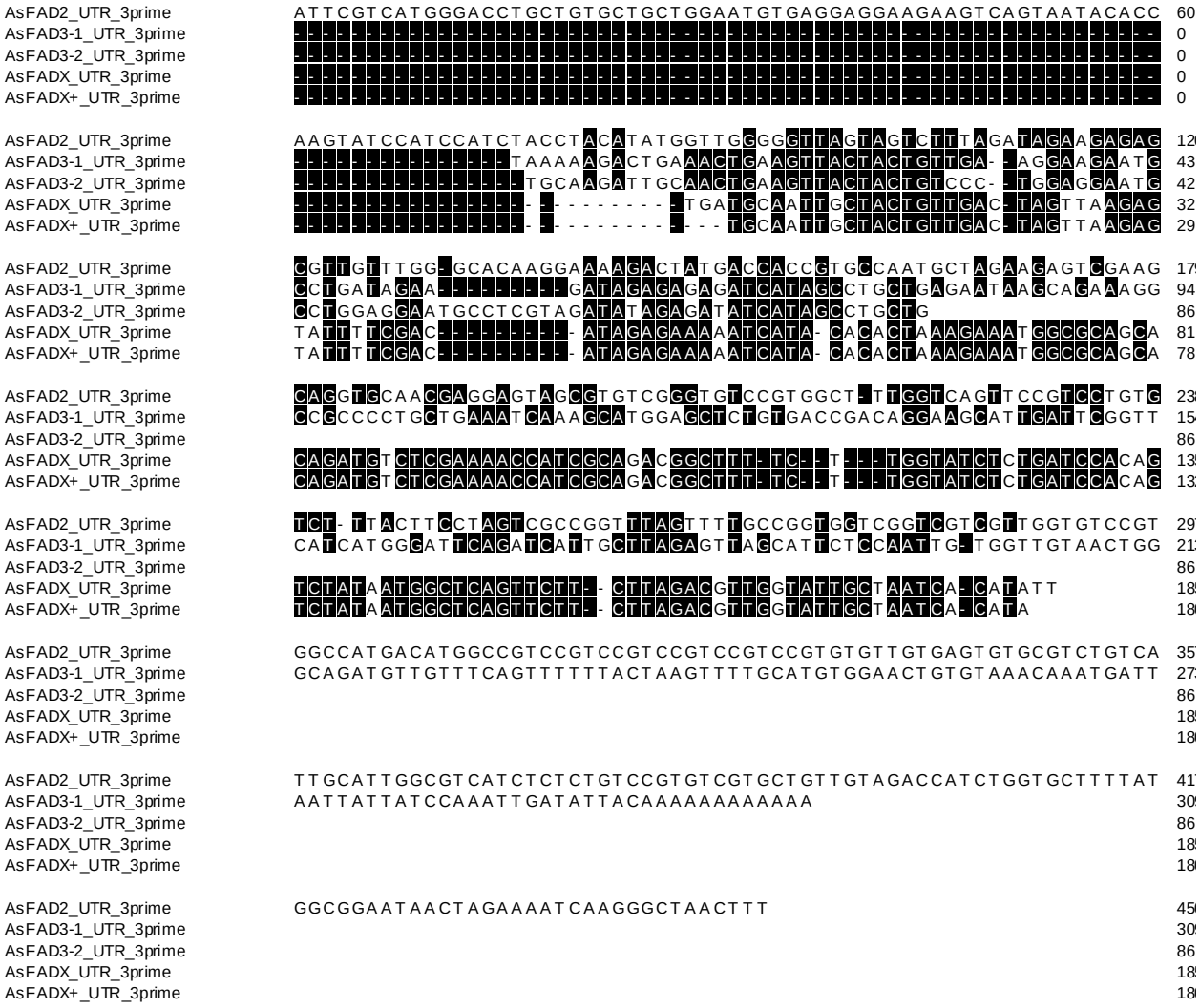

Figure 46. A ClustalW nucleotide alignment of entire 3' UTRs identified downstream from the putative translation termination codon of each putative oat *FAD*-like gene CDS.

Table 20. Relative percent nucleotide identities of the 3' UTRs of each putative oat *FAD*-like gene CDS.

1	2	3	4	5	
	35.5	36.5	41.3	42.5	1
		80.5	50.5	51.4	2
			54.7	57.4	3
				100.0	4
					5

AsFAD2_UTR_3prime
AsFAD3-1_UTR_3prime
AsFAD3-2_UTR_3prime
AsFADX_UTR_3prime
AsFADX+_UTR_3prime

5.3. Appendix 3: AsFADX+ aligned with all *Arabidopsis* FADs

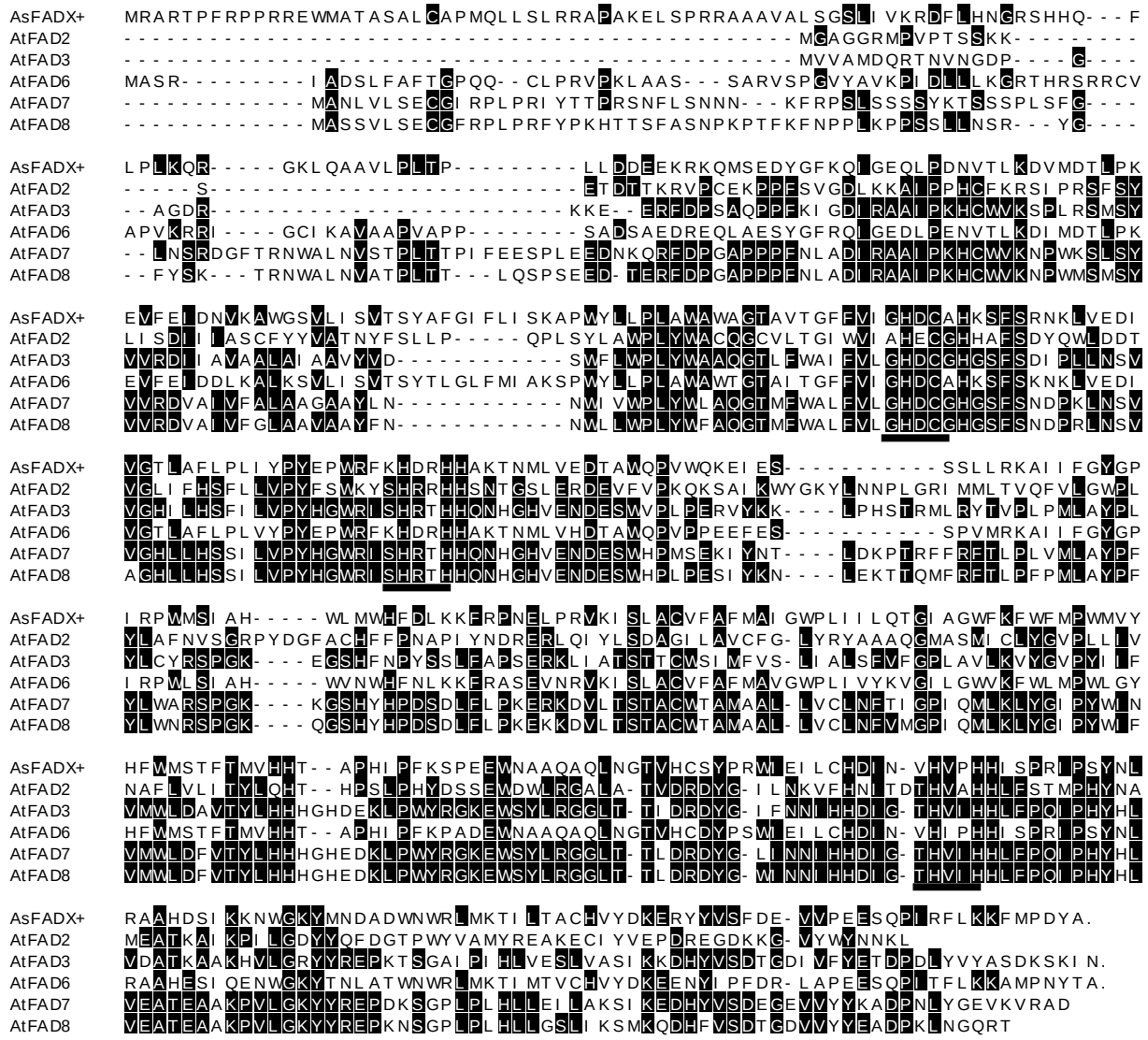

Figure 47. A ClustalW alignment of the Avena AsFADX+ with *Arabidopsis* (At) FAD-like proteins. Histidine boxes are underlined.

Table 21. Relative percent identities of AsFADX+ to *Arabidopsis* FAD-like proteins.

1	2	3	4	5	6		
	19.7	22.5	71.1	24.2	23.3	1	AsFADX+
		36.2	19.9	33.2	33.9	2	AtFAD2
			22.1	65.6	67.6	3	AtFAD3
				21.5	22.4	4	AtFAD6
					82.2	5	AtFAD7
						6	AtFAD8

5.4. Appendix 4: qRT-PCR Data

Table 22. qRT-PCR results from germinating seed tissue.

			Biological repetition		
			1	2	3
GAPDH	Ct of technical repetition	1	23.61150602	24.19553754	25.87484571
		2	23.61513763	24.34631908	25.67443897
		3	23.51587898	23.53420053	25.34771909
	mean Ct		23.58084088	24.02535239	25.63233459
	SD_{Ct}		0.05628795	0.431979601	0.266073679
	Quantity [$2^{(mean\ Ct)}$]		12547015.28	17074646.66	52011762.41
	$SD_{Quantity}$		775890.2777	8103253.33	15203652.59
Actin 1	Ct of technical repetition	1	28.24952602	28.47327266	30.42343932
		2	28.30033366	28.94140556	30.24109673
		3	28.22067192	28.68187332	29.68154973
	mean Ct		28.25684387	28.69885051	30.11536193
	$SD_{mean\ Ct}$		0.040331894	0.234527768	0.386596655
	Quantity [$2^{(mean\ Ct)}$]		3207432955.3	4357273745	1163127358
	$SD_{Quantity}$		14211851.41	112267375	4940032607
	Normalization Factor (NF)		**63437930.5**	**86254802.52**	**245959963.8**
	SD_{NF}		**14478007.34**	**139735299.5**	**380443555.7**

			Biological repetition			Adjusted to Multiplification Factor
			1	2	3	749.76
AsFAD2	tech Ct of technical repetition	1	28.12010772	28.89502636	29.46015759	
		2	27.94848182	28.81573482	29.4598478	
		3	27.83725798	29.27117277	29.58609618	
	mean Ct		27.96861584	28.99397798	29.50203386	
	$SD_{mean\ Ct}$		0.142495709	0.243309474	0.072800272	
	Quantity [$2^{(mean\ Ct)}$]		262659011	534634605	760321241.7	
	$SD_{Quantity}$		41118621.33	142909314.9	60809940.13	
	Normalized Expression Level (EL)		0.241522003	0.161334118	0.323494794	
	SD_{EL}		0.06684226	0.264899883	0.501040587	
	Mean EL			**0.24212**		**181.53**
	$SD_{Mean\ EL}$			0.081082		60.792
AsFAD3-1	Ct of technical repetition	1	31.58782073	32.8474612	33.43017419	
		2	31.51366862	32.91629539	34.00854574	
		3	31.48603008	33.39803509	33.95635885	
	mean Ct		31.52917315	33.05393056	33.79835963	
	$SD_{mean\ Ct}$		0.052636741	0.299984137	0.319923824	
	Quantity [$2^{(mean\ Ct)}$]		3099037670	8917119204	14938949235	
	$SD_{Quantity}$		179209199	2938781621	5250626022	
	Normalized Expression Level (EL)		0.020470203	0.009672945	0.016464342	
	SD_{EL}		0.004819411	0.015991425	0.026115741	
	Mean EL			**0.015536**		**11.648**
	$SD_{Mean\ EL}$			0.0054582		4.0923
AsFAD3-2	Ct of technical repetition	1	29.57739355	31.53564291	32.21349901	
		2	29.48793624	31.49254211	31.9231278	
		3	29.57353319	31.44624322	32.08197273	
	mean Ct		29.54628766	31.49147608	32.07286651	
	$SD_{mean\ Ct}$		0.050570664	0.04470938	0.145399628	
	Quantity [$2^{(mean\ Ct)}$]		784005025.4	3019109800	4517465738	
	$SD_{Quantity}$		43557400.81	148293463.9	721610121.9	
	Normalized Expression Level (EL)		0.080915209	0.028569614	0.054464448	
	SD_{EL}		0.019006028	0.046304878	0.084664041	
	Mean EL			**0.054644**		**40.970**
	$SD_{Mean\ EL}$			0.026173		19.624

Table 23. qRT-PCR results from root tissue.

Gene		Technical repetition	Biological repetition 1	Biological repetition 2	Biological repetition 3
GAPDH	Ct of technical repetition	1	25.2332847	30.15527477	30.62110918
		2	25.09682746	30.16586114	30.33949959
		3	25.19392476	31.44[illegible]	30.33620944
	mean Ct		25.17467898	30.16056795	30.43227273
	SD_{Ct}		0.070234923	0.007485695	0.163545431
	Quantity [$2^{(mean\ Ct)}$]		37873330.94	1200150305	1448861690
	$SD_{Quantity}$		2922342.19	9869888.275	260321355.3
Actin1	Ct of technical repetition	1	30.77004099	34.64336628	35.67128582
		2	31.00734337	34.31572057	35.54050831
		3	30.87187923	34.57921976	36.27130864
	mean Ct		30.88308786	34.51276887	35.82770092
	$SD_{mean\ Ct}$		0.119047598	0.173636745	0.389700585
	Quantity [$2^{(mean\ Ct)}$]		1980321972	24511995260	60983543168
	$SD_{Quantity}$		259000675.3	4675895036	26108875261
	Normalization Factor (NF)		**273863815.4**	**5423843524**	**9399825500**
	SD_{NF}		**124760472.1**	**3106831550**	**13093110276**

Gene		Technical repetition	Biological repetition 1	Biological repetition 2	Biological repetition 3	Adjusted to Multiplication Factor
						749.76
AsFAD2	tech Ct of technical repetition	1	31.13830707	36.57343436	35.10143842	
		2	31.09038017	36.17442723	34.62307879	
		3	31.28321178	36.5705151	34.78619587	
	mean Ct		31.170633	36.43945889	34.83690436	
	$SD_{mean\ Ct}$		0.100397867	0.229528798	0.243177909	
	Quantity [$2^{(mean\ Ct)}$]		2417105007	93190180520	30686910608	
	$SD_{Quantity}$		266602647.1	23499130175	8198261003	
	Normalized Expression Level (EL)		0.113302407	0.058201878	0.306313842	
	SD_{EL}		0.053106997	0.036426077	0.434444567	
	Mean EL			**0.15927**		**119.42**
	$SD_{Mean\ EL}$			0.13029		97.684
AsFAD3-1	Ct of technical repetition	1	34.14760703	40.50672402	35.10143842	
		2	33.98841032	40.75451785	34.62307879	
		3	33.98023233	42.31148391	34.78619587	
	mean Ct		34.03874989	41.1909086	34.83690436	
	$SD_{mean\ Ct}$		0.094361682	0.978323684	0.243177909	
	Quantity [$2^{(mean\ Ct)}$]		17647562656	2.51015E+12	30686910608	
	$SD_{Quantity}$		1829468175	2.6979E+12	8198261003	
	Normalized Expression Level (EL)		0.015518506	0.002160768	0.306313842	
	SD_{EL}		0.007250293	0.002631619	0.434444567	
	Mean EL			**0.10800**		**80.972**
	$SD_{Mean\ EL}$			0.17188		128.87
AsFAD3-2	Ct of technical repetition	1	32.94230555	38.82725807	38.78724231	
		2	32.74716653	38.86844518	37.97200708	
		3	32.94690451	40.12682721	37.62126149	
	mean Ct		32.8787922	39.27417682	38.12683696	
	$SD_{mean\ Ct}$		0.114014361	0.738704006	0.598211531	
	Quantity [$2^{(mean\ Ct)}$]		7897737094	6.64822E+11	3.00138E+11	
	$SD_{Quantity}$		989251416.7	5.39536E+11	1.97252E+11	
	Normalized Expression Level (EL)		0.034676239	0.008158341	0.031318303	
	SD_{EL}		0.01638324	0.008104003	0.048235406	
	Mean EL			**0.024718**		**18.532**
	$SD_{Mean\ EL}$			0.014439		10.826

Table 24. qRT-PCR results from leaf tissue.

			Biological repetition		
			1	2	3
GAPDH	Ct of technical repetition	1	22.11726163	24.37123627	28.53601528
		2	21.98613982	23.85740924	28.34636914
		3	21.81813291	23.60312354	28.13208942
	mean Ct		21.97384479	23.94392302	28.33815795
	SD_{Ct}		0.149942903	0.391296263	0.202088082
	Quantity [$2^{(\text{mean Ct})}$]		4118948.869	16137603.57	339340397.9
	$SD_{Quantity}$		678510.8063	6937279.551	75339150.47
Actin1	Ct of technical repetition	1	28.44265365	30.87256725	35.50204044
		2	28.38416191	30.62422368	34.55476288
		3	28.30215763	30.43938867	33.98745541
	mean Ct		28.3763244	30.6453932	34.68141958
	$SD_{mean\ Ct}$		0.070575154	0.217363821	0.765195005
	Quantity [$2^{(\text{mean Ct})}$]		348437436.6	1679509953	27551648237
	$SD_{Quantity}$		27016003.18	401064565.7	23161365711
	Normalization Factor (NF)		**37883980.59**	**164630695.3**	**3057676778**
	SD_{NF}		**20691932.19**	**242874438.7**	**7975727841**

			Biological repetition		
			1	2	3
AsFAD2	tech Ct of technical repetition	1	25.90199291	28.54760129	32.00513453
		2	26.04239354	28.93742573	32.29709809
		3	25.78700589	28.54921201	32.31926
	mean Ct		25.91046411	28.67807968	32.20716421
	$SD_{mean\ Ct}$		0.127904393	0.224601716	0.175313379
	Quantity [$2^{(\text{mean Ct})}$]		63070590.7	429499043.7	4958182430
	$SD_{Quantity}$		8862511.485	105978977.4	954953038.6
	Normalized Expression Level (EL)		0.600659993	0.383308642	0.616693077
	SD_{EL}		0.338758907	0.573338262	1.612978247
	Mean EL			**0.53355**	**400.04**
	$SD_{Mean\ EL}$			0.13036	97.741
AsFAD3-1	Ct of technical repetition	1	35.03970341	39.59453697	39.99567484
		2	36.08079926	37.66214675	39.99567484
		3	35.83139294	37.44187172	39.99567484
	mean Ct		35.65063187	38.23285181	39.99567484
	$SD_{mean\ Ct}$		0.543577102	1.184385966	0
	Quantity [$2^{(\text{mean Ct})}$]		53939828065	3.23024E+11	1.09622E+12
	$SD_{Quantity}$		32211812614	4.20313E+11	0
	Normalized Expression Level (EL)		0.000702338	0.000509654	0.002789291
	SD_{EL}		0.000568395	0.001002542	0.007275662
	Mean EL			**0.0013338**	**1.0000**
	$SD_{Mean\ EL}$			0.0012642	0.94785
AsFAD3-2	Ct of technical repetition	1	32.18566341	35.36551756	38.18121464
		2	32.2481421	35.11219831	38.34536815
		3	32.63103546	34.83993778	38.30417879
	mean Ct		32.35494699	35.10588455	38.27692053
	$SD_{mean\ Ct}$		0.241131767	0.262846773	0.08540406
	Quantity [$2^{(\text{mean Ct})}$]		5492999403	36976369995	3.33044E+11
	$SD_{Quantity}$		1455152245	10677544146	31248141457
	Normalized Expression Level (EL)		0.006896775	0.004452322	0.009181008
	SD_{EL}		0.004186651	0.006693015	0.02396348
	Mean EL			**0.0068434**	**5.1309**
	$SD_{Mean\ EL}$			0.0023648	1.7730

Adjusted to Multiplification Factor
749.76

Table 25. qRT-PCR results from developing seed (milky stage) tissue.

			Biological repetition		
			1	2	3
GAPDH	Ct of technical repetition	1	21.79908498	23.7285254	25.12513164
		2	21.76936191	23.16193805	24.7347323
		3	21.67376346	22.89615713	24.46625891
	mean Ct		21.74740345	23.26220686	24.77537429
	SD_{Ct}		0.065482831	0.425146574	0.331311254
	Quantity [$2^{(\text{mean Ct})}$]		3520633.09	10060557.1	28716454.23
	$SD_{Quantity}$		253275.1979	4698996.985	10452290.1
Actin1	Ct of technical repetition	1	27.49595968	29.48963945	30.43701827
		2	27.3287828	29.45420167	30.38366341
		3	27.48044134	29.10496716	30.08423391
	mean Ct		27.43506127	29.34960276	30.30163853
	$SD_{mean\ Ct}$		0.092366336	0.212600311	0.190158519
	Quantity [$2^{(\text{mean Ct})}$]		181458106.8	684086138.5	1323433475
	$SD_{Quantity}$		18413423.66	159778793.8	276479130.4
	Normalization Factor (NF)		**25275431.06**	**82959554.34**	**194946959**
	SD_{NF}		**9431928.921**	**129968124**	**245442976.1**

			Biological repetition		
			1	2	3
AsFAD2	tech Ct of technical repetition	1	26.07139313	27.81743209	27.72958383
		2	26.02921031	27.58619527	27.5718265
		3	25.92299745	27.11040099	27.29197246
	mean Ct		26.00786696	27.50467612	27.5311276
	$SD_{mean\ Ct}$		0.076465502	0.360495871	0.221626323
	Quantity [$2^{(\text{mean Ct})}$]		67475805.73	190428757	193952428.1
	$SD_{Quantity}$		5668368.509	75418394.07	47223809.06
	Normalized Expression Level (EL)		0.374585094	0.435646147	1.005127705
	SD_{EL}		0.14328053	0.703973249	1.288927114
	Mean EL			**0.60512**	
	$SD_{Mean\ EL}$			0.34776	
AsFAD3-1	Ct of technical repetition	1	30.20016649	31.47173762	32.79076773
		2	30.123386	32.03543381	32.52548885
		3	30.24445702	31.8459993	32.45296458
	mean Ct		30.1893365	31.78439024	32.58974038
	$SD_{mean\ Ct}$		0.061257768	0.286853801	0.177831206
	Quantity [$2^{(\text{mean Ct})}$]		1224322517	3698748968	6463822274
	$SD_{Quantity}$		82395114.3	1165627859	1262821113
	Normalized Expression Level (EL)		0.020644422	0.02429085	0.030159703
	SD_{EL}		0.007828072	0.035842272	0.038426242
	Mean EL			**0.024411**	
	$SD_{Mean\ EL}$			0.0050578	
AsFAD3-2	Ct of technical repetition	1	28.49454953	31.12016543	32.25805412
		2	28.68090047	31.15457389	32.56157724
		3	28.53650239	31.23114639	32.54179519
	mean Ct		28.5706508	31.16862857	32.45380885
	$SD_{mean\ Ct}$		0.097756093	0.056809715	0.169816866
	Quantity [$2^{(\text{mean Ct})}$]		398678565	2413749086	5882608397
	$SD_{Quantity}$		42816500.97	150646548.5	1097476461
	Normalized Expression Level (EL)		0.063398019	0.034369585	0.033139544
	SD_{EL}		0.024618251	0.05388763	0.042179078
	Mean EL			**0.043636**	
	$SD_{Mean\ EL}$			0.017126	

Adjusted to Multiplification Factor
749.76
453.69
260.74
18.302
3.7921
32.716
12.840

6. REFERENCES CITED

Agriculture & Agri-Food Canada (2010) GRIN-CA Accession Area Queries. Plant Gene Resources of Canada. Accessed online March 29, 2012 <http://pgrc3.agr.gc.ca/acc/search-recherche_e.html#add>

Agriculture & Agri-Food Canada (2012) Canadian Agricultural Biodiversity. National Collections. Accessed online March 29, 2012 <http://www4.agr.gc.ca/AAFC-AAC/display-afficher.do?id=1273845048950&lang=eng>

Agriculture and Agri-Food Canada (2010a) Oats: Situation and Outlook (August 2010). Market Outlook Report. Accessed online 2014 January 3 < http://www.agr.gc.ca/eng/industry-markets-and-trade/statistics-and-market-information/by-product-sector/crops/crops-market-information-canadian-industry/market-outlook-report/oats-situation-and-outlook-august-2010/?id=1378843401619>

Agriculture Saskatchewan (2008) Oats. Crops. Accessed online February 12, 2012 <http://www.agriculture.gov.sk.ca/oats>

Alexander DE, Seif RD (1963) Relation of kernel oil content to some agronomic traits in maize. *Crop Sci.* 3(4):354-355. doi:10.2135/cropsci1963.0011183X000300040022x

American Oil Chemists' Society (2012) Trimethylsilyl Ether Derivatives of Alcohols. Part 2. Derivatives Other than Nicotinates. Accessed online March 20, 2012 <http://lipidlibrary.aocs.org/ms/ms35/index.htm>

American Oil Chemists' Society (2012b) Free (unesterified) fatty acids. The AOCS Lipid Library. Accessed online 2014 March 2 < http://lipidlibrary.aocs.org/Lipids/fa_poly/index.htm>

American Oil Chemists' Society (2012c) Fatty acids: methylene-interrupted double bonds. The AOCS Lipid Library. Accessed online 2014 January 6 <http://lipidlibrary.aocs.org/Lipids/fa_poly/index.htm>

An YQ, Huang S, McDowell JM, McKinney EC, Meagher RB (1996) Conserved expression of the Arabidopsis ACT1 and ACT 3 actin subclass in organ primordia and mature pollen. *Plant Cell.* 8(1):15-30. doi: 10.1105/tpc.8.1.15

Arondel V, Lemieux B, Hwang I, Gibson S, Goodman HM, Somerville CR. (1992) Map-based cloning of a gene controlling omega-3 fatty acid desaturation in *Arabidopsis*. *Science* 258(5086):1353-5. PMID: 1455229

Banas A, Debski H, Banas W, Heneen WK, Dahlqvist A, Bafor M, Gummeson PO, Marttila S, Ekman A, Carlsson AS, Stymne S (2007) Lipids in grain tissues of oat (*Avena sativa*): differences in content, time of deposition, and fatty acid composition. *J Exp Bot.* 58(10):2463-70. PMID: 17586606

Banik M, Duguid S, Cloutier S (2011) Transcript profiling and gene characterization of three fatty acid desaturase genes in high, moderate, and low linolenic acid genotypes of flax (Linum usitatissimum L.) and their role in linolenic acid accumulation. Genome. 54(6):471-83. doi: 10.1139/g11-013.

Bell RM, Ballas LM, Coleman RA (1981) Lipid topogenesis. *J Lipid Res.* 22(3):391-403. PMID: 7017050

Bhushan S, Kuhn C, Berglund AK, Roth C, Glaser E (2006) The role of the N-terminal domain of chloroplast targeting peptides in organellar protein import and miss-sorting. *FEBS Lett.* 580(16):3966-72. PMID: 16806197

BioBasic (2013) Plasmid DNA, Gel Extraction and PCR Product Purification Kits. Accessed online 2013 October 17 <http://store.biobasic.com/category/molecular-biology-kits_dna-isolation-kits_plasmid-dna-gel-extraction-and-pcr-product-purification-ki/>

BioRad (2013) SsoFast™ EvaGreen® supermix. Accessed online 2013 June 5 <http://www.bio-rad.com/webroot/web/pdf/lsr/literature/Bulletin_10014647.pdf>

Bloch K (1969) Enzymatic synthesis of monounsaturated fatty acids. *Acc. Chem. Res*. 2(7):193–202. DOI: 10.1021/ar50019a001

Brash AR, Schneider C, Hamberg M (2012) Applications of Stereospecifically-labeled Fatty Acids in Oxygenase and Desaturase Biochemistry. *Lipids*. 47(2):101–116. doi: 10.1007/s11745-011-3612-7

Brenna JT (2002) Efficiency of conversion of alpha-linolenic acid to long chain n-3 fattyacids in man. *Curr Opin Clin Nutr Metab Care*. 5(2):127-32. PMID: 11844977

Broun P, Boddupalli S, Somerville C (1998a) A bifunctional oleate 12-hydroxylase: desaturase from *Lesquerella fendleri. Plant J* 13(2):201-210. PMID: 9680976

Broun P, Shanklin J, Whittel E, and Somerville C (1998b) Catalytic plasticity of fatty acid modification enzymes underlying chemical diversity of plant lipids. *Science.* 282(5392):1315-1317. PMID: 9812895

Browse J, McConn M, James DJ, Miquel M (1993) Mutants of *Arabidopsis* deficient in the synthesis of alpha-linolenate. biochemical and genetic characterization of the endoplasmic reticulum linoleoyl desaturase. *J Biol Chem*. 268(22):16345-51. PMID: 8102138

Browse J, Xin Z (2001) Temperature sensing and cold acclimation. *Curr Opin Plant Biol*. 4(3):241-6. PMID: 11312135

Bugg TDH (2003) Dioxygenase enzymes: catalytic mechanisms and chemical models. *Tetrahedron.* 59(36):7075–7101. http://dx.doi.org/10.1016/S0040-4020(03)00944-X

Buist PH (2004) Fatty acid desaturases: selecting the dehydrogenation channel. *Nat. Prod. Rep.,* 21:249-262. DOI: 10.1039/B302094K

Burdge GC, Jones AE, Wootton SA (2002) Eicosapentaenoic and docosapentaenoic acids are the principal products of alpha-linolenic acid metabolism in young men. *Br J Nutr*. 88(4):355-63. PMID: 12323085

Cahoon EB1, Ripp KG, Hall SE, McGonigle B (2002) Transgenic production of epoxy fatty acids by expression of a cytochrome P450 enzyme from *Euphorbia lagascae* seed. *Plant Physiol.*128(2):615-24. PMID: 11842164

Carlsson AS, Yilmaz JL, Green AG, Stymne S, Hofvander P (2011) Replacing fossil oil with fresh oil – with what and for what? *Eur J Lipid Sci Technol* 113: 812-831. PMID: 22102794

Carnielli VP, Wattimena DJ, Luijendijk IH, Boerlage A, Degenhart HJ, Sauer PJ (1996) The very low birth weight premature infant is capable of synthesizing arachidonic and docosahexaenoic acids from linoleic and linolenic acids. *Pediatric Research.* 40(1):169-174. PMID: 8798265

Chaw SM, Chang CC, Chen HL, Li WH (2004) Dating the monocot-dicot divergence and the origin of core eudicots using whole chloroplast genomes. *J Mol Evol*. 58(4):424-41. PMID: 15114421

Christie WW (2011) Chapter 4: The preparation of derivatives of fatty acids. Part 2: The analysis of fatty acids. Gas chromatography and lipids. James Hutton Institute (and Mylnefield Lipid Analysis), Invergowrie, Dundee. Scotland. Accessed online 2014 May 08 <http://lipidlibrary.aocs.org/GC_lipid/04_deriv/index.htm>

Christie WW (2012) Part 1B. 10- to omega-Hydroxy Acids. Mass spectra of hydroxy fatty acids. Accessed online 2014 February 10 <http://lipidlibrary.aocs.org/ms/ms23a/index.htm>
Christie WW (2012b) Mass spectra of epoxy, furanoid and alkoxy fatty acids. Accessed online 2014 February 26 <http://lipidlibrary.aocs.org/ms/ms25/index.htm>
Cleland LG, James MJ, Proudman SM (2005) Fish oil: what the prescriber needs to know. *Arthritis Res Ther.* 8(1): 202. doi:10.1186/ar1876
Coffman, FA (1977) "The species of *Avena* Technical bulletin no. 1516: Oat history, identification, and classification." Agricultural Research Service, United States Department of Agriculture. Washington, D.C.
Comai L (2005) The advantages and disadvantages of being polyploidy. *Nature Reviews Genetics* 6:836-846. doi:10.1038/nrg1711
Covello PS, Reed DW (1996) Functional expression of the extraplastidial Arabidopsis thaliana oleate desaturase gene (FAD2) in *Saccharomyces cerevisiae. Plant Physiol.* 111(1): 223–226. PMID: 8685264
Dangour AD, Andreeva VA, Sydenham E, Uauy R (2012) Omega 3 fatty acids and cognitive health in older people. *Br J Nutr.* Suppl 2:S152-8. doi: 10.1017/S0007114512001547.
Davidson MH, Kling D, Maki KC (2011) Novel developments in omega-3 fatty acid-based strategies. *Curr Opin Lipidol*. 22(6):437-44. doi: 10.1097/MOL.0b013e32834bd642.
Deshpande SS, Damodaran S (1990) "Chapter 3: Food legumes: chemistry and technology" In Advances in Cereal Science and Technology, Volume X, Pomeranz Y ed. (147-241) American Association of Cereal Chemists, St. Paul, MN
Dhanda RK (2011) Fatty acid composition in diverse oat germplasm. Electronic Theses and Dissertations. University of Saskatchewan. Accessed online 2014 January 08 <http://hdl.handle.net/10388/etd-03202011-224522>
Dieticians of Canada (2013) Food Sources of Omega-3 Fats. *Resources.* Accessed online 2014 January 3 < http://www.dietitians.ca/Nutrition-Resources-A-Z/Factsheets/Fats/Food-Sources-of-Omega-3-Fats.aspx>
Dohm JC, Minoche AE, Holtgräwe D, Capella-Gutiérrez S, Zakrzewski F, Tafer H, Rupp O, Sörensen TR, Stracke R, Reinhardt R, Goesmann A, Kraft T, Schulz B, Stadler PF, Schmidt T, Gabaldón T, Lehrach H, Weisshaar B, Himmelbauer H (2014) The genome of the recently domesticated crop plant sugar beet (*Beta vulgaris*). *Nature*. 505(7484):546-9. doi: 10.1038/nature12817
Dyer JM, Chapital DC, Cary JW, Pepperman AB (2001) Chilling-sensitive, post-transcriptional regulation of a plant fatty acid desaturase expressed in yeast. *Biochem Biophys Res Commun.* 282(4):1019-25. PMID: 11352654
Dyer JM, Chapital DC, Kuan JCW, Shepherd HS, Tang F, Peperman AB (2004) Production of Linolenic Acid in Yeast Cells Expressing an Omega-3 Desaturase from Tung (*Aleurites fordii*). *Journal of the American Oil Chemists' Society*. 81(7): 647-651. Doi: 10.1007/s11746-004-956-x
Dyer JM, Mullen RT (2001) Immunocytological localization of two plant fatty acid desaturases in the endoplasmic reticulum. *FEBS Letters.* 494(1-2):44-7. PMID: 11297732
Ekman A, Hayden DM, Dehesh K, Bülow L, Stymne S (2008) Carbon partitioning between oil and carbohydrates in developing oat (*Avena sativa* L.) seeds. *J Exp Bot.* 59(15):4247-57. doi: 10.1093/jxb/ern266.
Emanuelsson O, Nielsen H, von Heijne G (1999) ChloroP, a neural network-based method for predicting chloroplast transit peptides and their cleavage sites. *Protein Science.* 8(5):978-84. PMID: 10338008

Finnzymes (2012) High Performance PCR from Finnzymes. Accessed online April 5 2012 <http://www.finnzymes.com/pdf/high_performance_pcr_2_low.pdf#search=%22high%20fidelity%20phusion%22>

Frey KJ, Hammond EG (1975) Genetics, characteristics, and utilization of oil in caryopses of oat species. *J. Am. Oil Chem. Soc.* 52(9):358-362. Doi: 10.1007/BF02639196

Gibson S, Arondel V, Iba K, Somerville C (1994) Cloning of a temperature-regulated gene encoding a chloroplast omega-3 desaturase from *Arabidopsis thaliana*. *Plant Physiol*. 106(4): 1615–1621. PMID: 7846164

Gietz RD, Schiestl RH (2007) High-efficiency yeast transformation using the LiAc/SS carrier DNA/PEG method. *Nature Protocols* 2: 31 – 34 doi:10.1038/nprot.2007.13

Goff SA, Ricke D, Lan TH, Presting G, Wang R, Dunn M, Glazebrook J, Sessions A, Oeller P, Varma H, Hadley D, Hutchison D, Martin C, Katagiri F, Lange BM, Moughamer T, Xia Y, Budworth P, Zhong J, Miguel T, Paszkowski U, Zhang S, Colbert M, Sun WL, Chen L, Cooper B, Park S, Wood TC, Mao L, Quail P, Wing R, Dean R, Yu Y, Zharkikh A, Shen R, Sahasrabudhe S, Thomas A, Cannings R, Gutin A, Pruss D, Reid J, Tavtigian S, Mitchell J, Eldredge G, Scholl T, Miller RM, Bhatnagar S, Adey N, Rubano T, Tusneem N, Robinson R, Feldhaus J, Macalma T, Oliphant A, Briggs S (2002) A draft sequence of the rice genome (*Oryza sativa* L. ssp. *japonica*). *Science*. 296(5565):92-100.

Graham D, Patterson BD (1982) Responses of plants to low, nonfreezing temperatures: proteins, metabolism, and acclimation. *Annual Review of Plant Physiology* 33: 347-372 . DOI: 10.1146/annurev.pp.33.060182.002023

Greenspan FP, Gall RJ (1956) Epoxy fatty acid ester plasticizers. Preparation and properties. *Journal of the American Oil Chemists Society.* 33(9):391-394. DOI: 10.1021/ie50528a048

Hamberg M, Hamberg G (1996) 15(R)- Hydroxylinoleic Acid, an Oxylipin from Oat Seeds. *Phytochemistry* 42(3):729-732. PMID: 12226220

Hamberg M, Liepinsh E, Otting G, Griffiths W (1998) Isolation and structure of a new galactolipid from oat seeds. *Lipids*. 33(4):355-63. PMID: 9590622

Health Canada (2012) Fats: The Good the Bad and the Ugly. Healthy Living. Accessed online 2014 January 02 <http://www.hc-sc.gc.ca/hl-vs/iyh-vsv/med/fats-gras-eng.php>

Helmreich EJ (2003) Environmental influences on signal transduction through membranes: a retrospective mini-review. *Biophys Chem*. 100(1-3):519-34. PMID: 12646388

Heneen WK, Karlsson G, Brismar K, Gummeson PO, Marttila S, Leonova S, Carlsson AS, Bafor M, Banas A, Mattsson B, Debski H, Stymne S (2008) Fusion of oil bodies in endosperm of oat grains. *Planta*. 228(4):589-99. doi: 10.1007/s00425-008-0761-x.

Hermes-Lima M, Storey KB (1993) Antioxidant defences in the tolerance of freezing and anoxia by garter snakes. *Am. J. Physiol.* 265:R646–R652. PMID: 8214160

Holland JB, Frey KJ, Hammond EG (2001) Correlated responses of fatty acid composition, grain quality and agronomic traits to nine cycles of recurrent selection for increased oil content in oat. *Euphytica.* 122,(1):69-79. 10.1023/A:1012639821332

Huis R, Hawkins S, Neutelings G (2010) Selection of reference genes for quantitative gene expression normalization in flax (*Linum usitatissimum* L.). *BMC Plant Biol.* 10:71. doi: 10.1186/1471-2229-10-71.

Iba K, Gibson S, Nishiuchi T, Fuse T, Nishimura M, Arondel V, Hugly S, Somerville C (1993) A gene encoding a chloroplast omega-3 fatty acid desaturase complements alterations in fatty acid desaturation and chloroplast copy number of the fad7 mutant of Arabidopsis thaliana. *J Biol Chem.* 268(32):24099-105. PMID: 8226956

Inaba M, Suzuki I, Szalontai B, Kanesaki Y, Los DA, Hayashi H, Murata N (2003) Gene-engineered rigidification of membrane lipids enhances the cold inducibility of gene expression in *Synechocystis*. *J Biol Chem.* 278(14):12191-8. PMID: 12502718

International Barley Genome Sequencing Consortium, Mayer KF, Waugh R, Brown JW, Schulman A, Langridge P, Platzer M, Fincher GB, Muehlbauer GJ, Sato K, Close TJ, Wise RP, Stein N (2012) A physical, genetic and functional sequence assembly of the barley genome. *Nature.* 491(7426):711-6. doi: 10.1038/nature11543.

Invitrogen (2002) T4 DNA Ligase manual. Accessed online 2012 April 27 <http://tools.invitrogen.com/content/sfs/manuals/t4dnaligase_1U_man.pdf>

Invitrogen (2004) SuperScript III Reverse Transcriptase. Manuals. Accessed Online 2012 February 27. <http://www.invitrogen.com/site/us/en/home/Products-and-Services/Applications/Nucleic-Acid-Amplification-and-Expression-Profiling/Reverse-Transcription-and-cDNA-Synthesis/RT___cDNA_Synthesis-Misc/SuperScript.html>

Invitrogen (2008) pYES2. Yeast Expression Vectors. Accessed online 2012 February 27 <http://products.invitrogen.com/ivgn/product/V82520>

Invitrogen (2010a) TRIzol Reagent. Manuals. Accessed Online 2012 February 27. <http://tools.invitrogen.com/content/sfs/manuals/trizol_reagent.pdf>

Ishimaru A, Yamazaki I (1977) Hydroperoxide-dependent hydroxylation involving "H2O2-reducible hemoprotein" in microsomes of pea seeds. A new type enzyme acting on hydroperoxide and a physiological role of seed lipoxygenase. *J Biol Chem*. 252(17):6118-24. PMID: 19466

IUPAC (2013) IUPAC Periodic Table of the Elements. Accessed online 2014 March 17 < http://www.iupac.org/fileadmin/user_upload/news/IUPAC_Periodic_Table-1May13.pdf>

Jacq C, Miller JR, Brownlee GG (1977) A pseudogene structure in 5S DNA of *Xenopus laevis.* *Cell*. 12(1):109-20. PMID: 561661

Jian B, Liu B, Bi Y, Hou W, Wu C, Han T (2008) Validation of internal control for gene expression study in soybean by quantitative real-time PCR. BMC *Molecular Biology*. 9:59 doi:10.1186/1471-2199-9-59

Jiang ZD, Gerwick WH (1990) Galactolipids from the Temperate Red Marine Alga *Gracilariopsis lemaneiformis*. *Phytochemistry* 29:1433–1440. http://dx.doi.org/10.1016/0031-9422(90)80096-Y

Jiang ZD, Gerwick WH (1991) An Aldehyde-Containing Galactolipid from the Red Alga *Gracilariopsis lemaneiformis*. *Lipids* 26:960–963. PMID: 1805099

Karr JE, Alexander JE, Winningham RG (2011) Omega-3 polyunsaturated fatty acids and cognition throughout the lifespan: A review. *Nutr Neurosci.* 14(5):216-25. doi: 10.1179/1476830511Y.0000000012.

Kumar P, Gupta VK, Misra AK, Modi DR, Pandey BK (2009) Potential of Molecular Markers in Plant Biotechnology. *Plant Omics.* 2(4):141-162.

Kurumbail RG, Stevens AM, Gierse JK, McDonald JJ, Stegeman RA, Pak JY, Gildehaus D, Miyashiro JM, Penning TD, Seibert K, Isakson PC, Stallings WC (1996) Structural basis for selective inhibition of cyclooxygenase-2 by anti-inflammatory agents. *Nature*. 1996 Dec 19-26;384(6610):644-8. PMID: 8967954

Kyte J, Doolittle RF (1982) A simple method for displaying the hydropathic character of a protein. *J Mol Biol*. 5;157(1):105-32. PMID: 7108955

Langer SH, Connell S, Wender I (1958) Preparation and Properties of Trimethylsilyl Ethers and Related Compounds. J. Org. Chem 23(1):50-58. DOI: 10.1021/jo01095a017

Laroche C, Beney L, Marechal PA, Gervais P (2001) The effect of osmotic pressure on the membrane fluidity of *Saccharomyces cerevisiae* at different physiological temperatures. *Appl Microbiol Biotechnol*. 56(1-2):249-54. PMID: 11499939

Leach MD, Brown AJP (2012) Posttranslational modifications of proteins in the pathobiology of medically relevant fungi. *Eukaryotic Cell* 11(2):98-108. doi: 10.1128/EC.05238-11

Lee M, Lenman M, Banaś A, Bafor M, Singh S, Schweizer M, Nilsson R, Liljenberg C, Dahlqvist A, Gummeson PO, Sjödahl S, Green A, Stymne S (1998) Identification of non-heme diiron proteins that catalyze triple bond and epoxy group formation. *Science*. 280(5365):915-8. PMID: 9572738

Leonova S, Grimberg Å, Marttila S, Stymne S, Carlsson AS (2010) Mobilization of lipid reserves during germination of oat (*Avena sativa* L.), a cereal rich in endosperm oil. *J Exp Bot.* 61(11): 3089–3099. doi: 10.1093/jxb/erq141

Leonova S, Shelenga T, Hamberg M, Konarev AV, Loskutov I, and Carlsson AS (2008) Analysis of oil composition in cultivars and wild species of oat (*Avena* Sp.) *J Agric Food Chem.*. 56 (17): 7983-7991. PMID: 18707115

Li B, Birdwell C, Whelan J (1994) Antithetic relationship of dietary arachidonic acid and eicosapentaenoic acid on eicosanoid production in vivo. *J Lipid Res.* 35(10):1869-77. PMID: 7852864

Ling HQ, Zhao S, Liu D, Wang J, Sun H, Zhang C, Fan H, Li D, Dong L, Tao Y, Gao C, Wu H, Li Y, Cui Y, Guo X, Zheng S, Wang B, Yu K, Liang Q, Yang W, Lou X, Chen J, Feng M, Jian J, Zhang X, Luo G, Jiang Y, Liu J, Wang Z, Sha Y, Zhang B, Wu H, Tang D, Shen Q, Xue P, Zou S, Wang X, Liu X, Wang F, Yang Y, An X, Dong Z, Zhang K, Zhang X, Luo MC, Dvorak J, Tong Y, Wang J, Yang H, Li Z, Wang D, Zhang A, Wang J (2013) Draft genome of the wheat A-genome progenitor *Triticum urartu*. *Nature*. 496(7443):87-90. doi: 10.1038/nature11997

Los A, Murata N (1998) Structure and expression of fatty acid desaturases. *Biochimica et Biophysica Acta* 1394(1):3-15. PMID: 9767077

Los DA, Murata N (2004) Membrane fluidity and its roles in the perception of environmental signals. *Biochim Biophys Acta.* 1666(1-2):142-57. PMID: 15519313

Lu C, Xin Z, Ren Z, Miquel M, Browse J (2009) An enzyme regulating triacylglycerol composition is encoded by the ROD1 gene of *Arabidopsis*. *PNAS* 106(44):18837-18842. doi: 10.1073/pnas.0908848106

Lyons JM, Raison JK (1970) Oxidative activity of mitochondria isolated from plant tissues sensitive and resistant to chilling injury. *Plant Physiol*. 45(4): 386–389. PMCID: PMC396419

Mathias JR, Martin JL, Burns TW, Carlson GM, Shields RP (1978) Ricinoleic acid effect on the electrical activity of the small intestine in rabbits. *J Clin Invest*. 61(3):640-4. PMID: 641145

May WE, Hume DJ (1995) Free fatty acid contents in developing seed of three summer rape cultivars in Ontario. *Canadian Journal of Plant Science*, 1995, 75(1): 111-116, 10.4141/cjps95-018

McCartney AW, Dyer JM, Dhanoa PK, Kim PK, Andrews DW, McNew JA, Mullen RT (2004) Membrane-bound fatty acid desaturases are inserted co-translationally into the ER and contain different ER retrieval motifs at their carboxy termini. *The Plant J* 37:156-173. PMID: 14690501

Meesapyodsuk D, Qiu X (2008) An oleate hydroxylase from the fungus *Claviceps purpurea*: Cloning, functional analysis, and expression in *Arabidopsis*. Plant Physiology. 147(3):1325-33. http://dx.doi.org/10.1104/pp.108.117168

Meesapyodsuk D, Qiu X (2011) A peroxygenase pathway involved in the biosynthesis of epoxy fatty acids in oat. *Plant Physiol.* 157(1):454-63. PMID: 21784965

Meesapyodsuk D, Reed DW, Covello PS, Qiu X (2007) Primary structure, regioselectivity, and evolution of the membrane-bound fatty acid desaturases of *Claviceps purpurea. J Biol Chem.* 282(28):20191-9. PMID: 17510052

Morris G J, Coulson GE, Clarke KJ (1988) Freezing injury in *Saccharomyces cerevisiae*. The effects of growth conditions. *Cryobiology* 25:471–472. http://dx.doi.org/10.1016/0011-2240(88)90055-7

Murata N, Los DA (1997) Membrane Fluidity and Temperature Perception. *Plant Physiol.* 115(3): 875–879. PMC158550

Muthamilarasan M (2013) Wheat genome sequencing: a milestone in cereal genomics and its future potential. News. *Current Science*, 104(3):286. Accessed online 2014 March 20 <http://www.currentscience.ac.in/Volumes/104/03/0286.pdf>

MyHits (2013) Motif Scan. Accessed online 2013 December 03 <http://myhits.isb-sib.ch/cgi-bin/motif_scan>

Napier JA (2007) The production of unusual fatty acids in transgenic plants. *Annu Rev Plant Biol* 58:295-315. PMID: 17472567

National Center for Biotechnology Information (2012) BLAST. Basic BLAST. Accessed online 2012 February 3, <http://blast.ncbi.nlm.nih.gov>

National Centre for Biotechnology Information (2013b) Conserved Domains. Structure. Accessed online 2013 December 03 < http://www.ncbi.nlm.nih.gov/Structure/cdd/wrpsb.cgi>

National Centre for Biotechnology Information (2014a) Genomes & Maps. Accessed online 2014 March 20. http://www.ncbi.nlm.nih.gov/guide/genomes-maps/

National Centre for Biotechnology Information (2014b) Index of /genbank/genomes/Eukaryotes/plants/. Accessed online 2014 March 20. ftp://ftp.ncbi.nih.gov/genbank/genomes/Eukaryotes/plants/

New England Biolabs Inc. (2013) Q5® High-Fidelity DNA Polymerase. Accessed online 2013 October 17. <https://www.neb.com/products/m0491-q5-high-fidelity-dna-polymerase#tabselect0>

Nielsen H, Engelbrecht J, Brunak S, von Heijne G (1997) Identification of prokaryotic and eukaryotic signal peptides and prediction of their cleavage sites. *Protein Engineering*, 10(1):1-6. PMID: 9051728

Nishida I, Murata N (1996) Chilling sensitivity in plants and cyanobacteria: the crucial contribution of membrane lipids. *Annu Rev Plant Physiol Plant Mol Biol*. 47:541-568. PMID: 15012300

Okada S, Zhou XR, Damcevski K, Gibb N, Wood C, Hamberg M, Haritos VS (2013) Diversity of Δ12 fatty acid desaturases in santalaceae and their role in production of seed oil acetylenic fatty acids. *J Biol Chem.* 288(45):32405-13. doi: 10.1074/jbc.M113.511931.

Okuley J, Lightner J, Feldmann K, Yadav N, Lark E, Browse J (1994) *Arabidopsis* FAD2 gene encodes the enzyme that is essential for polyunsaturated lipid synthesis. *Plant Cell.* 6(1):147-58. doi: http://dx.doi.org/10.1105/tpc.6.1.147

Oo KC, Teh SK, Khor HT, Ong ASH (1985) Fatty acid synthesis in the oil palm (*Elaeis guineensis*): Incorporation of acetate by tissue slices of the developing fruit. *Lipids.* 20(4) 205-210. DOI 10.1007/BF02534189

Orchard TS, Pan X, Cheek F, Ing SW, Jackson RD (2012) A systematic review of omega-3 fatty acids and osteoporosis. *Br J Nutr. Suppl* 2:S253-60. doi: 10.1017/S0007114512001638.

Pan A, Chen M, Chowdhury R, Wu JH, Sun Q, Campos H, Mozaffarian D, Hu FB (2012) α-Linolenic acid and risk of cardiovascular disease: a systematic review and meta-analysis. *Am J Clin Nutr*. 96(6):1262-73. doi: 10.3945/ajcn.112.044040

Pan X, Siloto RM, Wickramarathna AD, Mietkiewska E, Weselake RJ (2013) Identification of a pair of phospholipid:diacylglycerol acyltransferases from developing flax (*Linum usitatissimum* L.) seed catalyzing the selective production of trilinolenin. *J Biol Chem.* 288(33):24173-88. doi: 10.1074/jbc.M113.475699

Potato Genome Sequencing Consortium (2011) Genome sequence and analysis of the tuber crop potato. *Nature*. 475(7355):189-95. doi: 10.1038/nature10158.

Prochnik S, Marri PR, Desany B, Rabinowicz PD, Kodira C, Mohiuddin M, Rodriguez F, Fauquet C, Tohme J, Harkins T, Rokhsar DS, Rounsley S (2012) The Cassava Genome: Current Progress, Future Directions. *Trop Plant Biol*. 5(1):88-94. Doi: 10.1007/s12042-011-9088-z

Promega (2009) pGEM-T and pGEM-T Easy Vector Systems Technical Manual. Accessed online 2012 April 8 <http://www.promega.com/~/media/Files/Resources/Protocols/Technical%20Manuals/0/pGEM-T%20and%20pGEM-T%20Easy%20Vector%20Systems%20Protocol.pdf>

Qiagen (2013) RNeasy Mini Kit, Part 1 - (EN). Accessed online 2013 June 5 < http://www.qiagen.com/knowledge-and-support/resource-center/resource-download.aspx?id=0e32fbb1-c307-4603-ac81-a5e98490ed23&lang=en>

Rajhathy T, Thomas H (1974) Cytogenetics of oats (*Avena* L.). Miscellaneous Publications of the Genetics Society of Canada – No. 2. The Genetics Society of Canada. Ottawa, ON.

Rajwade AV, Kadoo NY, Borikar SP, Harsulkar AM, Ghorpade PB, Gupta VS (2013) Differential transcriptional activity of SAD, FAD2 and FAD3 desaturase genes in developing seeds of linseed contributes to varietal variation in α-linolenic acid content. *Phytochemistry*. doi: 10.1016/j.phytochem.2013.12.002.

Reed DW, Schäfer UA, Covello PS (2000) Characterization of the Brassica napus Extraplastidial Linoleate Desaturase by Expression in *Saccharomyces cerevisiae. Plant Physiol*. 122(3):715-720. PMID: 10712534

Rodríguez-Vargas S, Sánchez-García A, Martínez-Rivas JM, Prieto JA, Randez-Gil F (2007) Fluidization of membrane lipids enhances the tolerance of Saccharomyces cerevisiae to freezing and salt stress. *Appl Environ Microbiol*. 73(1):110-6. PMID: 17071783

Russo GL (2009) Dietary n-6 and n-3 polyunsaturated fatty acids: from biochemistry to clinical implications in cardiovascular prevention. *Biochem Pharmacol*. 77(6):937-46. doi: 10.1016/j.bcp.2008.10.020.

Salem N Jr, Pawlosky R, Wegher B, Hibbeln J (1999) In vivo conversion of linoleic acid to arachidonic acid in human adults. *Prostaglandins Leukot Essent Fatty Acids*. 60(5-6):407-10. PMID: 10471130

Sambrook J, Russel DW, Eds. (2001) "Chapter 8.13: Design of oligonucleotide primers for basic PCR." Molecular Cloning: A Laboratory Manual, Third Edition, V. 2. Cold Spring Harbor Laboratory Press, Cold Spring Harbor, New York.

Sander I, Flagge A, Merget R, Halder TM, Meyer HE, Baur X (2001) Identification of wheat flour allergens by means of 2-dimensional immunoblotting. *J Allergy Clin Immunol*. 107(5):907-13. PMID: 11344361

Sanders-Loehr J, Wheeler WD, Shiemke AK, Averill BA, Loehr TM (1989) Electronic and raman spectroscopic properties of oxo-bridged dinuclear iron centers in proteins and model compounds *J. Am. Chem. Soc.* 111(21):8084-8093. DOI: 10.1021/ja00203a003

Saskatchewan Ministry of Agriculture (2011) Factsheet: Oat production and markets. Oats. Accessed online 2014 January 3 <http://www.agriculture.gov.sk.ca/Default.aspx?DN=432e8940-b38a-4ad6-9194-728c3c903849>

Schmitz G, Ecker J (2008) The opposing effects of n-3 and n-6 fatty acids. *Prog Lipid Res.* 47(2):147-55. doi: 10.1016/j.plipres.2007.12.004.

Schmutz J, Cannon SB, Schlueter J, Ma J, Mitros T, Nelson W, Hyten DL, Song Q, Thelen JJ, Cheng J, Xu D, Hellsten U, May GD, Yu Y, Sakurai T, Umezawa T, Bhattacharyya MK, Sandhu D, Valliyodan B, Lindquist E, Peto M, Grant D, Shu S, Goodstein D, Barry K, Futrell-Griggs M, Abernathy B, Du J, Tian Z, Zhu L, Gill N, Joshi T, Libault M, Sethuraman A, Zhang XC, Shinozaki K, Nguyen HT, Wing RA, Cregan P, Specht J, Grimwood J, Rokhsar D, Stacey G, Shoemaker RC, Jackson SA (2010) Genome sequence of the palaeopolyploid soybean. *Nature*. 463(7278):178-83. doi: 10.1038/nature08670.

Schnable PS, Ware D, Fulton RS, Stein JC, Wei F, Pasternak S, Liang C, Zhang J, Fulton L, Graves TA, Minx P, Reily AD, Courtney L, Kruchowski SS, Tomlinson C, Strong C, Delehaunty K, Fronick C, Courtney B, Rock SM, Belter E, Du F, Kim K, Abbott RM, Cotton M, Levy A, Marchetto P, Ochoa K, Jackson SM, Gillam B, Chen W, Yan L, Higginbotham J, Cardenas M, Waligorski J, Applebaum E, Phelps L, Falcone J, Kanchi K, Thane T, Scimone A, Thane N, Henke J, Wang T, Ruppert J, Shah N, Rotter K, Hodges J, Ingenthron E, Cordes M, Kohlberg S, Sgro J, Delgado B, Mead K, Chinwalla A, Leonard S, Crouse K, Collura K, Kudrna D, Currie J, He R, Angelova A, Rajasekar S, Mueller T, Lomeli R, Scara G, Ko A, Delaney K, Wissotski M, Lopez G, Campos D, Braidotti M, Ashley E, Golser W, Kim H, Lee S, Lin J, Dujmic Z, Kim W, Talag J, Zuccolo A, Fan C, Sebastian A, Kramer M, Spiegel L, Nascimento L, Zutavern T, Miller B, Ambroise C, Muller S, Spooner W, Narechania A, Ren L, Wei S, Kumari S, Faga B, Levy MJ, McMahan L, Van Buren P, Vaughn MW, Ying K, Yeh CT, Emrich SJ, Jia Y, Kalyanaraman A, Hsia AP, Barbazuk WB, Baucom RS, Brutnell TP, Carpita NC, Chaparro C, Chia JM, Deragon JM, Estill JC, Fu Y, Jeddeloh JA, Han Y, Lee H, Li P, Lisch DR, Liu S, Liu Z, Nagel DH, McCann MC, SanMiguel P, Myers AM, Nettleton D, Nguyen J, Penning BW, Ponnala L, Schneider KL, Schwartz DC, Sharma A, Soderlund C, Springer NM, Sun Q, Wang H, Waterman M, Westerman R, Wolfgruber TK, Yang L, Yu Y, Zhang L, Zhou S, Zhu Q, Bennetzen JL, Dawe RK, Jiang J, Jiang N, Presting GG, Wessler SR, Aluru S, Martienssen RA, Clifton SW, McCombie WR, Wing RA, Wilson RK (2009) The B73 maize genome: complexity, diversity, and dynamics. *Science.* 326(5956):1112-5. doi: 10.1126/science.1178534.

Schrickel, DJ (1986) "Chapter 1: Oats production, value, and use." In Oats: Chemistry and Technology, Webster FH, ed. American Association of Cereal Chemists, Inc. St. Paul, Minnesota

Shakespeare, W. *The Tragedy of Hamlet, Prince of Denmark.* Accessed online <http://shakespeare.mit.edu/hamlet/full.html >

Shanklin J, Cahoon EB (1998) Desaturation and related modifications of fatty acids. Annual Review of Plant Physiology and Plant Molecular Biology, *Annu. rev. plant physiol. plant mol. biol.* 611-641. DOI: 10.1146/annurev.arplant.49.1.611

Shanklin J, Whittle E, Fox BG (1994) Eight histidine residues are catalytically essential in a membrane associated iron enzyme, stearoyl-coA desaturase, and are conserved in alkane hydroxylase and xylene monooxygenase. *Biochemistry* 33:12787-12794. PMID: 7947684

Siddiqui RA, Harvey KA, Zaloga GP (2008) Modulation of enzymatic activities by n-3 polyunsaturated fatty acids to support cardiovascular health. *J Nutr Biochem*. 19(7):417-37. PMID: 17904342

Simopoulos AP (1998) The importance of the omega-6/omega-3 fatty acid ratio in cardiovascular disease and other chronic diseases. *Exp Biol Med* 233(6):674-88. doi: 10.3181/0711-MR-311

Simopoulos AP (2002) Omega-3 Fatty Acids in Inflammation and Autoimmune Diseases. *J Am Coll Nutr.* 21:6(495–505) PMID: 12480795

Strittmatter PP, Spatz LL, Corcoran DD, Rogers MJM, Setlow BB, Redline RR (1974) Purification and properties of rat liver microsomal stearyl coenzyme A desaturase. *Proc Natl Acad Sci U S A.* 71(11), 4565-4569. PMID: 4373719

Sukharev S (1999) Mechanosensitive channels in bacteria as membrane tension reporters. *FASEB J.* 13 Suppl:S55-61. PMID: 10352145

Swiss Institute of Bioinformatics (2013a) Prosite. Accessed online 2013 December 03 < http://prosite.expasy.org/scanprosite/>

Swiss Institute of Bioinformatics (2013b) ProtScale tool. ProtScale. Accessed online 2013 December 03 < http://web.expasy.org/protscale/>

Swiss Institute of Bioinformatics (2013c) Prediction of transmembrane regions and orientation. TMpred Accessed online 2013 April 27 <http://www.ch.embnet.org>

Tai SL, Daran-Lapujade P, Walsh MC, Pronk JT, Daran JM (2007) Acclimation of Saccharomyces cerevisiae to low temperature: a chemostat-based transcriptome analysis. *Mol Biol Cell.* 18(12):5100-12. PMID: 17928405

Tasaka Y, Gombos Z, Nishiyama Y, Mohanty P, Ohba T, Ohki K, Murata N (1996) Targeted mutagenesis of acyl-lipid desaturases in Synechocystis: evidence for the important roles of polyunsaturated membrane lipids in growth, respiration and photosynthesis. *EMBO J.* 15(23): 6416–6425. PMCID: PMC452467

The Arabidopsis Genome Initiative (2000) Analysis of the genome sequence of the flowering plant *Arabidopsis thaliana*. *Nature*. 408:796-815 doi:10.1038/35048692.

The International Brachypodium Initiative (2010) Genome sequencing and analysis of the model grass *Brachypodium distachyon*. *Nature* 463:763-768. doi:10.1038/nature08747

Tokishita S, Mizuno T (1994) Transmembrane signal transduction by the *Escherichia coli* osmotic sensor, EnvZ: intermolecular complementation of transmembrane signalling. *Mol Microbiol.* 13(3):435-44. PMID: 7997160

Tomato Genome Consortium (2012) The tomato genome sequence provides insights into fleshy fruit evolution. *Nature*. 485(7400):635-41. doi: 10.1038/nature11119.

Torija MJ, Beltran G, Novo M, Poblet M, Guillamón JM, Mas A, Rozès N (2003) Effects of fermentation temperature and Saccharomyces species on the cell fatty acid composition and presence of volatile compounds in wine. *Int J Food Microbiol.* 85(1-2):127-36. http://dx.doi.org/10.1016/S0168-1605(02)00144-7

Tunaru S, Althoff TF, Nüsing RM, Diener M, Offermanns S (2012) Castor oil induces laxation and uterus contraction via ricinoleic acid activating prostaglandin EP3 receptors. *Proc Natl Acad Sci U S A.* 109(23):9179-84. doi: 10.1073/pnas.1201627109.

UniProt (2013) BLAST. UniProt. Accessed online 2013 December 03 < http://www.uniprot.org/ >

United States Department of Agriculture (2010) BatcBLAST Search. *Avena*. Accessed online 2012 February 9, <http://*Avena*.pw.usda.gov/CORE/dataO/blast/batchblast.php>

van Bakel H, Stout JM, Cote AG, Tallon CM, Sharpe AG, Hughes TR, Page JE (2011) The draft genome and transcriptome of *Cannabis sativa. Genome Biol.* 12(10):R102. doi: 10.1186/gb-2011-12-10-r102.

van de Loo FJ, Broun P, Turner S, Sommerville C (1995) An oleate 12-hydroxylase from *Ricinus communis* L. is a fatty acyl desaturase homolog. *Proc Natl Acad Sci USA*. 92(15):6743-6747. PMID: 7624314

van Meer G, Voelker DR, Feigenson GW (2008) Membrane lipids: where they are and how they behave. *Nat Rev Mol Cell Biol.* 9(2):112-24. doi: 10.1038/nrm2330.
Vanin EF (1985) Processed pseudogenes: characteristics and evolution. *Annu Rev Genet.* 19:253-72. PMID: 3909943
Vrinten P, Hu Z, Munchinsky MA, Rowland G, Qiu X (2005) Two *FAD3* desaturase genes control the level of linolenic acid in flax seed. *Plant Physiol*. 139(1):79–87. doi: 10.1104/pp.105.064451
Wada H, Gombos Z, Murata N (1990) Enhancement of chilling tolerance of a cyanobacterium by genetic manipulation of fatty acid desaturation. *Nature.* 347(6289):200-3. PMID: 2118597
Wanamaker S, Close T (2014) HarvEST. University of California. Accessed online 2014 March 20. http://harvest.ucr.edu/
Wang Z, Hobson N, Galindo L, Zhu S, Shi D, McDill J, Yang L, Hawkins S, Neutelings G, Datla R, Lambert G, Galbraith DW, Grassa CJ, Geraldes A, Cronk QC, Cullis C, Dash PK, Kumar PA, Cloutier S, Sharpe AG, Wong GK, Wang J, Deyholos MK (2012) The genome of flax (*Linum usitatissimum*) assembled de novo from short shotgun sequence reads. *Plant J.* 72(3):461-73. doi: 10.1111/j.1365-313X.2012.05093.x.
Wheat CAP (2007) MAS Wheat. University of California, Davis. Accessed online 2014 March 20. http://maswheat.ucdavis.edu/index.htm
Whitehead Institute for Biomedical Research (2006) Primer3Plus. Accessed online 25 July 2013 http://www.bioinformatics.nl/cgi-bin/primer3plus/primer3plus.cgi/
Wolfe J, Bryant G (1999) Freezing, drying, and/or vitrification of membrane-solute-water systems. *Cryobiology* 39:103–129. PMID: 10529304
Wood JM (1999) Osmosensing by bacteria: signals and membrane-based sensors. *Microbiol Mol Biol Rev. 63*(1):230-62. PMID: 10066837
Wood TE, Takebayashi N, Barker MS, Mayrose I, Greenspoon PB, Rieseberg LH (2009) The frequency of polyploid speciation in vascular plants. *Proc Natl Acad Sci U S A.* 106(33):13875-9. doi: 10.1073/pnas.0811575106.
Xu Y, Crouch JH (2008) Marker-Assisted Selection in Plant Breeding: From Publications to Practice. *Crop Science.* 48:2(391-407) doi:10.2135/cropsci2007.04.0191
Zhang XP, Glaser E (2002) Interaction of plant mitochondrial and chloroplast signal peptides with the Hsp70 molecular chaperone. *Trends Plant Sci.* 7(1):14-21. PMID: 11804822